THE

THERMAL DECOMPOSITION

OF

IRRADIATED SILVER PERMANGANATE

By

M. J. SOLE B.Sc. HONS. (RHODES).

A thesis submitted in fulfilment of the requirements for the Degree of Master of Science of Rhodes University.

Department of Chemistry,
Rhodes University,
Grahamstown.
SOUTH AFRICA.

November, 1958.

ACKNOWLEDGEMENTS.

It is with sincere gratitude that acknowledgements are made to:

Dr. E.G. Prout, for his very able guidance and direction and for his stimulating enthusiasm throughout the course of this research.

Dr. F.H. Herbstein, for helpful guidance in regard to the X-ray work and for assistance in the interpretation of results.

Prof. J.A. Gledhill, for much useful advice and discussion.

Mr. F. van de Water, for his skilful assistance in the construction of apparatus.

Mr. G. Walters, who did the reproduction and printing of photographs.

Mr. W.S Eastwood of Harwell, who arranged for the irradiations.

The author is also deeply indebted to the South African Council for Scientific and Industrial Research for grants without which this research could not have been undertaken.

PAPERS AND PUBLICATIONS.

1. "The Thermal Decomposition of Irradiated Silver Permanganate"

By

E.G. Prout and M.J. Sole.

(Journal of Inorganic and Nuclear Chemistry - in the press.)

2. "X-Ray Studies on the Thermal Decomposition of Silver Permanganate"

By

F.H. Herbstein and M.J. Sole.

(A paper read at the South African Institute of Physics Conference, Pretoria, July 1953).

CONTENTS.

1. INTRODUCTION.

1.1 THE GENERAL NATURE OF SOLID DECOMPOSITIONS.

Solid decompositions are of two main types - exothermic and endothermic. A detailed survey of the latter is beyond the scope of this introduction. It is sufficient to mention that investigations in this field have been confined almost exclusively to hydrates and carbonates. Endothermic reactions do, however, sometimes yield useful information on the nature of nucleation and the interface reaction, so examples will be quoted whenever they will aid the understanding of exothermic decompositions.

Exothermic decompositions are mainly of the type:

$$\underset{\text{(solid)}}{A} \longrightarrow \underset{\text{(solid)}}{B} + \underset{\text{(gas)}}{C}$$

The course of the decomposition is usually followed by plotting α, the fraction decomposed (or alternatively, p, the pressure of gas developed) as a function of time. Typical α, t curves are shown below.

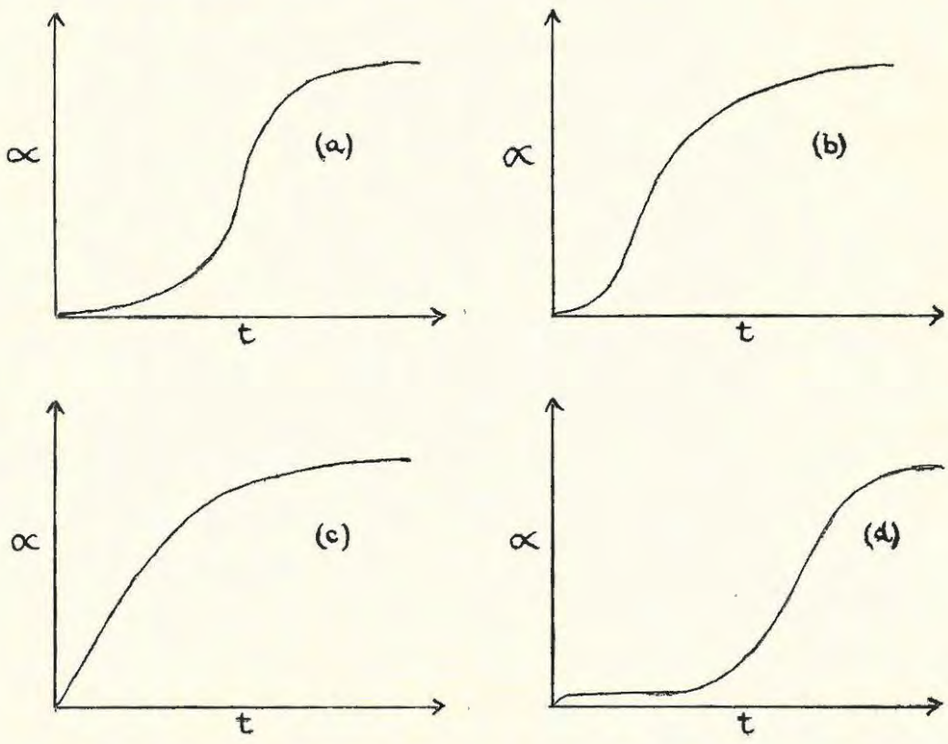

Three important characteristics are clear from these curves. However, it does not necessarily follow that all three are present in any particular decomposition. These characteristics may be de-

-2-/....

scribed as:

(a) A period of quiescence.

During this period there occur processes which result in the formation of centres of decomposition. Various explanations of the nature of these processes will be given later. This induction period is therefore associated with little or no measurable decomposition. At the end of this period, the decomposition centres, or 'nuclei', which have been formed begin to grow resulting in measurable decomposition.

(b) A period of acceleration.

This period involves the rapid spread of the reaction through the material from the nuclei. The bulk of past research work has been concentrated on this phase of the decomposition. It has indicated that in general the nuclei are three-dimensional and increase in area as the square of the time. However variations in the rate and mode of growth do often occur and these will be dealt with subsequently.

(c) A period of decay.

This period occurs after the maximum rate of decomposition has been reached. The reactant/product interface then starts shrinking and the rate of decay usually becomes proportional to the amount of reactant left undecomposed.

The nature of the decomposition curves given above may be interpreted as follows. In general they are sigmoidal, indicating an autocatalytic reaction (a). These curves sometimes show very marked induction periods where the rate of formation of nuclei is slow (1). The rather assymmetric curve (b) results from a short acceleratory period followed by a marked decay (e.g. lead styphnate (2) and mercuric oxalate (3).). In some cases the induction period is virtually absent (c), indicating instant nucleation (e.g. lead azide (4)) while in others (d), the reaction is a two-stage process with an initial evolution of gas followed by the general autocatalytic process (e.g. potassium azide (5) and lithium aluminium hydride (6)).

-3-/.....

1.2. NUCLEATION IN CRYSTALS.

It has been indicated above that thermal decompositions of solids are characterised by the formation and growth of nuclei. The process of nucleation is, as will be discussed later, a structure-sensitive process, since nuclei are only formed at certain favoured or 'potential' sites. That induction periods are associated with the formation of nuclei is shown by the fact that they are shortened by increasing the number of potential sites. This is easily done by crushing or grinding (1), or by scratching the surface of the crystal (7). Pre-irradiation with ultra-violet light (8) also shortens the induction periods of some substances, though there are indications that a different type of nucleus may be produced (9). Other means which are effective in shortening induction periods are pre-bombardment with electrons (10), neutrons (11), x-rays (11), atomic particles and γ-rays (12). Incorporation of impurities can also speed up the decomposition (13).
Previous work in these fields will be considered in section 1.4.

Nuclei vary in shape and size and both these characteristics depend upon several factors, for example, relative activation energies for nucleus formation and for nucleus growth, the particular crystal face on which they are formed, the crystal structures of parent and product phases, the mode of formation and the substance concerned.

Plate A shows some reproductions which illustrate the diversity of shapes encountered. Nuclei are usually compact, often being spherical (e.g. barium azide (14)) or perhaps hexagonal (e.g. potassium hydrogen oxalate (15)). In a few cases nuclei are diffuse, an example of this type being nickel sulphate heptahydrate (16) where they exist as two dimensional bands. In copper sulphate pentahydrate star-shaped nuclei are found, their shape being attributed to preferential growth along certain crystal planes (17). In the decomposition of silver azide the silver atoms are considered to take up the parent azide structure which at the end of the decomposition suddenly collapses to the normal silver structure (18).

-4-/.....

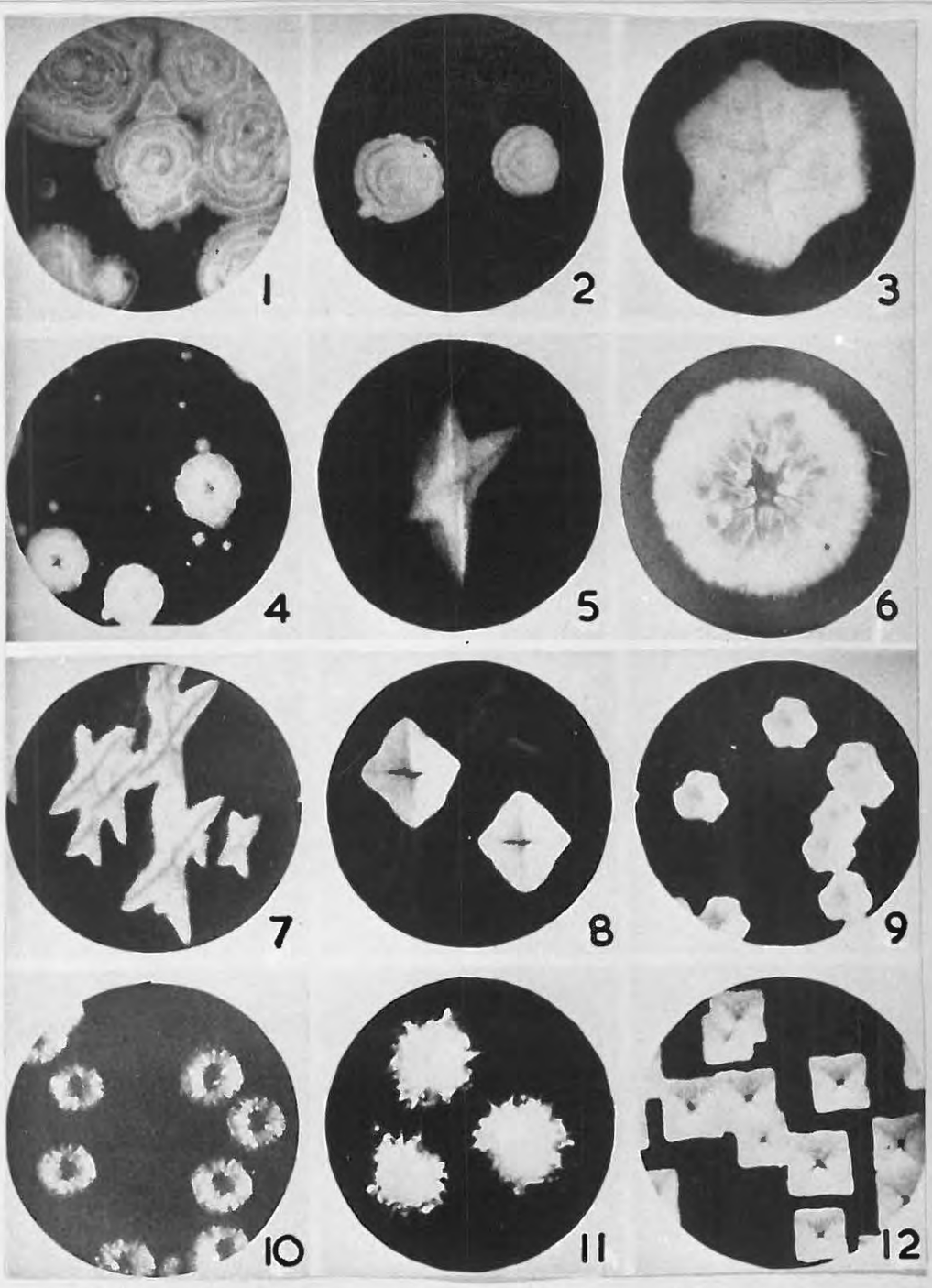

PLATE A.

1, 2, 4. —— MIXED ALUMS.
3, 9. —— COMMON ALUM, III FACE.
6. —— CHROME ALUM, III FACE.
5. —— $CuSO_4.5H_2O$.
7. —— $CuSO_4.5H_2O$ IN VACUO.
8. —— COMMON ALUM, OII FACE.
10. —— $CuSO_4.5H_2O$ IN H_2O.
11. —— AMMONIUM ALUM + H_2O.
12. —— COMMON ALUM, OOI FACE.

There is also evidence for nuclei which grow by means of linear branching chains which may interfere with one another (e.g. potassium permanganate (1)) and there is the possibility too of branching plate-like nuclei (e.g. silver oxalate (19)).

The study of solid decompositions has been too largely concerned with the increase in number with time and with the growth of nuclei. It was only when Mott and Gurney (20), in their classic work on the photolysis of the silver halides, explained the method of formation of decomposition centres that the most important aspect of the problem was treated.

However following the historical development of the field the phenomenon of nucleus growth will be considered first. Past theoretical considerations have divided the problem of nucleation into (i) the laws of nucleus formation and (ii) the laws of nucleus growth, the main aspects of which are detailed below.

(i) The Laws of Nucleus Formation.

(a) Nucleation involving a single step.

It is assumed that the decomposition of one molecule leads to the formation of a nucleus.

The probability of this decomposition is

$$k_1 = \upsilon \exp\ (-\Delta G_1 / RT) \qquad \text{(1.1)}$$

where υ = frequency of the lattice vibration.

$$\Delta G_1 = \Delta U_1 - T\Delta S_1$$
$$= E_1 - T\Delta S_1$$
$$= \text{activation energy of nucleus formation}$$

Equation (1.1) may be written

$$k_1 = s_1 \upsilon \exp\ (-E_1 / RT) \qquad \text{(1.2)}$$

where

s_1 = entropy factor, $\exp.(\Delta S_1 / R)$

If there are N_o potential nucleus forming sites, the rate of nucleus formation is

$$\frac{dN}{dt} = k_1\ (N_o - N) \qquad \text{(1.3)}$$

-5-/.....

where N = the number of nuclei at time t.

Neglecting the ingestion of potential sites by growing nuclei, equation (1.3) may be integrated to give

$$N = N_o \left[1 - \exp(-k_1 t)\right] \qquad (1.4)$$

and so from eqn. (1.3)

$$\frac{dN}{dt} = k_1 N_o \exp(-k_1 t) \qquad (1.5)$$

This is known as the 'exponential law'.

In the early stages of the reaction, especially if ΔG_1 is large and k_1 is small, the exponential term in equation (1.4) may be expanded to give approximately

$$N = k_1 N_o t \qquad (1.6)$$

or $$\frac{dN}{dt} = k_1 N_o \qquad (1.7)$$

so that the number of nuclei increases linearly with time. This has been verified for the initial stages of the dehydration of $CuSO_4.5H_2O$ (21) and of chrome alum (22).

(b) Nucleation involving more than one step.

However, cases often occur where the number of nuclei increase as powers of time which are greater than unity. In the dehydration of $NiSO_4.7H_2O$ (16) for example, they increase as t^2 and in the decompositions of barium azide (14) and of silver oxalate (23) they increase as t^3 and as t^4 respectively.

This may be accounted for in two ways. Either several successive decompositions may be required to produce a stable nucleus or alternatively a nucleus may be formed as a result of a bi-molecular process involving two or more active intermediaries, both of which are formed at a constant rate. Both hypotheses lead to the same power law (24) viz.

$$\frac{dN}{dt} = DBt^{B-1} \qquad (1.8)$$

where D = a constant

B = the number of successive decompositions (1st theory)

or B-1 = the number of separate entities required (2nd theory)

Which of the two theories is more likely, can sometimes be determined from a knowledge of the activation energy of nucleus formation.

-6-/....

Before considering how nuclei may grow it is necessary to see whether or not they will grow. In reactions of the type

$$A_{(s)} \longrightarrow B_{(s)} + C_{(g)} \qquad (1.9)$$

the probability of formation of a fragment of B embedded in the matrix of A depends not only on statistical energy fluctuations but also on the possible deformation arising if B has a different molecular volume to that of A. This deformation is associated with a certain strain energy, γ.

Consider a fragment of B containing m molecules. Then the free energy change accompanying the formation of the fragment is

$$\Delta G_1 = m\Delta G_B + \sigma\gamma \qquad (1.10)$$

where ΔG_B = bulk free energy change/molecule.

σ = a shape factor

(= $4\pi r^2$ for a spherical interface)

If u_m is the volume/molecule of the product phase, then for spherical fragments

$$m = \frac{4\pi r^3}{3u_m} \qquad (1.11)$$

Equation (1.10) can then be rewritten as

$$\Delta G_1 = m\Delta G_B + \gamma(36\pi u_m^2)^{\frac{1}{3}} m^{\frac{2}{3}} \qquad (1.12)$$

$$= am^{\frac{2}{3}} - bm \qquad (1.13)$$

where a is proportional to γ

b is the negative of ΔG_B

Thus when γ is positive ΔG_1 must pass through a maximum at m = m* when a fragment has a critical size to be in equilibrium with its surroundings.

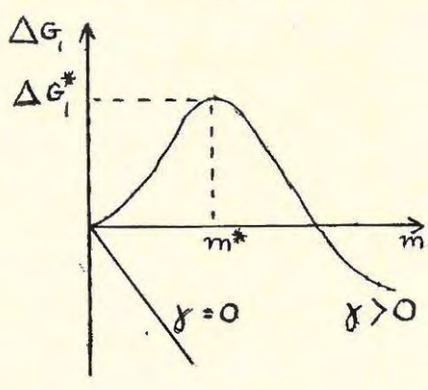

-7-/.....

As a consequence of the strain induced by the formation of the new phase, small fragments of B will be unstable and tend to revert back to A whereas large fragments are stable with respect to the transformation A $\longrightarrow$ B + C. Thus further reaction tends to occur at the interface rather than lead to the initiation of a large number of small fragments of B, and the reaction spreads out from those points where it first commenced.

Following the curve of (a) the autocatalytic nature of the reation is explained in terms of rapid growth of nuclei which are formed at certain localised spots, provided that the activation energy of nucleus growth is less than that for formation of nuclei. This has been verified in the case of barium azide (14) by Wischin and for various hydrates by Garner and his co-workers.

However if the activation energy for nucleus growth is of the same order as the activation energy for nucleus formation, then a large number of small nuclei are formed (curve (b)). The accelerator period is reduced and may virtually be removed by crushing or grinding (curve (c)). Curve (d) is simply a combination of (a) and (c) and represents two phases of the reaction, one of which is initiated extremely rapidly.

(ii) The Laws of Nucleus Growth.

A general relationship governing the growth of nuclei may now be derived.

Let r = a size parameter

i.e. for one dimension, r = the length of the nucleus.

" two " , r = the radius of a circular nucleus or side of a square nucleus

" three " , r = mean radius

Let G(x) = a growth function.

Then the size of the nucleus which started growing at t = y is determined by the parameter

$$r(t,y) = \int_y^t G(x)\,dx \qquad \text{(1.14)}$$

-8-/.....

Thus the volume of the nucleus is given by

$$v(t,y) = \sigma \left[r(t,y) \right]^{\lambda} \qquad (1.15)$$

where σ = a shape factor $\left\{ = \frac{4\pi}{3} \text{ for a spherical nucleus} \right\}$

λ = 1, 2 or 3, depending on the number of dimensions of the nucleus.

The total volume of all nuclei at time t is therefore

$$V(t) = \int_{o}^{t} v(t,y) \left[\frac{dN}{dt} \right]_{t=y} dy \qquad (1.16)$$

and substituting for (1.14) and (1.15) we get

$$V(t) = \int_{o}^{t} \sigma \left[\int_{y}^{t} G(x)dx \right]^{\lambda} \left[\frac{dN}{dt} \right]_{t=y} dy \qquad (1.17)$$

If the appropriate forms of the functions describing the rate of nucleus formation and the rate of growth are known, it is possible to calculate V(t) and hence the degree of decomposition. For example, if a constant growth rate and power law nucleation are assumed, it is found that

$$\alpha = C^{1} t^{n} \qquad (1.18)$$

where C^{1} = a constant

$$n = B + \lambda$$

and since $\alpha = \frac{P}{P_f}$

where p = pressure of evolved gas at time t

p_f = final gas pressure

equation (1.18) can be written in the form

$$p = Ct^{n} \qquad (1.19)$$

This relationship is found to hold for barium azide (14), (8), where n = 6-8; for calcium azide (25), silver oxide (26) and aged mercury fulminate (27), where n = 3, and for small crystals of barium styphnate monohydrate (25), where n = 2.

However experiment revealed certain discrepancies. For example, in the case of barium azide n was found to vary between 6.8 and 8.2 at varying temperatures of decomposition, instead of giving the theoretical value of 6. This anomaly could be explained by postulating abnormally slow initial growth.

-9-/.....

Subsequently it was shown by Thomas and Tompkins (8) that equation (1.19) could be modified to give

$$p = C(t - \gamma)^n \qquad (1.20)$$

where γ is the period of slow growth.

The above theory cannot be applied to certain substances notably silver oxalate (19) and mercury fulminate (23). Garner and Hailes were led therefore to the concept of linear branching chains, where the rate of nucleation is relatively unimportant and is effectively constant. They further postulated a constant branching coefficient k_3. Hence the net rate of production of nuclei becomes

$$\frac{dN}{dt} = k_1N + k_3N \qquad (1.21)$$

from which it can be shown that

$$p = c.e^{k_3t} \qquad (1.22)$$

i.e. the decomposition follows an exponential law.

Further work has shown that the concept of linear branching chains requires some modification since the chains would tend to separate the crystal into mosaic blocks which would decompose slowly. By postulating branching plate-like nuclei, this objection is overcome without any departure from the general exponential relationship.

The concepts outlined above take no account of the possibility of chains interfering during growth. Taking this factor into consideration Prout and Tompkins (1) put forward a chain theory applicable to permanganates. As this theory is of particular interest to this work, its derivation will be given in full.

Let k_4 = probability of termination of nuclei

Then $$\frac{dN}{dt} = k_1N_o + (k_3 - k_4)N \qquad (1.23)$$

Soon after the reaction has commenced the second term in (1.23) predominates and so

$$\frac{dN}{dt} = (k_3 - k_4)N \qquad (1.24)$$

Further, it may be supposed that

-10-/.....

$$\frac{d\alpha}{dt} = k^1 N \qquad \text{(1.25)}$$

where k^1 is another constant.

In the case of $KMnO_4$ which has a symmetrical p-t curve, we can apply certain boundary conditions to permit of integration, since at the point of inflexion $\alpha_i = \frac{1}{2}$.

Thus:

at $t = o$, $\alpha = o$, $k_4 = o$

at $t = t_i$, $\alpha_i = \frac{1}{2}$, $\frac{d\alpha}{dt}$ is a maximum

and $k_3 = k_4$ since $\frac{dN}{dt}$ changes sign.

The boundary condition is therefore

$$k_4 = k_3 \frac{\alpha}{\alpha_i} \qquad \text{(1.26)}$$

Hence (1.24) becomes

$$\frac{dN}{dt} = k_3 \left[1 - \frac{\alpha}{\alpha_i}\right] N \qquad \text{(1.27)}$$

and (1.25) becomes

$$\frac{dN}{d\alpha} = k \left[1 - \frac{\alpha}{\alpha_i}\right] \qquad \text{(1.28)}$$

where $k = \frac{k_3}{k^1}$

On integration (1.28) yields

$$N = k\left[\alpha - \frac{\alpha^2}{2\alpha_i}\right] \qquad \text{(1.29)}$$

and using (1.25) we get

$$\frac{d\alpha}{dt} = k_3 \alpha (1 - \alpha) \qquad \text{(1.30)}$$

Integration of (1.30) then yields

$$\log \frac{\alpha}{1-\alpha} = k_3 t + C \qquad \text{(1.31)}$$

or

$$\log \frac{p}{p_f - p} = k_3 t + C \qquad \text{(1.32)}$$

This is known as the 'Prout-Tompkins equation' and has been found valid for substances other than permanganates, notably nickel formate (29) ammonium perchlorate (30) and lead oxalate (31).

Prout and Tompkins (32) used a modified form of the above equation to explain the decomposition curve of silver permanganate. The details of this will be considered later.

-11-/.....

1.3 PHYSICAL MECHANISMS OF NUCLEATION.

It is noticeable in the theoretical work so far discussed that the full explanation of favoured points of decomposition and the exact reasons for decomposition at these points are not available.

The study of the thermal decomposition and photolysis of azides and halides however, has yielded information which has shed considerable light on the actual physical processes involved in the formation (and growth) of nuclei. Ideas developed in these studies when taken in conjunction with the modern knowledge of the crystal disorganisation resulting from bombardment of solids with high energy photons or particles, are of considerable value in the elucidation of the mechanisms of thermal decompositions. For this reason the relevant work on the halides and azides will be outlined below. However, a clear understanding of these processes is impossible without some prior knowledge of imperfections in crystals and their influence on the solid state. Thus a short survey of the nature of imperfections in crystals will first be given.

The lattice theory of crystal structure first originated in the thinking of Huygens and Hooke in the 17th and of Haüy in the 18th century. Though many of the ideas associated with the concept of a perfect crystal lattice are still used, the inadequacy of this theory has been clearly demonstrated. Subsequent work has shown that the crystal lattice is far from perfect and contains a number of imperfections, the more important of which are discussed below.

(i) Dislocations.

The low observed values of the critical shear stress can be explained in terms of motion through a crystal of an imperfection known as a dislocation of which there are two main types.

The edge dislocation may be thought of as caused by the insertion of an extra partial plane of atoms in the crystal. Near the dislocation line marking the termination of the extra plane the crystal is highly strained. The simple edge dislocation extends indefinitely in the slip plane in a direction normal to the slip direction. The

-12-/.....

second type of dislocation is the screw dislocation where the slip is parallel to the dislocation line. Various arrays of dislocations are said to form grain boundaries (33).

The number of dislocations varies from 10^6 to $10^{12}/cm^2$, but for artificially prepared inorganic crystals is of the order of $10^9/cm^2$. Their strain energy is about 1 ev. per atomic plane, being about the same as the energy of an interatomic bond. It has further been shown by Frank (34) that these dislocations may be a controlling factor in crystal growth. One must therefore accept that crystal faces are always heterogeneous and that steps in the crystal face should have different properties (e.g. catalytic) from those of the open lands between the steps.

It is theoretically likely that dislocation lines provide routes along which diffusion occurs more rapidly. The main reasons for this are the enhanced concentration of atoms there; the negative pressure on one side of a dislocation having an edge component; and the fact that atomic rearrangements may occur more frequently owing to the disordered nature of a dislocation.

Dislocation lines provide regions where foreign atoms will congregate in enhanced concentration (35) and should provide preferential sites for nucleation. They can also act as shallow traps for electrons and positive holes and can provide a source of vacancies which are able to 'evaporate' (36).

(ii) Frenkel, Schottky and Impurity Defects.

Unlike dislocations, these defects through scattered arbitrarily throughout the crystal, have associated regions of disturbance usually localised about individual lattice points.

A Frenkel defect exists where a cation (or anion) is displaced to a distant interstitial position leaving behind a 'vacancy'. Frenkel defects are usually favoured when the crystal is such that there is a considerable disparity of ionic size, the crystal has a high van der Waals energy and the dielectric constant is large. Silver bromide is a good example and is found to have $\sim 10^{14}$ defects/cm^3 at 300° K and $\sim 10^{-7}/cm^3$ at 100°K (36).

-13-/.....

Schottky defects consist of equal numbers of anion and cation vacancies within the crystal, the removed ions being located on the surfaces of the crystal. Schottky defects are favoured in crystals where the ionic sizes are not greatly different and for which the van der Waals energy and dielectric constant are not too high. In the main the alkali halides meet these requirements. The vacancies tend to form pairs of positive and negative ion vacancies or even clusters of about 5000 Å in size (37). Often they 'condense' on dislocations resulting in a change of pattern of these dislocations. Schottky defects are associated with an increase of volume of the crystal.

Impurities tend to accumulate at dislocations but may be found elsewhere too. They influence the colours of solids under ionising radiations, directly by providing new traps for electrons and holes, and indirectly by altering the concentration of trapping defects in the solid due to mismatch in size, polarisation properties and electrostatic charge (38). They can also act as sensitisers for speeding up chemical reactions (13).

(iii) Colour Centres.

The experimental work of Pohl (39) and of Estomann, Leivo and Stern (40) who studied the absorption bands in the alkali halides when irradiated by x-rays, has established the existence of a defect known as an F-centre. This consists of an anion vacancy which has trapped an electron. The energy of its formation is about 2.5 ev. for the alkali halides. F-centres may aggregate to form pairs or clusters which have a lower associated energy. Centres of this type are R_1 - and R_2 - centres which are anion vacancy pairs containing one and two trapped electrons respectively, and the M-centre which is a complex of two anion vacancies and a cation vacancy, which has one trapped electron. Another centre is the F^1 - centre which is simply an F-centre which has trapped a second electron.

Furthermore, there may exist V-centres of various kinds, which are simply antimorphs of the above i.e. they are cationic

-14-/.....

vacancies with trapped positive holes.

(iv) Excitons.

When photons interact with solids they may excite anions so that they eject an electron into the conduction band leaving behind a 'positive hole'. Alternatively the electron may be raised to an 'exciton level' below the conduction band. In this case the electron is still in a bound state. The 'exciton' so formed can travel through the crystal giving up its energy of formation on recombination. It is electrically neutral and does not contribute directly to the conductivity of the crystal.

An exciton may get trapped at certain points such as vacancies, dislocation or impurities before it has lost all its kinetic energy. An exciton thus trapped has a certain average lifetime before it returns to the ground state. If, before this happens, another exciton is trapped at the same trap, the two may react with one another.

The above resumé provides the essential background to the processes of nucleation which will now be discussed.

The photolysis of silver bromide because of its importance in photographic processes has been extensively studied and the early work of Gurney and Mott (20) is of particular significance since their theory is still the basis of the modern viewpoint (41). This theory is now presented.

A light quantum near 4500 A is absorbed forming a free electron and a positive hole. The electron is mobile and gets trapped on the surface, while the hole produces neutral Br absorbed on the surface elsewhere. An interstitial silver ion from a Frenkel defect migrates to the trapped electron forming a silver atom. When a second photon is absorbed the hole produced forms a second Br atom and Br_2 escapes from the surface. The electron joins the silver atom to form an Ag^- ion which attracts another interstitial silver ion to form Ag_2. This process can be repeated and the silver speck grows in size. The first trapped

-15-/.....

electron thus represents the start of a nucleus at which the product of decomposition forms.

Mitchell (42) extended the work of Mott and Gurney by examining the effects of impurities on the nucleation of AgBr. Previously Sheppard (43), (44), had shown that sulphur from the gelatin emulsion might be instrumental in forming on the surface of the halide grain so-called 'sensitivity specks' which act as nuclei on which silver forms during photolytic action. It was suggested that the sensitivity specks were minute crystals of silver sulphide.

Mitchell on the other hand suggests that silver halides dissolve silver sulphide which goes into solution as an S^{--} ion and an F-centre. Plate-like aggregates are formed which, if big enough, break away from the halide matrix to form colloidal silver. These aggregates form the 'sensitivity specks' of Sheppard's theory. Under illumination electrons leave the F-centres and are transferred to the aggregates which then increase in size by a process of ionic migration.

The process of migration may be of two types: (a) a transport of cations as described above (Gurney and Mott). This will set up internal strains in forming the specks and is usually possible only on the surface where the silver can be pushed out, or (b) the motion towards the centre of vacant anion sites which may result from the removal of electrons from F-centres or which may be present initially as Frenkel defects.

The second alternative is not very clear but is presumably intended to mean that F-centre aggregates containing extra electrons can trap vacancies before they trap silver ions, thus building themselves up. They then trap silver ions which take up the volume of the vacancies and so do not set up internal strains.

The concepts developed in the study of the halides were transferred to the field of thermal decomposition, with and without preirradiation. Mott (45) was the first to do this in his work on the decomposition of metallic azides.

-16-/.....

Previous work by Garner and Maggs (9) had shown that the threshold for absorption of ultra-violet light by N_3^- ions in barium azide was 2600-2700 A. Pre-illumination with U-V shortened the induction period and prolonged irradiation with light of wavelength shorter than 2360 A produced metallic nuclei at room temperature. Furthermore, Wischin (14) had shown that the number of nuclei formed when the salt was heated for a time t was given by

$$N = At^3 \qquad (1.33)$$

The rate of growth of the nucleus was constant and given by

$$\frac{dr}{dt} = B \qquad (1.34)$$

The pressure of nitrogen after a time t was observed to be

$$p = Ct^x \quad (x = 6\text{-}8) \qquad (1.35)$$

The activation energies for nucleus formation, nucleus growth and development of pressure were found to be 74, 23.5 and 166 Kcals/mole respectively.

Mott showed that equation (1.35) followed from (1.33) and (1.34) by substituting them in (1.17). He further supposed that since pre-irradiation only had the effect of increasing the constants A and C, the subsequent thermal decomposition followed the same laws of nucleus formation and growth as before. It was also known that when ZnO is heated in a vacuum, oxygen is evolved and zinc atoms go into solid solution where they dissociate into interstitial zinc ions and mobile electrons. Mott therefore, assumed that a similar state of affairs existed in barium azide and came to the conclusion that the mechanisms of nucleation were similar to those occurring in silver halides.

When barium azide is heated, nitrogen is driven off from the surface, barium atoms are formed which go into solution and dissociate, thus increasing the number of interstitial barium ions there already (assuming barium azide is a cationic conductor). At first during the induction period, nitrogen is driven off slowly, being later catalysed by the presence of nuclei which are subsequently formed.

-17-/.....

During the slow emission, n, the number of electrons/unit volume increases linearly with time. Thus there are a large number of interstitial ions plus a few electrons, a state of affairs similar to that found in the halide grain. It is probable that there exist on the surface a number of electron traps which are similar to the 'sensitivity specks' found in photographic emulsions. These traps may be anion vacancies.

When an electron becomes trapped, a cation is attracted but the nucleus so formed is unstable and after a certain time the electron will escape unless a second electron gets trapped first. The probability that an electron will be trapped is proportional to n; that of a second electron being trapped is also proportional to n. Thus if σ electrons are required to form a stable nucleus the probability of nucleus formation is proportion to n^{σ} .

$$\therefore \frac{dN}{dt} = n^{\sigma} \cdot \text{constant} \qquad \text{(1.36)}$$

but $n = t \cdot \text{constant}$

$$\therefore \frac{dN}{dt} = t^{\sigma} \cdot \text{constant} \qquad \text{(1.37)}$$

$$\text{or } N = t^{\sigma + 1} \cdot \text{constant} \qquad \text{(1.38)}$$

Comparing (1.38) with (1.33) we see that $\sigma = 2$. It follows that a nucleus with two electrons and one interstitial barium ion is stable or can catalyse the thermal decomposition.

Once the nucleus is formed it can grow as follows. Every now and then an adjacent azide ion receives enough thermal energy to lose an electron to the metal. The positive hole so formed diffuses away to the surface by a process of electron exchange and N_2 is given off. This may be a slow process further accounting for the induction period. The $(Ba_2)^{-}$ ion will grow by attracting another interstitial barium ion and so the process may continue.

Since there is no escape of metallic atoms and no azide ions are removed from the interior of the crystal, a nucleus must be formed on the surface or at internal cracks, otherwise the crystal would split due to the strains produced. This was confirmed experimentally by Wischin (14) who found nuclei growing outwards

-18-/.....

from the surface.

Further information on the effects of pre-irradiation with ultra-violet light led Thomas and Tompkins (8) to believe that the mechanism of nucleation in azides was due to 'exciton' formation. They discounted Motts' theory, for barium azide had been found not to show photoconductance. Hence the production of free electrons was unlikely. Furthermore, barium azide is a poor conductor, its conductance being mainly due to anion migration. A very thorough analysis (46) of the rate of growth of nuclei in barium azide had shown that this was far too high to be accounted for by any mechanism involving the transport of both cations and electrons.

Bagdassarian's mechanism (47) of nucleus formation as a series of decompositions, (see Section 1.2(i)b) in this case three, seemed equally improbable. This is so because the activation energy for nucleus formation is 74 Kcals/mole and that for growth is 29 Kcals/mole. It was pointed out by Thomas and Tompkins that the activation energy of each of the three consecutive nucleus-forming processes must be greater than that of growth, and it was not possible to have three such processes having an overall activation energy as low as 74 Kcals/mole.

Mitchell's theory involved the aggregation of F-centres present initially. These would be present in barium azide because of the presence of impurity $CO_3^{=}$ ions. The mobility of the F-centres would then be approximately

$$\text{const. } c\ e^{-E/RT}$$

where c = concentration of anion vacancies

E = activation energy for their mobility

The rate of formation of double F-centres would therefore be

$$\text{const. } c\ e^{-E/RT}\ C^2$$

where C = concentration of single F-centres at t = o.

The number of double centres formed after a time t is

$$\text{const. } c\ e^{-E/RT}\ C^2 t$$

-20-/.....

To obtain experimental dependence of N upon t i.e. N = const. t^3, the nucleus must be a four centre complex and the number present at time ti is approximately

const. $c^3 e^{-3E/RT} c^4 t^3$

Thomas and Tompkin's results on the pre-irradiation with U-V of intensity I for a time τ show c^3c^4 = const. $I\tau$, hence either (i) F-centres are produced at a rate proportional to $(I\tau)^{\frac{1}{4}}$, or (ii) vacancies at a rate proportional to $(I\tau)^{\frac{1}{3}}$. Both conclusions they considered improbable and so proposed the following mechanism.

Two adjacent azide ions are excited thermally and decompose to give nitrogen. For the activation energy of nucleus formation (74 Kcals) not to be exceeded it is necessary that each azide ion be excited separately such that the first excitation is rate determining. They therefore postulate that the electron is ejected into the conduction band being eventually trapped at an impurity centre. Meanwhile the mobile positive hole also gets trapped at some surface defect. If now an adjacent azide ion is thermally excited to give an exciton, this reacts with the hole and nitrogen is evolved.

An alternative viewpoint is that a positive hole reacts with an adjacent azide ion whenever sufficient activation energy is available - this energy must necessarily be less than that required to produce a positive hole. The complex remaining (F-centre + anion vacancy) later dissociates. The F-centres now aggregate as in Mitchell's theory to form double F-centres or nuclei. The rate of formation of nuclei is then given by

$$\frac{dN}{dt} = (te^{-E_1/RT})^2 . ce^{-E/RT} \qquad (1.39)$$

where E_1 = energy to eject an electron from the azide full band to the conduction band (~ 31 Kcals).

E = activation energy for mobility of anion vacancies (~ 11 Kcals).

c = concentration of vacancies.

Equation (1.39) is in agreement with the experimental fact N = const. t^3 and is consistent with the effects of photolysis, pre-irradiation

-21-/.....

and ageing of the salt.

The mechanism of nucleus growth is considered to be a reaction in which nitrogen is produced at the salt-metal interface, followed by its outward diffusion through the crystal. The metal nuclei facilitate the formation of an adjacent hole from an azide ion since the energy required to raise an electron to the metal is less than that required to raise it to the conduction band. When another adjacent azide ion in the interface receives sufficient thermal energy an exciton is formed which reacts with the positive hole to form nitrogen. The electron returns to the ground state forming an F-centre complex bound to the nucleus.

The activation energy for reaction between a hole and an exciton is $\sim$ 0.5 Kcals. The rate determining process is therefore the electron transfer to the metal which is associated with an energy difference of 29 Kcals - the same as the activation energy for nucleus growth. As the double F-centre is more stable than a single F-centre because the electrons move in a larger volume, the size of the aggregate can increase by decomposition and by trapping conduction electrons and subsequently anion vacancies.

The effect of incorporating an impurity into the azide lattice was investigated by Gray and Waddington (13) in their study of the thermal decomposition of silver and thallous azides. The kinetics of the reaction of the pure salts were found to fit the equation

$$\frac{d(N_2)}{dt} = k(AgN_3)^{\frac{2}{3}} \qquad (1.40)$$

which transforms to

$$1 - \left[1 - \frac{p}{p_f}\right]^{\frac{1}{3}} = k_f^{-\frac{1}{3}} t \qquad (1.41)$$

The kinetics and activation energies were unchanged by incorporating impurities but the rate constant k was found to increase.

The behaviour of silver and thallous azides differs markedly from that of the alkali and alkaline earth azides. These differences are summarised below.

-22-/.....

	Azides of silver and thallium.	Alkali and alkaline earth azides.
1.	The decomposition has no induction period	Curves of sigmoid shape have induction periods.
2.	The decomposition has been sensitised by divalent anions.	The decomposition has <u>not</u> been sensitised in this way.
3.	Ionic conductivities are high - mainly due to cation migration.	Ionic conductivities are low - mainly due to anionic migration.
4.	Show photoconductance.	Show no photoconductance.
5.	Nuclei are very small and do not grow.	At least in the case of BaN_3 nuclei are discrete, 3-dimensional and grow in size.

Gray and Waddington attribute these differences to the stability of the exciton formed in each case. For example, the energy difference between the exciton level and the conduction band in AgN_3 is 1.8 Kcals mole^{-1} whereas in KN_3 it is 13.7 Kcals mole^{-1}. Thus the silver salt excitons will dissociate thermally into electrons and positive holes.

They therefore proposed the following mechanism for decomposition. Using the notation

N_3^- : a normal azide ion

e : an electron

h^+ : a positive hole

T : a trap

$\square$: a vacancy

they set out the following equations:

$$N_3^- \xrightarrow{k_1} h^+ + e \qquad \text{I}$$

$$2h^+ \xrightarrow{k_2} 2\square + 3N_2 \qquad \text{II}$$

$$h^+ + e \xrightarrow{k_3} N_3^- \qquad \text{III}$$

$$T + e \xrightarrow{k_4} Ag \text{ (finally)} \qquad \text{IV}$$

The electron traps are of the type invoked by Seitz (36). They are incipient anion vacancies with effective charge $\frac{e}{2}$ which

-23-/.....

occur at slip planes and dislocations. After the capture of an electron the traps may be reset by the migration of an interstitial cation to them. The traps are produced when the crystal is formed and are not generated optically or thermally. In the course of the reaction, T may therefore be assumed constant.

The electrons and holes formed will be mobile and may be treated by conventional means so that the rate of evolution of nitrogen is given by

$$\frac{d(N_2)}{dt} = k_2 (h^+)^2 \qquad \text{(1.42)}$$

Furthermore, since electrons and holes are unstable intermediates, stationary state assumptions may be applied to them which results in two limiting cases being distinguishable (i) Reaction II predominates over III. This leads to the first order reaction

$$\frac{d(N_2)}{dt} = k_2 (h^+)^2 = k_1 (N_3^-) \qquad \text{(1.43)}$$

(ii) Reaction III predominates over II in which case

$$\frac{d(N_2)}{dt} = k_2 (h^+)^2$$

$$= (k_1^2 . k_2 . k_4^2 . k_3^{-2} . T^2)^{\frac{1}{3}} \; (N_3^-)^{\frac{2}{3}} \qquad \text{(1.44)}$$

and this agrees with the experimental result (c.f. equation (1.40).)

If E_1, E_2, E_3 and E_4 are the activation energies for the appropriate individual steps, then the composite activation energy is given by

$$E = \frac{2}{3}E_1 + \frac{1}{3}E_2 - \frac{2}{3}E_3 + \frac{2}{3}E_4 \qquad \text{(1.45)}$$

To a good approximation E_2, E_3 and E_4 are small so that $E = \frac{2}{3} E_1$. Gray and Waddington give a theoretical calculation of E_1 and the value of E derived from this is in good agreement with the experimental value. This they take as confirmation of the above mechanism.

Further evidence in support of this mechanism is the absence of an induction period and the absence of pre-irradiation effects. This shows that the rate determining step is not taking place at the nuclei where the process is the accretion of silver by the migration of silver ions. These nuclei are groups of electron

-24-/.....

traps that are continually trapping electrons and being reset. Sawkill's observation (18) that these nuclei do not grow but only increase in density supports this. The rate determining step is therefore the homogeneous generation of free electrons and holes.

When cyanamide ions are incorporated they are presumed to produce additional electron traps and so affect the $T^{\frac{2}{3}}$ term in (1.44). They are situated on azide ion sites as CN_2^{2-} and for electrical neutrality there are presumably additional interstitial silver ions or additional anion vacancies which can act as electron traps. The additional interstitials would speed up the resetting of traps.

In the case of barium azide, the decomposition depends on exciton formation and because of this, an increase in the number of free electron traps would not increase the rate. This is borne out by the fact that its decomposition has not been sensitised by the incorporation of divalent anions.

1.4 EFFECTS OF PRE-IRRADIATION ON THERMAL DECOMPOSITIONS.

As has been indicated, the results of thermal decomposition alone could not adequately explain the physical mechanisms of nucleation. Thus the effects of pre-irradiation with U-V became an important and integral part of the work done on azides in particular, which culminated in the exciton theory of Thomas and Tompkins.

When barium azide is decomposed the pressure of gas developed is given by

$$p = C.(t-y)^x \qquad (1.46)$$

where y is a slow growth correction.

Pre-irradiation with U-V shortens the induction period and increases the value of C to C_τ which was found to be proportional to the exposure $I\tau$ for small exposures. Thus during irradiation an electron is ejected from an azide ion and is trapped at a deep impurity centre. The mobile hole is trapped at a cation vacancy where it can react with an activated adjacent azide ion to give

-25-/.....

nitrogen forming an anion vacancy and an F-centre. The F-centre is destroyed during the warming up period preceeding thermal decomposition by its electron tunnelling to other mobile holes present at the surface, giving an azide ion and a further anion vacancy. The acceleration of the thermal rate is due to the anion vacancies rendering mobile the F-centres created thermally, thereby allowing them to aggregate to form nuclei. As the number of impurity centres is limited, for larger energies of pre-irradiation the anion vacancies compete for the ejected electrons and F-centres are formed. These with existing vacancies are rendered mobile. There are two consequences:

(i) C increases more rapidly than linearly with the energy of the pre-irradiation.

(ii) The slope of the log p/log (t-y) plot decreases finally to 3 since the thermal process comprises predominately the growth of nuclei created during irradiation.

Garner and Moon (48) and Maggs (49) had previously shown that pre-bombardment with electrons produced similar effects on the induction period and rate of decomposition of barium azide. Groocock and Tompkins (10) made more detailed studies of these effects on barium and sodium azides. They came to the following conclusions.

In pre-bombardment, the slope of the log p/log (t-y) plots remained equal to 6 indicating that no nuclei were created during the pre-treatment. The initial act of the primary beam is to eject electrons from the azide ions and here there is sufficient energy for photo-emission. Because in pre-bombardment there is always a large excess of electrons, surface anion vacancies are converted to F-centres, but these are largely immobile since their mobility depends on the simultaneous presence of anion vacancies. Consequently nucleus formation during bombardment is improbable. During warming up regeneration of azide ions and vacancies from holes and F-centres occurs. These vacancies (greater in number after pre-bombardment) assist nucleus formation in the thermal process which is accelerated. The increased number of vacancies depending on i^2 (i is the beam current) suggests that this is a

-26-/..

bi-molecular process, which they show to be a combination of a pair of positive holes.

Prout and Tompkins (50) studied the effects of electron bombardment and U-V irradiation on the subsequent thermal decomposition of mercuric oxalate. They found higher initial rates of decomposition suggesting a surface effect which was found to reach a saturation value. The changes produced by pre-treatment were found to be stable at room temperature and there was no evolution of gas during the pre-treatment. Prout and Tompkins conclude that pre-treatment affects the individual molecules and that the effect penetrates at least two or three molecular layers. The primary act of pre-treatment is to free an electron from a surface oxalate group and this electron is subsequently trapped by an Hg 'ion' in the second layer. The process thus corresponds to an electron transference, which when followed by an intramolecular change, can result in the production of 'mercurous oxalate' and this occurs without the evolution of gas.

In recent years much attention has been given to the effects of other types of radiation on the thermal decomposition of various solids.

Bowden and Singh (11) irradiated several inorganic azides with neutrons, electrons and γ-rays. Decreased induction periods and increased maximum rates of reaction resulted when these substances were subsequently decomposed. Groocock (51) observed similar effects in the case of α-lead azide irradiated with X-rays and the same is true of barium azide (52). In the case of the latter, however, it was found that after an initial increase of the maximum rate of decomposition with increased irradiation dose, the rate later decreased as the dose was increased still further.

Flanagan (53) has recently investigated the effects of nuclear radiations on the thermal decomposition of lead styphnate monohydrate. Gamma rays from Co^{60} had no apparent effect but neutrons greatly accelerated subsequent thermal decomposition. He suggests that the irradiated material decomposes from a large number of evenly distributed sites formed by fast particle damage in the crystal. The un-

-27-/..

irradiated decomposition is considered to proceed at a smaller number of more localised regions such as cracks, grain boundaries and other imperfections.

Prout (12) has presented a new approach to the study of thermal decompositions. As a result of studies of the effects of protons, neutrons and γ-rays on potassium permanganate he presents a theory involving the annealing of point defects. As it is considered that a similar mechanism is operative in the case of irradiated silver permanganate a detailed consideration of the theory will be reserved till later. However, as this will involve a thorough knowledge of radiation effects in crystalline solids generally a survey of current ideas in this field is presented in the next chapter.

The foregoing account may be summarised as consisting of two main points. Firstly, there is the earlier method of approach to the problem of thermal decomposition. This was the rather arbitrary use of mathematical expressions which fitted the experimental decomposition curves. This method has a serious drawback in that it provides little information on the physical processes involved in the decomposition.

Secondly, there is the more satisfactory approach in which modern views on crystal imperfections are applied to solid state reactions by the use of complementary techniques such as pre-irradiation or pre-bombardment or by the incorporation of impurities. These applications have been dealt with in some considerable detail, but this was considered necessary in order to show clearly the various ways in which the concepts associated with the generation and movement of interstitials, vacancies, etc. have been used in this fresh approach to thermal decomposition, an approach which is of particular significance in the research work to be described.

2. RADIATION DAMAGE IN CRYSTALLINE SOLIDS.

An energetic particle traversing a crystalline solid may lose energy in two ways: by elastic collisions with the lattice atoms thus creating Frenkels, or by excitation and ionisation of atoms through charge interactions. In order to displace an atom from its equilibrium position to an interstitial position some minimum energy (E_d) is required. Seitz and Koehler (51) estimate this to be about 25 ev for most materials. This value has generally become accepted as it is in reasonable agreement with experimental results (52, 53, 54, 55).

The types of radiation used in the following experiments were thermal neutron radiation and γ- radiation from ^{60}Co. However, as will be shown subsequently, γ- rays are similar to fast electrons in the damage they produce, and so all three types of radiation will be considered.

2.1 NEUTRONS.

The energies of neutrons vary considerably. Discussion will be limited to fast neutrons ($\sim$ 2 Mev) and 'thermal' neutrons ($\sim$ 0.025 ev). Neutrons produce damage in two ways: directly, by knocking atoms out of place, and indirectly by producing changes in atomic nuclei which then cause radiation damage. Being uncharged, most neutrons pass right through matter without any changes occurring. Occasionally, however, one collides with a nucleus, but the cross-sections (σ_n) for such encounters are only of the order of a few barns. For a material with a cross-section of one barn only about one neutron in 10^9 would strike the nucleus of the atom through which they pass. When a neutron "collides" with a nucleus it may be scattered or captured.

Damage as a result of scattering can only occur in the case of fast neutrons since only they are capable of giving sufficient recoil energy to the affected nucleus. It can be shown (56) that the maximum energy (E_{max}) imparted to the atom is given by

$$E'_{max} = \frac{4 M_1 M_2}{(M_1 + M_2)^2} E \qquad \text{(2.1)}$$

where M_1 = mass of the neutron

M_2 = mass of the struck atom

E = energy of the neutron.

The average energy transferred is $\frac{1}{2} E_{max}$. This may be far in excess of E_d (e.g. 0.12 Mev for Cu) so that the primary knock-on becomes a fast moving ion which ploughs a track through the material.

These charged ions will interact electrically with extra nuclear electrons and nuclei they meet on their way. The cross-section for electrostatic collisions is large and they are brought quickly to rest. The energy transferred (ΔE) to a stationary particle is then given by (56)

$$\Delta E = \frac{M_1 Z_1^2 Z_2^2 e^4}{M_2 b^2 E} \qquad \text{(2.2)}$$

where M_1 = mass of moving particle.

$Z_1 e$ = charge of moving particle.

M_2 = mass of atationary particle.

$Z_2 e$ = charge of stationary particle.

b = distance of closest approach.

provided that $\Delta E < E_{max}$. Since M_2 is much smaller for an electron than a nucleus, electrons absorb about a thousand times more energy than do the nuclei (provided that the ion is moving faster than the electrons.) There is a cut-off energy (L_c) below which the ion moves too slowly to lose much energy to the electrons. For insulating materials this is given by (57)

$$L_c \approx \frac{M}{m} \frac{I_t}{8} \qquad \text{(2.3)}$$

where M = mass of the ion.

m = mass of the electron.

I_t = lowest excitation potential of the atom.

In general, for heavy elements ($Z_2 > 50$), $E_{max} < L_c$ and there is practically no ionisation.

When the moving ion collides with nuclei, collisions may be of

-29-/.....

two types; a Rutherford type for ions of high energy or an elastic collision of the hard-sphere type for ions of lower energies. In the case of heavy elements the latter type of collision occurs. In either case the energy of the ion is sufficient to create secondary knock-ons which in turn can displace other atoms. A 'cascade' of displaced atoms thus results until no atom has sufficient energy to displace another and the damage thus becomes densely grouped near the end of the ion track. In cases where $E_{max} < L_c$, Snyder and Neufeld (58) have shown that the total number (n) of displaced atoms (i.e. vacancy-interstitial pairs) per fast neutron collision is given by

$$n \simeq \frac{E_{max}}{4\,E_d} \qquad (2.4)$$

An alternative model for the distribution of displaced atoms is due to Seitz (59) and to Brooks (60). Since only about 5 % ev of the energy of the primary knock-on can be stored in lattice defects the remainder must be released to the vibrational system of the lattice in the form of phonons. Localised heating results and the region is heated to a high temperature for the short period of time ($\sim 10^{-11}$ secs.) that is necessary for the thermal pulse to disperse. In this region or 'thermal spike' the temperature rise is not considered sufficient to allow general recombination of vacancies and interstitials. Brinkman (61), however, has suggested that near the end of the ion path the region melts and freezes rapidly, forming a 'displacement spike'. During this process the point defects are largely eliminated and the region freezes back on to the surrounding lattice, and contains only a few quenched-in vacancies and interstitials, and perhaps a dislocation loop.

The capture of neutrons by atomic nuclei is complicated and the cross-section for capture varies considerably. For neutrons with energies greater than 0.1 Mev it is small but below 10 ev the cross-section increases with decreasing neutron energy so that for 'thermal' neutrons (0.025 ev) capture is the predominant process. The new nucleus formed is often unstable and transmutation may occur.

-30-/.....

Two main possible results of capture are thus the introduction of an impurity and the emission of γ- rays of capture and decay. The capture γ-ray released in the reaction may give sufficient recoil energy to the atom to displace it from its normal lattice position into an interstitial position (62).

2.2 ELECTRONS.

Electrons of sufficient energy to produce displacement are in the relativistic range. Even for electron energies considerably in excess of E_d, the cross-sections for displacement are about a hundred times smaller than for a charged nucleon. Furthermore, since the collisions are heavily biased toward small energy transfer, the knocked-on atoms seldom have sufficient energy to produce secondaries. Consequently, electrons tend to produce a simpler type of damage, namely isolated pairs of vacancies and interstitials. On the other hand the range of electrons is fairly short and their capacity for producing damage varies appreciably through the depth of the sample. Threshold energies for displacement of atoms by electrons have been measured. In the case of germanium (52) the threshold value was found to be 0.63 Mev.

2.3 γ - RAYS.

Recently Dugdale (63) has pointed out that γ- rays may have sufficient energy so that some of the Compton and photoelectrons generated by them exceed the threshold for displacement. He showed that disordering could be produced in Cu_3Au by means of γ- rays from ^{60}Co. Cleland et al (64) have also used γ -rays to produce displacements in Ge. They point out that disordering of solids by γ -rays is essentially the same as by electron bombardment except that (i) the energies of the Compton electrons will vary with the angle of scattering, and (ii) there will be uniform damage throughout the specimen as the absorption of γ -rays is small enough to ensure this. Gamma radiation therefore produces the simplest type of damage. The energies of the electrons are close enough to threshold so that only isolated vacancy-interstitial pairs are produced

-31-/.....

and these are distributed uniformly throughout the specimen. Kinchin and Pease (57) state that for light elements ($Z_2 < 50$) the predominant interaction is the Compton effect while for heavy elements there may be direct displacement of atoms by recoil from the photoelectric effect.

Two other mechanisms have been suggested for the production of defects as a result of γ-radiation. Seitz (65) suggests the following process to account for the production of colour-centres in KBr when irradiated with X-rays. The X-rays produce photoelectrons which dissipate their energy in the formation of electrons, holes and excitons. Initially electrons and holes are trapped at positive and negative incipient vacancies (jogs at Taylor-Orowan dislocations) where they may annihilate one another if sufficiently close together. Excitons are also trapped at incipient vacancies producing point thermal spikes which may be violent enough to evaporate vacancies from the dislocation, and these vacancies become situated near the dislocation. However, the main effect is considered as being due to the electrons and holes. If it is assumed that the incipient vacancies occur in oppositely charged pairs, then if either an electron or hole is captured, the two centres tend to repel each other. This in addition to the thermal spike produced, causes vacancies or clusters of vacancies near the dislocation. Some of these vacancies will be in the form of coupled pairs and if an electron is then captured, repulsion occurs and an F-centre and positive ion vacancy are produced. Dexter (66) discusses the above mechanism more quantitatively and finds certain major difficulties associated with it.

Varley (67) has proposed another mechanism by which ionising radiation may engender vacancies in salts like the alkali halides. through multiple ionisation. He proposes that anions which have lost more electrons than the number they normally possess in excess of the value of the neutral atom, will find themselves at a position where the electrostatic potential energy is near a maximum rather than a minimum, if the ideal arrangement of ions in the crystal prevails.

-32-/.....

Very strong forces will act to move such anions to positions where they are surrounded preferably by negative rather than by positive ions. That is, they will leave normal sites for interstitial sites. An anion vacancy will remain behind.

The preceding paragraphs may be summed up by saying that, with any of the types of radiation considered, point defects will be produced. These may be randomly distributed (electrons or γ-rays) or be clustered in groups (neutron irradiation). If the displacement spike model is valid, distribution of defects will be approximately uniform, since clusters of defects in the spike will be self annealed.

3. PREVIOUS WORK ON SILVER PERMANGANATE.

Moles and Crespi (68) were amongst the first to study the kinetics of the decomposition of $AgMnO_4$. They showed that the reaction could be represented by an equation corresponding to the monomolecular reaction,

$$\frac{dx}{dt} = (k_1 + k_2x)\ (a-x) \qquad \text{(3.1)}$$

Roginsky (69) made a qualitative study of a series of permanganates including $AgMnO_4$ and found that the decompositions were of an autocatalytic nature. He considered that the reaction consisted of a splitting off of excess oxygen from the MnO_4^- ion to give manganese in the tetravalent form, and that the decompositions behaved like interface reactions.

Prout and Tompkins (32) found that the chemical nature of the decomposition was best represented by

$$4AgMnO_4 \longrightarrow 2Ag_2O + 4MnO_2 + 3O_2 \qquad \text{(3.2)}$$

They found that the reaction followed the normal sigmoid curve and that grinding decreased the acceleratory period and increased the rate of decay. Addition of end products shortened the induction period but had no subsequent effect on the acceleratory or decay periods. Decomposition in the presence of oxygen (pressure 10^{-2} cm. Hg) caused no change and the reaction was likewise unaltered by sudden cooling and reheating to the original temperature. Furthermore, pre-irradiation with ultra-violet light (full quartz mercury arc) for 30 minutes at 20 cms, or pre-bombardment with cathode rays (applied potential 20 Kv. and residual oxygen pressure 2×10^{-3} cm. Hg.) had no effect. The activation energies for the acceleratory and decay periods were found to be 29.4 Kcals $mole^{-1}$.

They considered that the growth of the nuclei involved the growth and interference of branching chains (c.f. $KMnO_4$.) However, they modified the 'Prout-Tompkins equation' by assuming that the branching coefficient varied inversely with time. viz. $k_3 = \frac{k_3^1}{t}$

-34-/.....

Thus equation (1.27) becomes

$$\frac{dN}{dt} = \frac{k_3'N}{t}(1 - 2\alpha) \qquad (3.3)$$

whence $$t\frac{d^2\alpha}{dt^2} = k_3'(1 - 2\alpha)\frac{d\alpha}{dt} \qquad (3.4)$$

Integration of (3.4) yields

$$t\frac{d\alpha}{dt} - \alpha = k_3'(\alpha - \alpha^2) \qquad (3.5)$$

and on further integration

$$\log \frac{\alpha}{\left[k_3' + 1\right] - k_3'} = (k_3' + 1)\log t + c' \qquad (3.6)$$

which reduces to

$$\log \frac{\alpha}{1 - \alpha} = k_3' \log t + c \qquad (3.7)$$

for $k_3' \gg 1$ i.e. $t \gg \frac{1}{k_3}$

Alternatively,

$$\log \frac{p}{pf - p} = k_3' \log t + c \qquad (3.8)$$

Equation (3.8) was found to fit the experimental curve well, but as in the case of $KMnO_4$, two constants (k_3') were necessary, the one valid during the acceleratory period, the other during the decay.

4. OBJECTS OF RESEARCH.

The thermal decompositions of $KMnO_4$ and $AgMnO_4$ are similar in that the kinetics of decomposition are unaffected by pre-irradiation with cathode rays or ultra-violet light and that a common theory of decomposition has been proposed. The effects of pre-irradiation with protons, neutrons and γ -rays, on the thermal decomposition of $KMnO_4$ has been studied by Prout (12). In view of the above similarities it was hoped that these effects would be repeated with $AgMnO_4$. This would provide a test of the theory proposed for irradiated $KMnO_4$. In particular, as will be shown later, the theory suggested that the activation energy (1.3 ev) found for the migration of defects could be attributed to the movement of cation vacancies and it was of interest to determine this value for $AgMnO_4$ where the cation was different.

In addition it was expected that an X-ray study of the course of the decompositions of irradiated and unirradiated $AgMnO_4$ would shed light on the mechanisms of decomposition in both cases.

5. APPARATUS AND MATERIALS.

5.1 DESCRIPTION OF APPARATUS.

The apparatus used was essentially a pumping system connected to a high-vacuum line which could be isolated from the pumps. The high-vacuum reaction line consisted of a constant temperature reaction chamber and a McLeod gauge which could be used to measure pressures in the range 10^{-5} - 10^{-1} cm. Hg.

The pumping system consisted of a two-stage rotary oil pump separated from a two-stage mercury diffusion pump by oil splash bulbs and a mercury vapour trap. The mercury pump was electrically heated by a 150 watt spiral heater encased in the bottom of an asbestos box into which the bottom of the pump fitted snugly. A device for automatically switching off the heater, should the water to the pump condenser fail, was also incorporated. A diagram of it is shown in fig. 2. A P_2O_5 trap was included in the pumping line to absorb any traces of moisture that might be present.

The reaction line could be isolated from the pumping system by means of a hollow, ground-glass tap of 8 mm. bore (T_2). The McLeod gauge was of the normal type having a calibrated bulb of capacity 123.1 cm^3 and capillaries of 2 mm. diameter. Provision was made for altering the reaction volume by including vessels of different cubic capacity via the ground-glass joint at tap T_3.

The reaction chamber (fig. 3) was a triple walled vessel of the type used by Prout (12). Standard ground glass joints facilitated its easy removal. The outer and inner boiling liquids were amyl acetate and glacial acetic acid respectively, or ethyl aceto acetate and amyl acetate respectively, depending on the temperature required. The heater was of a design similar to the one already described and had a power output of 350 watts. A calibrated 200°C thermometer, fixed at its upper end with vacuum wax and with its lower end touching the bottom of the reaction chamber, was used to measure the decomposition temperature.

The weighed crystals contained in the reaction bucket could be quickly lowered into the hot region of the chamber by means of a

-37-/.....

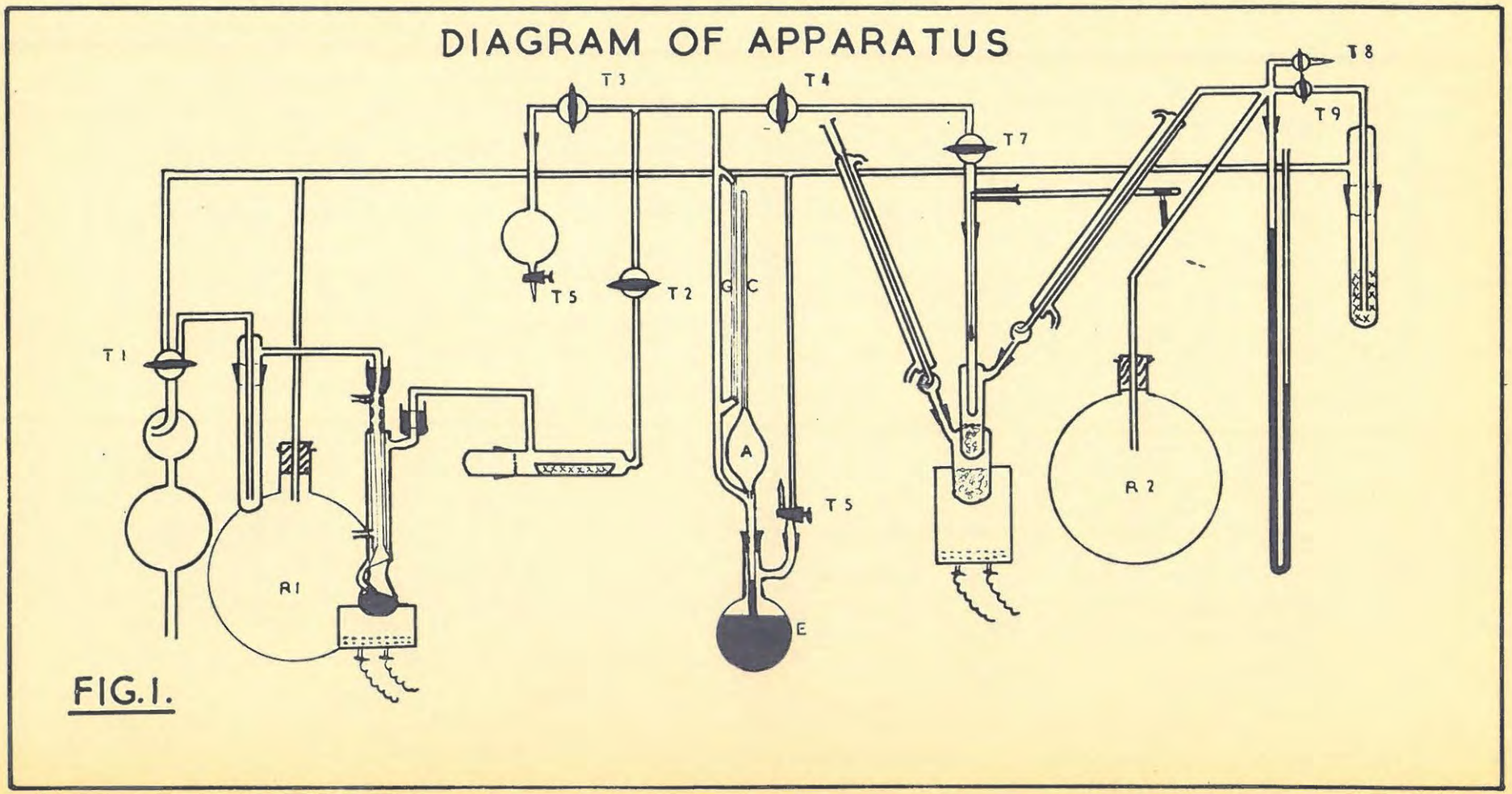

FIG.1.

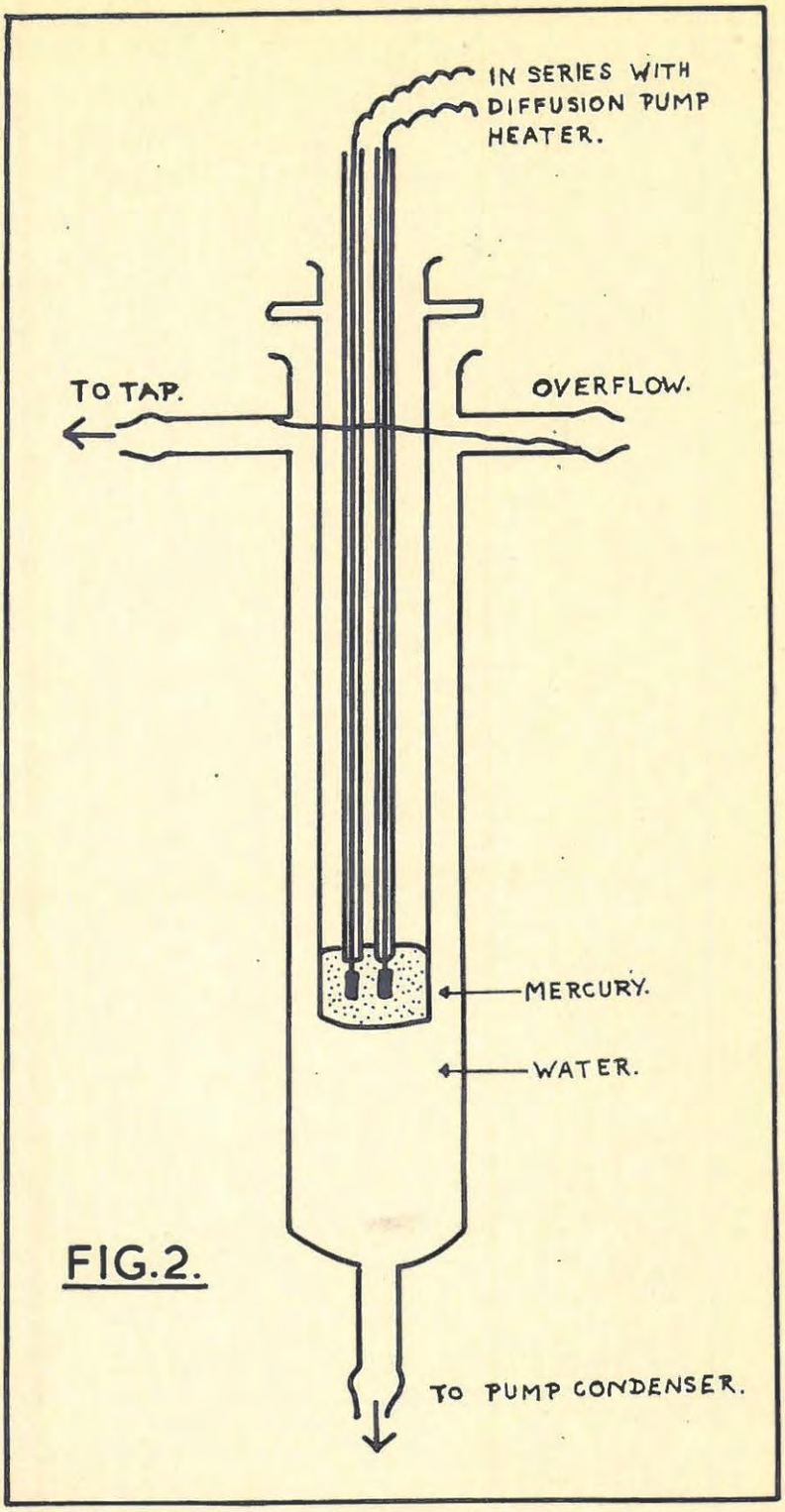
IN SERIES WITH
DIFFUSION PUMP
HEATER.
TO TAP.
OVERFLOW.
MERCURY.
WATER.
TO PUMP CONDENSER.

FIG.2.

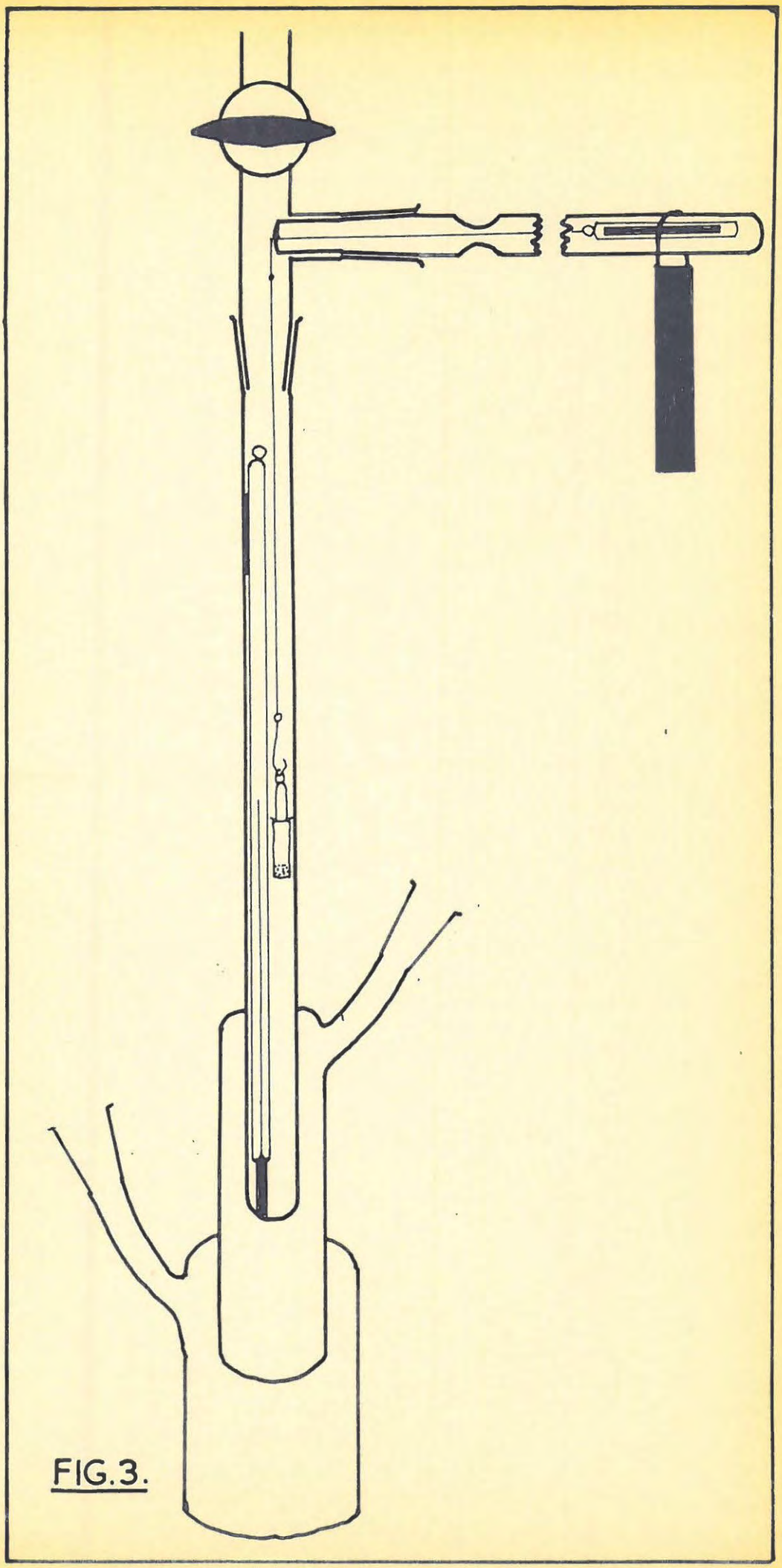

FIG.3.

magnetic device. This consisted of a detachable horizontal side arm containing a glass ampoule, attached to the Pt. hook on which the bucket hung by means of fine silk and then thin platinum wire. The bucket could thus be raised or lowered simply by moving the external permanent magnet which hung from the side arm.

A secondary vacuum line, connected to the mechanical pump through a two-way tap T_1 was used in the operation of the McLeod gauge and the temperature control system. The latter could be isolated by means of tap T_9 and easy control of the pressure above, and hence the temperature of the inner boiling liquid, was achieved by opening T_9 to vacuum or T_8 to the atmosphere. Reservoirs R_1 and R_2, each of 10 litre capacity were included to stabilise the pressure and to achieve fine pressure adjustment. Using the boiling liquids mentioned this method of temperature control regulated the temperature to within 0.1°C in the range 100°C - 130°C.

Two types of reaction bucket were used, platinum and pyrex. The former was made by rolling thin sheet platinum round a 5 mm diameter glass rod and then closing the one end of the cylinder by pinching it. The bucket was 15 mm. long and was fitted with a loose platinum lid and a handle of platinum wire.

Pyrex buckets were used in cases where it was desirable to study the behaviour of the crystals during decomposition or where incompletely decomposed samples had to be subsequently irradiated. These buckets were made by sealing off one end of a pyrex tube 4 mm. in diameter and 8 cm. long. The crystals were weighed in this tube and carefully tapped down to the bottom. Holding the tube vertical it was heated with a small hot flame at a distance of about 3.5 cm. from the sealed end, and the glass was drawn out to form a hollow hook through which the gas could subsequently escape.

It was found experimentally that the chemical nature of the bucket (platinum or pyrex) had no effect on the decomposition. With both types there was a slight delay in the attainment of the decomposition temperature. This was about five minutes.

-38-/....

5.2 CALIBRATION OF APPARATUS.

(i) Determination of the capillary constant of the McLeod.

A preliminary exploration of several lengths of clean dry 2 mm. bore capillary tubing was carried out by introducing a 1-2 cm. length of clean mercury into each and then measuring the lengths of the mercury beads at positions along the tubes, 5 cms. apart. The best 30 cms. of capillary was selected, thoroughly cleaned and dried. It was accurately calibrated as follows, another 30 cms. of the same tube being set aside for the comparison capillary.

A reference mark was first etched on the selected capillary at any convenient point along its length. A mercury bead was introduced as before and the tube was clamped horizontally. A blowing or suction tube, which included a silica gel trap, was attached to the one end of the capillary to facilitate the movement of the mercury bead along the length of the tube. The travelling microscope was adjusted to move in focus with the capillary. As the traverse on the microscope was only 14 cms. it was necessary to move it bodily and to realign it during the course of the measurements.

Starting with the mercury bead at one end of the tube readings A, B, C, and D (illustrated below) were taken successively.

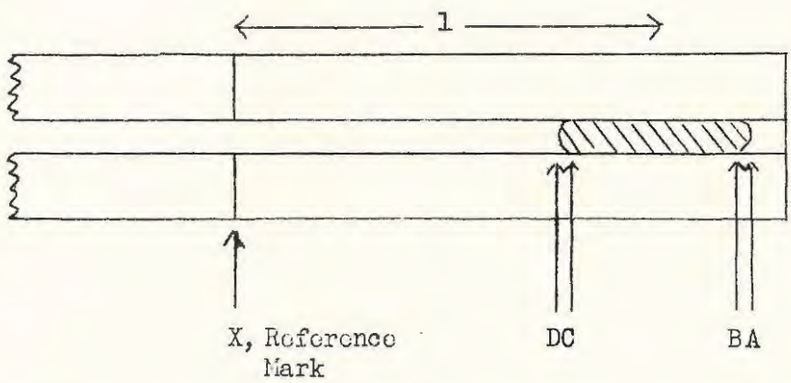

The mercury bead was moved a short distance along the tube so that the right hand end of it overlapped the previous position of the left hand end. Readings A, B, C, and D were repeated. This process was repeated along the whole length of the tube, the position X of the reference mark being noted when it was reached. The mercury bead was then weighed and knowing the density of Hg at the temperature of

-39-/.....

of the measurements, the cross-section of the capillary could be calculated for each position l of the mercury bead.

Two determinations of the variation of area of cross-section with length were made, using two separate beads of mercury. Using a very large sheet of graph paper this variation was plotted. By counting squares and knowing where the tube had been sealed off (in a manner which did not appreciably distort the bore of the tube) the volume of the capillary up to any point was known. A graph showing the variation of volume with distance from the sealed end was plotted, again using a very large sheet of graph paper. All the points, with negligible divergence, lay on a straight line passing through the origin. Thus the bore of the tube was taken as uniform and the capillary constant could be determined.

Results.

The volume of the mercury bead is made up of the volume of a right circular cylinder plus the volume of two spherical segments. It can be shown (71) that the area of cross section is given by

$$\pi r^2 = \frac{\frac{M}{D}}{F + \frac{1}{2}(E-F)} \qquad (5.1)$$

where r = radius of capillary

E = A - D

F = B - C

M = mass of mercury bead

D = density of Hg at the temperature of the experiment

1st Run.

M = 0.5091 gm.

$D_{22.5^{\circ}C}$ = 13.54 gm/cm^3

X = 8.02 cms.

TABLE 1. overleaf 40/.....

TABLE 1.

l cms	A cms	B cms	C cms	D cms	πr^2 cms^2
-7.32	14.928	14.884	13.780	13.742	0.03284
-6.26	13.868	13.824	12.723	12.680	0.03284
-5.20	12.811	12.770	11.662	11.629	0.03284
-4.17	11.778	11.724	10.630	10.594	0.03301
-3.10	10.706	10.660	9.558	9.552	0.03291
-2.00	9.610	9.570	8.470	8.432	0.03301
-0.95	8.560	8.514	7.414	7.372	0.03287
0.12	7.490	7.446	6.351	6.304	0.03296
1.21	6.400	6.354	5.250	5.212	0.03281
2.29	5.324	5.260	4.172	4.132	0.03298
3.35	4.262	4.202	3.100	3.068	0.03275
4.44	3.169	3.122	2.018	1.982	0.03281
5.52	2.092	2.036	1.939	1.898	0.03291
6.57	14.946	14.902	13.806	13.765	0.03301
*	1.040				
7.61	13.908	13.863	12.763	12.721	0.03287
8.73	12.792	12.755	11.658	11.613	0.03301
9.78	11.736	11.686	10.590	10.552	0.03298
10.86	10.660	10.616	9.516	9.478	0.03296
11.80	9.596	9.542	8.447	8.412	0.03298
12.90	8.495	8.543	7.354	7.312	0.03296
14.00	7.390	7.336	7.328	6.197	0.03281
15.07	6.316	6.262	6.164	5.126	0.03287
16.14	13.686	13.634	12.532	12.490	0.03273
*	5.254				
17.22	12.610	12.576	11.462	11.430	0.03278
18.33	11.524	11.472	11.376	11.338	0.03296
19.42	10.426	10.376	9.272	9.232	0.03273
20.52	9.330	9.286	8.178	8.142	0.03275
21.61	8.246	8.202	7.100	7.062	0.03291
22.7	7.164	7.105	6.015	5.978	0.03301
23.81	6.072	6.028	4.928	4.886	0.03291

Maximum percentage variation = 0.85

2nd Run.

M = 0.7149 gm.

$D_{22.5^{o}C}$ = 13.54 gm/cm^3.

X = 5.36 cms.

TABLE 2 Overleaf. (-41-)/.....

TABLE 2.

l cms	A cms	B cms	C cms	D cms	πr^2 cms^2
-8.76	14.956	14.918	13.350	13.300	0.03275
-7.25	13.436	13.392	11.828	11.794	0.03294
-5.74	11.924	11.866	11.318	11.386	0.03314
-4.20	10.380	10.326	8.774	8.742	0.03311
-2.69	8.866	8.820	7.262	7.226	0.03301
-1.16	7.340	7.290	5.736	5.696	0.03301
+0.36	5.820	5.776	4.220	4.182	0.03306
1.88	4.294	4.257	2.708	2.656	0.03313
3.39	2.792	2.748	1.186	1.152	0.03298
*	13.202				
4.94	1.242	13.160	11.600	11.564	0.03301
6.46	11.682	11.622	10.070	10.040	0.03306
8.00	10.138	10.094	8.538	8.496	0.03301
9.54	8.604	8.558	7.008	6.962	0.03308
11.07	7.074	7.016	5.466	5.434	0.03311
12.61	5.528	5.486	3.924	3.890	0.03311
14.13	4.000	3.946	2.388	2.354	0.03296
15.69	2.436	2.392	1.830	0.796	0.03298
*	14.416				
17.23	0.896	14.360	12.796	12.760	0.03279
18.79	12.860	12.818	11.252	11.216	0.03291
20.31	11.336	11.292	9.724	9.690	0.03286
21.87	9.778	9.730	8.170	8.134	0.03296
23.41	8.236	8.188	6.624	6.586	0.03286

Maximum percentage variation = 1.1

(* indicates where the travelling microscope had to be moved bodily and realigned).

The capillary constant k, is defined as the number of ccs/cm length of capillary. It was determined as previously described and was found to be 3.2965×10^{-2} ccs/cm.

(ii) Calibration of the bulb of the McLeod.

This was done after the capillary had been sealed on to the bulb. The other end of the capillary was, however, still open. The volume was determined weighing the bulb empty and then filled with distilled water at a known temperature. Knowing the density of water at the temperature of the experiment the volume of the bulb was easily calculated. Two determinations were made. Both gave the volume of the bulb to be 123.1 cms^3.

-42-/.....

(iii) Measurements of Pressure.

The McLeod gauge operates on the Boyles' Law principle. A known volume of rarified gas is compressed to another smaller known volume. In practice the mercury level in capillary G (fig.1) is brought approximately level with the top of the capillary C. The difference in heights of the mercury levels then gives the pressure of the gas confined in C. The volume of the gas in C is proportional to difference in height of the mercury level in C and the top of the capillary, provided that a correction is applied to account for the volume of the mercury meniscus.

If h = corrected length of enclosed gas column in C (cms)

$\triangle h$ = difference in height of mercury levels (cms)

$k = 3.2965 \times 10^{-2}$ ccs/cm

V_1 = volume of the bulb A.

$= 123.1$ cms^3.

P_1 = pressure to be determined

then

$$P_1 = \frac{k.h.\triangle h}{V_1} \text{ cm Hg}$$

$$= \frac{3.2965 \times 10^{-2} \times (h.\triangle h)}{123.1}$$

$$= K.\ (h.\triangle h) \text{ cm Hg.}$$

where K = proportionality constant

$= 2.678 \times 10^{-4}$ cm^{-2} cm Hg.

In the main only relative pressures were necessary and these were measured in terms of 'pressure units'. A 'pressure unit' is defined in terms of the product $(h.\triangle h)$. Pressures are converted to absolute values by multiplying by the constant K.

(iv) Check Calibration of McLeod Capillary.

The calibration of the McLeod was checked 'in situ' as follows. Some dry air was admitted into the vacuum line through taps T_5 and T_3. Suction was applied until on closing T_2 the pressure was about 10^{-2} cms of Hg. The mercury in the McLeod was raised until the bulb was sealed off. T_2 was then opened and the rest of the system was completely evacuated. The pressure was measured with the mer-

-43-/.....

cury level in C at varying heights.

Results.

If h = corrected reading of mercury level in C (cms)

p = pressure in 'pressure units'.

Then

h	p
9.75	68.70
13.54	69.00
20.02	69.40
24.81	69.40
26.16	69.25
Mean	69.15

Percentage variation = 1.01

This is in accordance with the previous calibration.

(v) Determination of the Reaction Volume of the Apparatus.

Dry air was admitted into the system and suction was applied until on closing T_2 the pressure was such that Δ h was 10-25 cms. With the mercury still trapping air at this pressure in the capillary, T_2 was opened and the system completely evacuated. This took about 10 minutes. T_2 was then closed and the previous gas pressure (P_1) was accurately measured. The mercury was then lowered to allow the imprisoned gas to expand into the volume to be determined. After allowing the pressure to equilibrate the mercury was again raised and the pressure (P_2) measured. This procedure was repeated several times. During these operations the reaction chamber was maintained at the decomposition temperature. Applying Boyles' Law the volume of the apparatus is easily calculated.

Results.

If V_1 = volume of the bulb A

= 123.1 cms^3.

V_2 = reaction volume (cms^3)

-44-/....

Then

P_1	P_2	V_2
267.0	46.15	714
517.0	89.30	713
89.5	15.43	713
175.0	30.30	711
447.0	77.80	707
	Mean	711.6 ccs.

This is a typical set of readings. As the volume of the apparatus was changed from time to time for various reasons, several re-calibrations were necessary. Using these, all pressures (unless otherwise stated) were corrected to correspond with the above volume viz. 711.6 cms^3.

5.3 PREPARATION OF CRYSTALS

Silver permanganate is prepared by mixing equimolar solutions of A.R. silver nitrate and A.R. potassium permanganate. The method used was similar to that employed by Prout and Tompkins (32).

Two 500 cc solutions containing 26.9 gms A.R. $AgNO_3$ and 25.0 gms A.R. $KMnO_4$ respectively were made up. The solutions were transferred to two 1 litre separating funnels with capillary outlets of the same bore to facilitate easy control of the dropping rate. The solutions were then run at the same rate, with stirring, and under dark room conditions, into 200 ccs of distilled water maintained at 45°C. The solution was cooled to 3°C and the crystals were filtered off, washed thoroughly with iced distilled water, and dried in a light-tight P_2O_5 vacuum desiccator

This procedure was repeated five times in all. The batches were pooled and yielded about 100 gms of $AgMnO_4$. Small crystals (0.3 mm x 0.03 mm) were recrystallised from a solution saturated at 40°C, by rapidly cooling it to 3°C in an ice-salt freezing mixture. The crystals were washed and dried as before. Larger crystals, weighing about 6 mgm. each, were prepared by placing the saturated

-45-/.....

solution in a vacuum oven at 40°C, containing silica gel. Pumping was continued for 24 hours. The mother liquor was decanted off and the crystals carefully dried with filter paper, but in doing so were rapidly transferred to fresh sheets to prevent oxidation.

Both batches of crystals were stored in a light-tight P_2O_5 desiccator.

5.4 METHODS OF PRE-IRRADIATION.

(i) Ultra-Violet Irradiation.

Crystals were given prolonged pre-irradiation using a Philips Type 5720 E/70 dark bulb. This bulb produces ultra-violet light of a wavelength of 2536 A. Crystals were placed at a distance of 9" from the bulb and were irradiated for 55 hours.

(ii) Pile Irradiation.

Irradiation was carried out by sealing the crystals in small silica ampoules which were placed inside standard irradiation cans. These were always inserted in the same hole of the atomic pile BEPO where the temperature was maintained at 30±5°C during irradiation. The crystals were thus bombarded by γ-rays and neutrons, the flux of the latter being 2 x 10^{11}/cm^2"sec.

(iii) Thermal Neutron Irradiation.

Crystals contained in A.R. lead ampoules, were placed in the 'thermal column' of BEPO. Here they were surrounded by a lead block which screened off any other type of irradiation. The flux of thermal neutrons was 7 x 10^9/cm^2/sec.

(iv) γ-Irradiation.

Crystals were sealed into pyrex ampoules which were placed in a Cobalt 60 "hotspot" of the type described by Eastwood (71). The energies of the γ-rays emitted by the Cobalt 60 are 1.33 and 1.17 Mev. The dose rate unless otherwise stated was 1.6 x 10^6 r.e.p./hour which was, as far as was known from the limited available information, comparable to that obtaining in the pile. The total activity of the hot-spot was 439 curies.

-46-/.....

COBALT 60 "HOTSPOT"

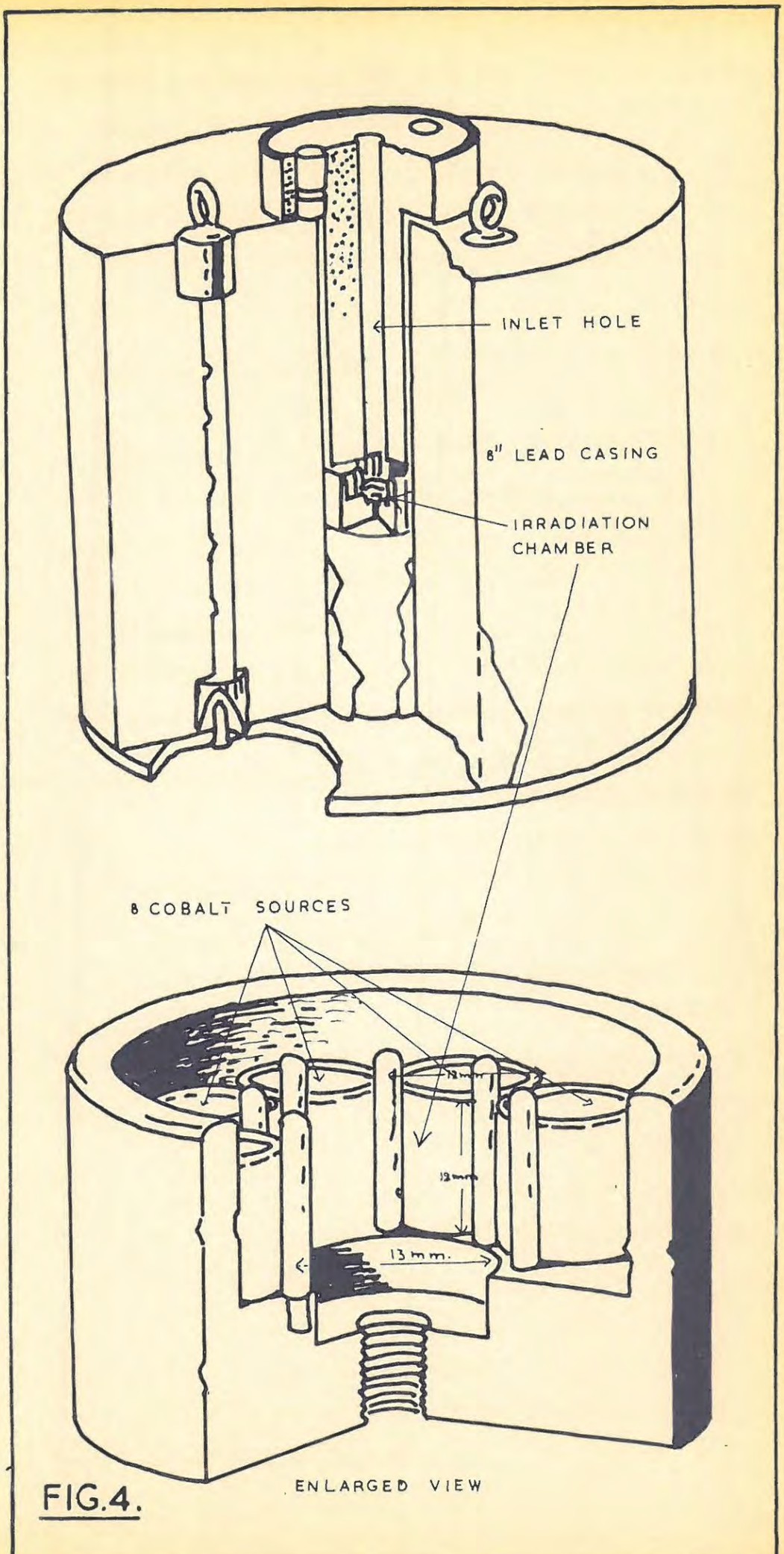

FIG.4.

ENLARGED VIEW

5.5 GENERAL EXPERIMENTAL PROCEDURE.

Before commencing any series of decompositions the apparatus was pumped out for a few days and was checked to ensure that the vacuum was maintained for 4 hours, the time required for a normal decomposition run. (Although liquid N_2 or solid CO_2 were not available for use with vapour traps it was found that the vacuum was satisfactorily maintained.) Tap T_7 was then closed and air was admitted to the reaction chamber by pulling out the side arm slightly. The reaction chamber was easily removed by slipping it down off the two ground glass joints.

About 20 mg of material was then accurately weighed into a reaction bucket - one of the types already described. After re-greasing the joints and hanging the bucket on the hook provided, the reaction chamber and side arm were replaced and the taps T_2 and T_7 were opened to vacuum. It was found necessary to seal externally with sealing wax the joint connecting the inner boiler to the condenser of the temperature control system, since grease was melted by the hot vapours of the boiling liquid.

The reaction chamber heater was switched on and the mercury manometer was adjusted to give the approximate temperature desired. It was found that two hours pumping thereafter was normally sufficient for complete evacuation. During this time the temperature was accurately adjusted by altering the pressure above the inner boiling liquid.

After two hours' pumping, maintenance of the vacuum was again checked. The reaction bucket was then lowered into the hot region and the time was noted. The pressure of evolved gas was measured at convenient intervals of time until no further increase of pressure was evident. Pressures were normally corrected to 20 mg weight, to a room temperature of 20°C and to correspond with a reaction volume of 711.6 ccs. Graphs showing the increase of pressure with time were plotted.

-47-/.....

6. RESULTS.

6.1 REPRODUCIBILITY OF RESULTS.

When new types of radiation or crystals were studied the degree of reproducibility was first checked. The graphs in fig.5 show that reproducibility was satisfactory for unirradiated and γ-irradiated crystals. This was less true of pile-irradiated whole crystals and in the case of the ground material the reproducibility was poor.

TABLE 3.

SMALL CRYSTALS, UNIRRADIATED., (105°C)					
t	p	t	p	t	p
20.0	4.2	115.5	73.0	200.0	415.0
40.0	14.2	126.5	95.6	210.0	432.0
55.6	20.6	148.5	166.5	220.0	480.3
65.0	25.4	155.5	197.3	261.0	555.6
78.0	33.6	170.0	270.3	273.0	565.9
90.5	42.2	181.0	320.0	300.0	569.0
102.5	55.6	190.0	366.1	350.0	574.0
22.0	5.9	141.0	143.1	241.0	530.9
40.0	13.2	160.0	220.5	256.0	555.0
60.0	23.2	180.0	320.5	270.0	559.6
80.0	34.9	201.0	417.0	300.0	565.1
100.0	53.6	220.0	482.0	340.0	570.1
120.0	86.9				

SMALL CRYSTALS, 2 hrs. BEPO. (105°C)					
t	p	t	p	t	p
21.0	4.1	95.0	151.0	130.5	419.2
31.5	9.1	98.0	174.0	136.0	444.9
41.5	15.2	100.0	189.5	140.0	458.2
50.0	21.4	102.5	210.5	146.0	473.2
62.5	32.2	105.5	235.5	150.0	481.5
74.0	49.7	110.0	274.5	157.0	491.5
84.0	77.8	117.0	335.0	167.0	498.0
90.0	112.5	120.0	384.5	175.0	502.3
93.0	135.7	125.0	386.0		
25.0	6.5	92.0	162.5	132.0	448.1
40.0	14.4	97.5	208.0	142.0	475.4
52.0	25.9	101.0	243.3	150.0	485.3
65.0	40.1	110.5	321.1	160.0	490.2
75.0	60.5	116.0	357.6	165.0	495.1
85.0	105.5	125.5	417.8		

REPRODUCIBILITY.

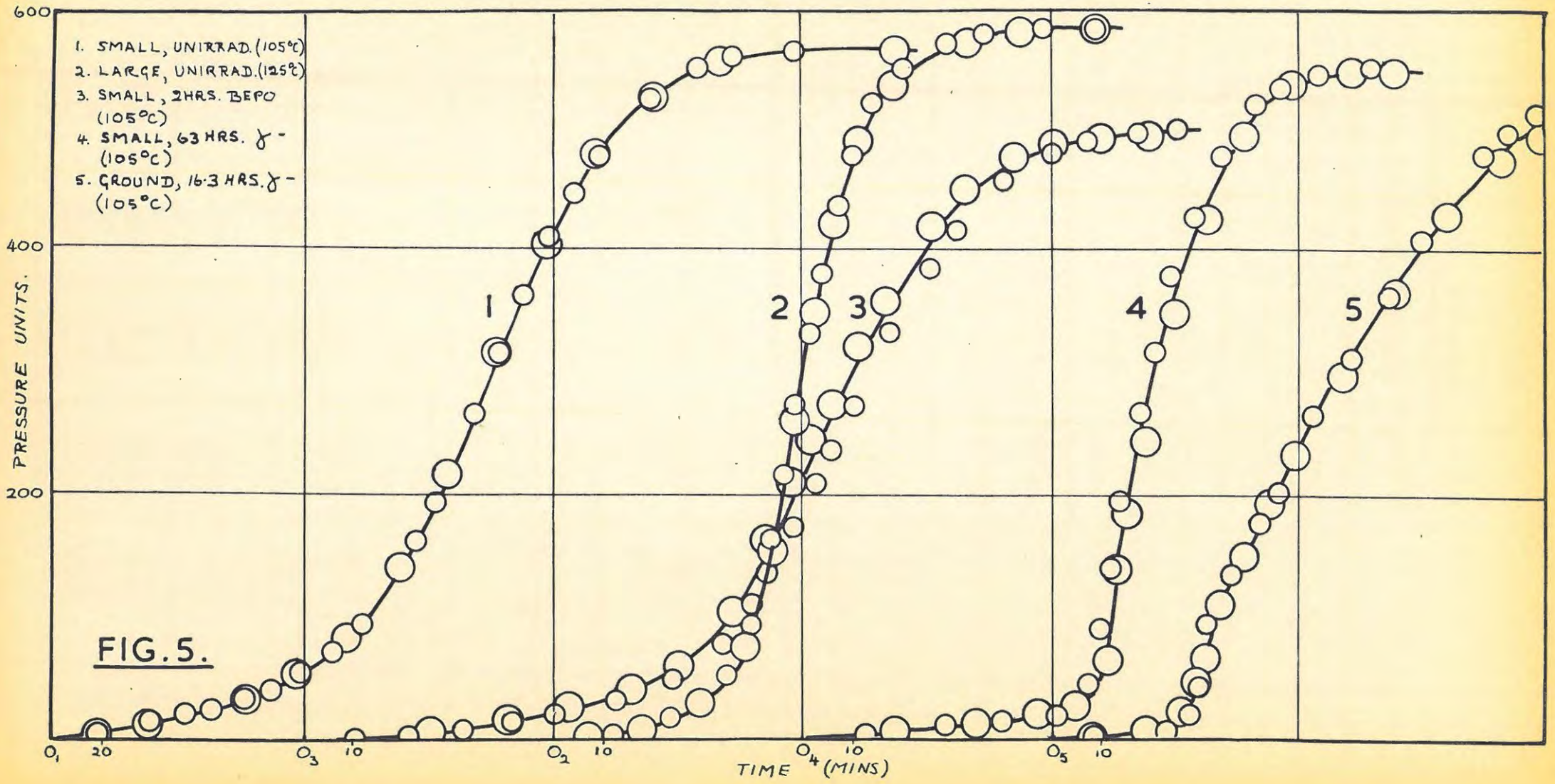

FIG. 5.

LARGE CRYSTALS UNIRRADIATED,
DECOMPOSED AT 125°C.

t	p	t	p	t	p
5.0	1.0	41.0	98.5	61.0	482.0
10.0	3.0	45.0	166.0	65.0	522.1
13.0	6.0	47.5	220.5	71.0	556.0
20.0	13.5	50.0	279.0	75.0	570.0
25.0	20.6	52.5	336.0	80.0	576.1
30.5	31.9	55.0	388.1	87.5	588.0
36.0	55.0	58.0	440.0	100.0	594.0
7.5	2.1	50.0	266.0	68.5	539.1
19.0	10.9	54.0	353.0	85.0	580.0
31.0	34.0	58.0	427.0	95.0	586.2
40.0	80.3	62.5	498.1	110.0	588.0
45.0	160.2				

SMALL CRYSTALS 63 hrs γ-IRRADIATION
DECOMPOSED AT 105°C.

t	p	t	p	t	p
5.0	0.6	61.0	95.0	75.0	386.3
14.0	7.8	62.0	118.1	80.0	431.1
22.0	11.0	63.0	140.0	85.5	483.0
30.0	13.8	65.0	197.1	92.0	523.0
41.0	18.9	67.0	240.5	97.0	537.1
52.0	23.6	69.0	271.0	105.0	550.0
59.0	47.1	72.0	320.0	115.0	554.0
60.0	70.6				
20.0	11.8	62.0	70.1	82.0	430.0
36.0	18.9	64.0	144.2	90.0	496.0
49.0	25.9	66.0	191.0	100.0	540.1
52.0	28.8	70.0	249.1	111.0	549.0
56.0	31.4	76.0	354.0	120.0	549.0
60.0	39.0				

GROUND CRYSTALS 16.3 hrs γ-IRRADIATION
DECOMPOSED AT 105°C.

t	p	t	p	t	p
10.0	0.2	40.0	158.1	75.0	413.0
20.0	1.5	43.0	183.5	87.5	482.1
25.0	10.7	46.0	203.5	92.0	496.0
28.0	26.0	50.0	238.0	98.0	515.0
30.0	48.0	53.0	275.5	103.0	522.0
32.5	99.0	60.5	315.0	122.0	534.0
35.0	120.0	68.0	365.0	120.0	537.0
37.5	138.0				

TABLE CONTINUED.

GROUND CRYSTALS 16.3 HRS γ-IRRADIATION DECOMPOSED AT 105°C.					
t	p	t	p	t	p
10.5	0.2	35.0	115.3	80.0	434.1
15.0	1.4	40.0	157.7	90.0	477.0
20.0	12.0	45.0	199.0	100.0	496.2
25.0	20.4	50.0	226.0	110.0	510.0
27.5	27.8	60.0	305.1	120.0	511.0
31.0	49.9	70.0	370.0	131.5	513.0
32.5	70.0				

6.2 EFFECT OF PRE-IRRADIATION WITH ULTRA-VIOLET LIGHT.

Prout and Tompkins (32) reported that pre-irradiation for 30 minutes with ultra-violet light from a quartz mercury-arc lamp had no effect on the thermal decomposition of $AgMnO_4$.

Before investigating other types of radiation it was felt desirable to confirm their findings. Consequently samples of both small and large crystals were pre-irradiated for 55 hours as previously described. The results, illustrated graphically in fig.6. show that ultra-violet light has no significant effect.

6.3 EFFECTS OF PRE-IRRADIATION FOR VARIOUS TIMES IN THE ATOMIC PILE BEPO.

Small crystals, which had been irradiated for varying times, as already described, were thermally decomposed at 105°C to ascertain whether thermal neutrons and/or γ-rays which are present in the pile had any effect. The results tabulated below and shown graphically in fig.7 indicate in the main a shortening of the induction period and increased acceleration of the reaction with increasing times of irradiation.

TABLE 4.

48 Hrs BEPO.					
t	p	t	p	t	p
5.0	0.1	50.0	114.1	68.0	425.0
10.0	0.5	52.0	151.0	71.0	454.0
15.0	2.0	54.0	189.1	75.0	492.0

ULTRA VIOLET IRRADIATION

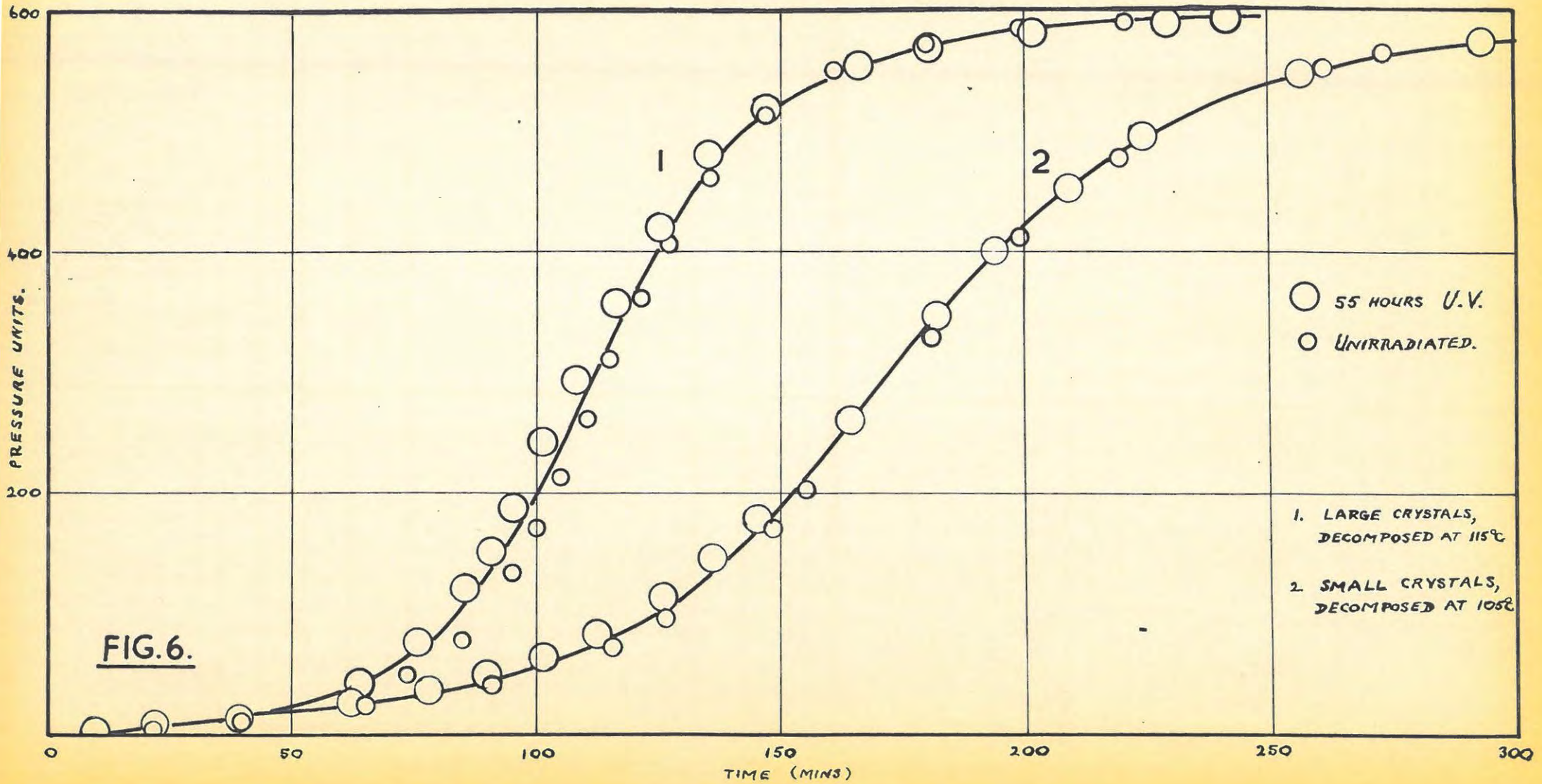

FIG.6.

TABLE CONTINUED.

48 hrs. BEPO.					
t	p	t	p	t	p
20.0	5.3	56.0	229.0	78.0	510.0
25.0	7.4	58.0	266.0	85.0	533.0
30.0	12.3	60.0	306.3	90.0	542.0
38.0	28.6	62.0	336.1	96.0	544.0
45.0	52.1	64.0	372.0	105.0	549.1
47.0	84.5	66.0	400.2		

15 hrs. BEPO.					
t	p	t	p	t	p
10.0	0.4	67.0	137.7	85.0	432.0
20.0	1.4	69.0	180.0	87.5	467.0
30.0	5.3	71.0	216.5	90.0	489.1
40.0	11.9	73.6	253.2	92.5	505.0
50.0	23.2	75.0	287.0	97.5	531.5
55.5	30.2	77.5	331.5	105.0	541.5
60.0	42.5	80.0	369.0	110.0	551.0
63.0	64.6	82.5	405.0	120.0	557.0
65.0	94.3				

4 hrs BEPO.					
t	p	t	p	t	p
11.0	0.5	82.5	121.0	105.0	417.0
21.0	1.6	95.0	152.1	107.5	440.0
30.0	5.6	87.5	187.5	110.0	463.4
40.0	11.9	90.0	224.6	115.0	497.1
50.0	19.0	92.5	256.0	120.0	518.0
60.0	29.8	95.0	297.5	125.0	535.0
70.0	43.4	97.5	328.0	130.0	543.0
76.0	66.0	100.0	359.5	135.0	548.5
80.0	91.7	102.5	393.0	145.0	552.0

2 hrs. BEPO.					
t	p(norm)	t	p(norm)	t	p(norm)
21.0	4.7	97.5	188.0	130.5	456.0
31.5	10.0	100.0	207.1	135.0	478.1
41.5	16.2	102.5	232.9	140.0	500.0
50.0	22.1	105.5	257.0	145.0	510.7
62.5	36.3	109.0	295.1	150.0	524.0
74.0	54.1	113.0	333.3	156.0	532.3
84.0	85.3	117.0	367.0	167.0	542.0
90.0	122.5	120.0	390.0	183.0	547.1
95.0	164.5	124.0	420.4		(p_f = 502.3)

SMALL CRYSTALS: PILE-IRRADIATED.

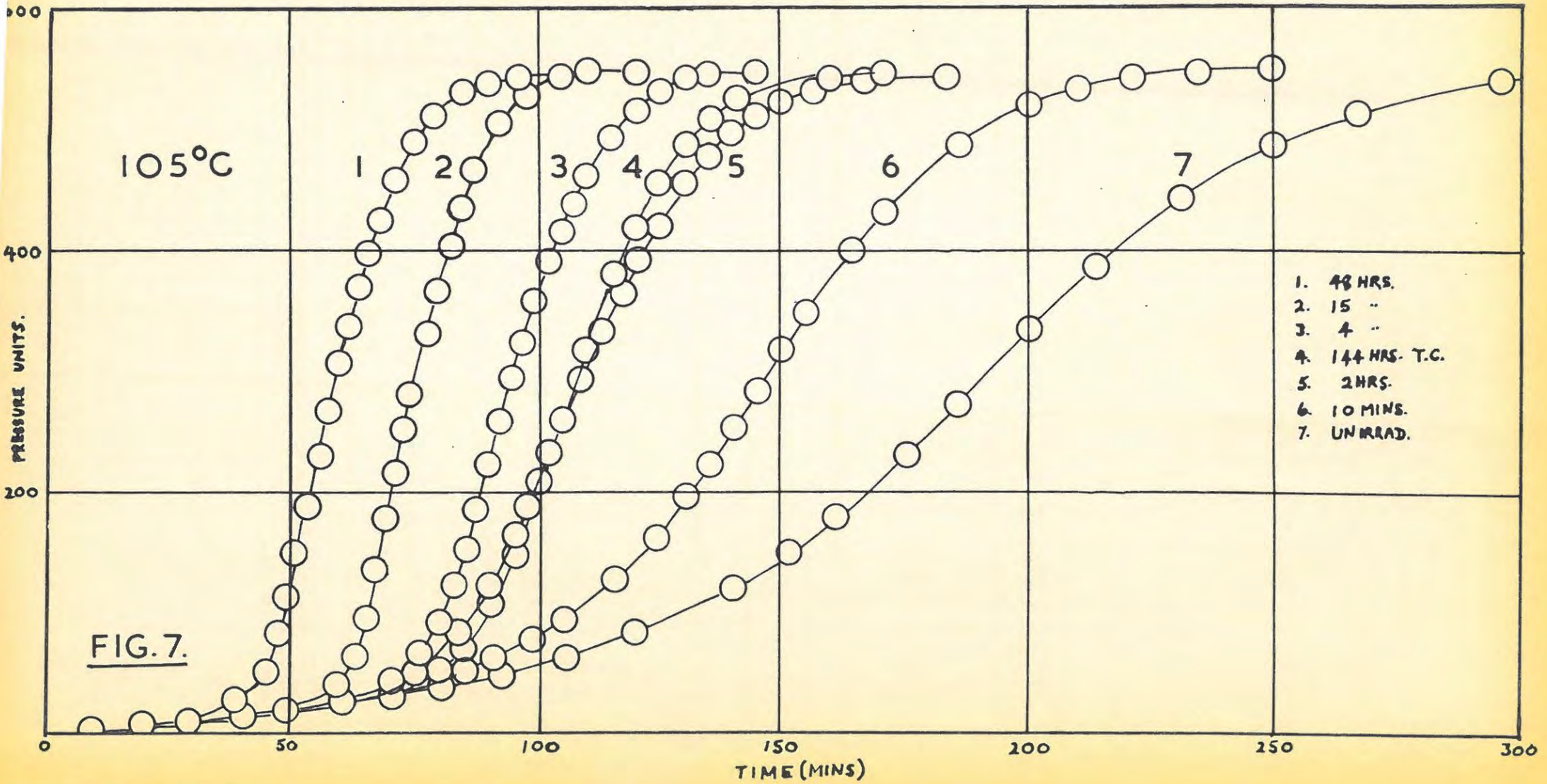

FIG. 7.

10 mins BEPO.					
t	p	t	p	t	p
25.0	4.7	120.0	144.5	165.0	403.0
40.0	12.8	125.0	167.7	170.0	431.0
60.0	27.0	130.0	196.0	185.5	486.1
70.0	37.2	135.0	225.1	190.0	498.5
80.0	47.8	140.0	250.0	200.0	522.0
85.0	55.3	145.0	287.0	210.0	533.5
92.0	66.6	150.0	318.1	220.0	538.1
100.0	79.5	155.0	346.3	235.0	544.0
106.5	95.5	160.0	377.0	230.0	546.0
115.0	123.5				

UNIRRADIATED.					
t	p	t	p	t	p
20.0	5.4	140.0	121.1	231.0	450.0
40.5	12.7	152.0	150.2	250.0	492.7
60.0	24.4	161.0	180.0	274.0	525.1
80.0	40.0	175.0	232.4	295.0	543.0
92.0	50.0	185.0	272.5	308.0	549.0
106.0	65.3	200.0	338.5	330.0	552.1
120.0	85.6	214.0	389.6		

The grinding of crystals serves to shorten the induction period by artificially creating nuclei (1). It was therefore desirable to know whether pre-irradiation in the pile produced any further nucleation in ground crystals. Thus ground crystals, irradiated for varying times in the pile, were thermally decomposed at 105°C.

The results tabulated below and illustrated in fig.8, show that the induction period is not markedly affected but that the accelerator and decay periods are. For all samples there is a sharp acceleration of the reaction after about 30 minutes followed by a definite and sudden change of slope of the curve after which the decay begins. However, the reproducibility of the p-t plots for these samples was not good, and this is shown by the irregularity of the curves in fig.8.

TABLE 5.

OVERLEAF/-52- .....

TABLE 5.

48 hrs. BEPO.					
t	p	t	p	t	p
10.0	0.5	32.5	106.5	57.0	440.0
15.0	1.5	35.0	137.8	60.0	469.1
17.5	2.7	37.5	168.7	65.0	503.0
20.5	4.9	41.0	219.5	70.0	524.1
23.0	7.8	44.0	264.0	75.0	531.0
25.0	11.7	47.0	311.5	80.0	536.0
27.5	19.1	50.0	354.5	105.0	540.0
30.0	58.8	54.0	409.0		

15 hrs. BEPO.					
t	p	t	p	t	p
10.5	0.3	37.5	94.4	65.5	376.3
15.0	0.9	40.0	143.0	70.0	413.0
21.0	1.6	42.5	167.0	75.0	447.0
25.0	4.4	45.0	189.0	80.0	471.0
27.5	9.3	50.0	236.0	90.0	506.0
30.0	15.8	55.0	282.1	100.0	513.0
32.5	25.8	60.0	326.5	110.0	519.0
35.0	40.7				

4 hrs. BEPO.					
t	p	t	p	t	p
10.0	0.2	35.0	104.2	74.0	380.1
20.0	0.9	37.5	124.2	81.0	419.0
22.5	4.1	40.0	142.1	90.0	464.0
25.0	9.1	46.0	187.0	104.0	513.4
27.5	21.0	50.0	216.3	115.5	527.0
30.0	46.3	56.5	262.3	130.0	536.0
32.5	84.2	62.0	299.0	148.0	533.0

2 hrs. BEPO.					
t	p	t	p	t	p
10.0	0.2	43.0	91.5	90.0	409.1
20.0	1.0	45.0	106.3	101.0	460.3
26.0	4.2	47.5	126.3	112.5	496.5
30.0	9.7	53.0	166.3	125.0	516.0
33.0	20.5	60.0	218.6	132.5	524.3
35.0	28.0	70.0	284.5	145.0	526.1
37.5	41.9	80.0	350.0	150.0	530.4
40.0	64.8				

GROUND CRYSTALS: PILE-IRRADIATED

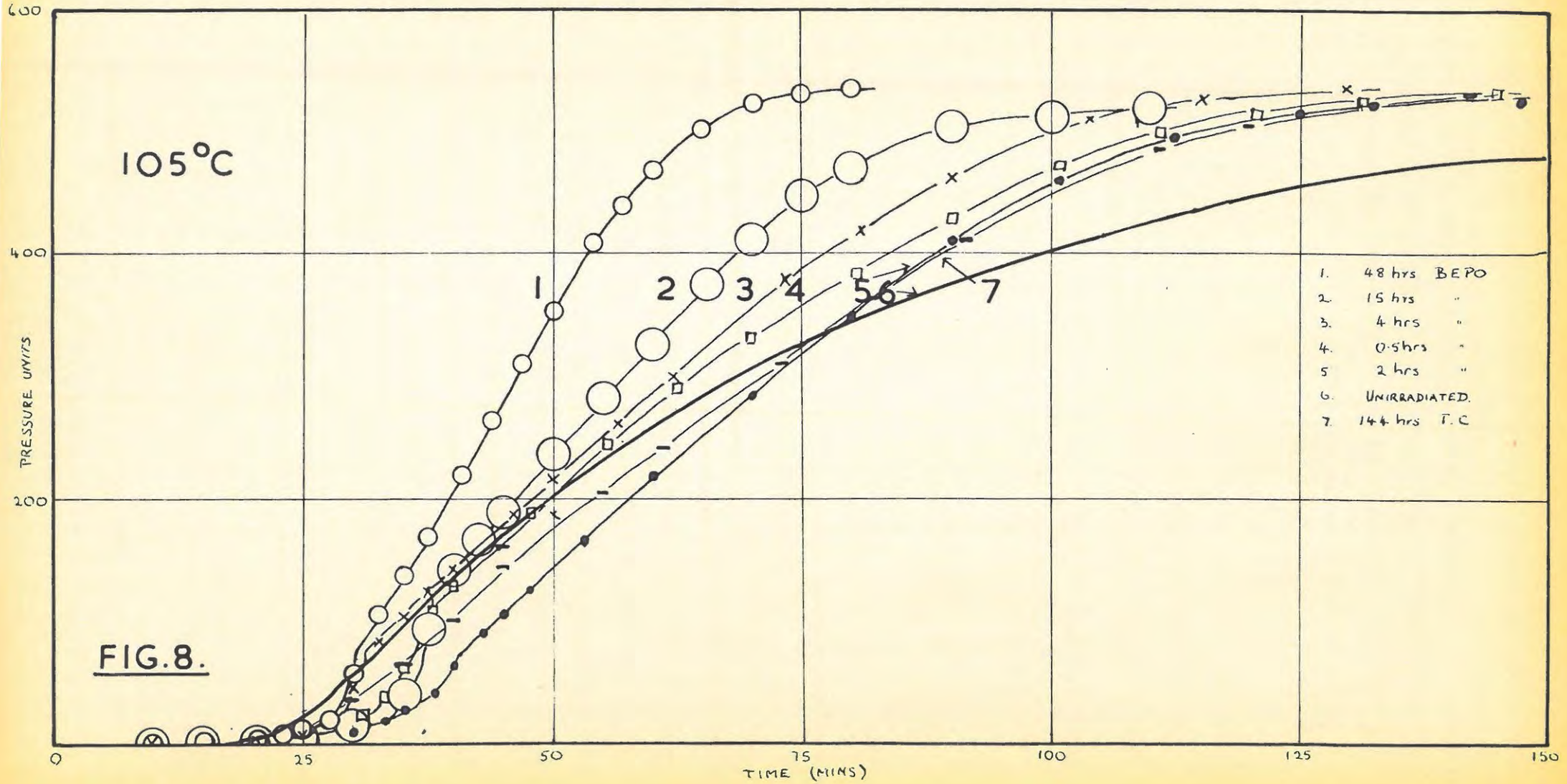

FIG.8.

0.5 hrs BEPO.					
t	p	t	p	t	p
10.0	0.2	37.5	107.0	90.0	431.9
21.5	1.2	40.0	129.1	101.0	472.0
25.0	4.8	48.0	193.4	111.0	500.0
27.5	10.2	55.5	246.0	121.0	516.3
31.0	25.1	62.5	291.0	132.0	526.1
33.0	39.1	70.0	334.0	145.0	530.4
35.0	62.5	80.5	386.3		

UNIRRADIATED.					
t	p	t	p	t	p
5.0	0.2	38.0	122.5	105.0	416.0
10.0	1.3	40.0	137.0	130.0	463.6
15.0	4.7	45.0	172.0	150.0	485.0
20.5	12.5	51.0	208.0	170.0	503.3
25.0	29.0	57.0	247.5	190.0	509.0
27.0	42.1	65.0	283.0	205.0	514.0
31.0	67.7	75.0	330.1	220.0	520.0
35.0	103.0	85.0	362.0		

6.4 EFFECTS OF PRE-IRRADIATION WITH THERMAL NEUTRONS.

Since both neutrons and γ-rays are present in the pile it was necessary to discover whether neutroms alone produced the same effects as did pile-irradiation.

Small and ground crystals were decomposed at 105°C after being irradiated for 144 hours in the "thermal columns" (T.C.) of BEPO. The integrated neutron flux was the same as that obtained in a normal five hour pile irradiation. The results are tabulated below and illustrated graphically in fig. 7 (for small crystals) and in fig. 8 (for ground crystals). The final pressure (p_f) in the case of the latter was somewhat low so the curve was normalised.

TABLE 6. Overleaf/.....

SMALL CRYSTALS.					
t	p	t	p	t	p
10.0	0.4	71.0	36.4	120.0	418.0
16.0	1.4	80.0	54.5	125.0	446.1
20.0	3.0	85.0	71.2	130.0	486.1
25.0	4.5	91.0	111.5	135.0	509.0
31.0	7.6	95.0	148.2	140.0	526.3
35.5	10.1	100.0	203.1	150.0	539.1
41.5	15.3	105.0	264.3	160.0	543.0
50.0	17.0	110.0	317.9	170.0	546.0
61.0	25.8	116.0	381.2		

GROUND CRYSTALS.					
t	p (norm)	t	p (norm)	t	p (norm)
10.0	0.4	45.0	143.4	111.0	485.8
20.0	3.0	55.0	204.0	120.5	503.2
25.0	12.9	61.0	242.8	140.0	514.1
30.0	34.9	73.0	311.1	150.0	515.4
35.0	67.0	82.0	364.0	210.0	520.0
40.0	101.3	91.0	409.0		(p_f=468.0)

6.5 EFFECT OF PRE-IRRADIATION WITH γ-RAYS ONLY.

Pile-irradiation (γ-rays plus neutrons) and neutron irradiation alone had been shown to affect subsequent thermal decomposition. However, it had not been established whether the neutrons or the γ-rays were the chief agents for producing the changes observed, since even neutron bombardment alone would produce γ-rays of capture and decay within the crystal.

Small crystals, irradiated for 6 hours in the "hotspot" previously described, were thermally decomposed at 105°C. Fig.9 shows a comparison of the curve obtained with curves of similarly dosed specimens which had received pile and thermal column treatment.

It was thus apparent that γ-rays alone produced similar effects to those produced in the pile and by thermal neutrons. As treatment with γ-rays offered the simplest approach, the complicating factor of the effects of neutron capture being absent, further study was combined to γ-irradiated crystals.

Firstly, the effect of varying dosage was investigated for batches

-55-/.....

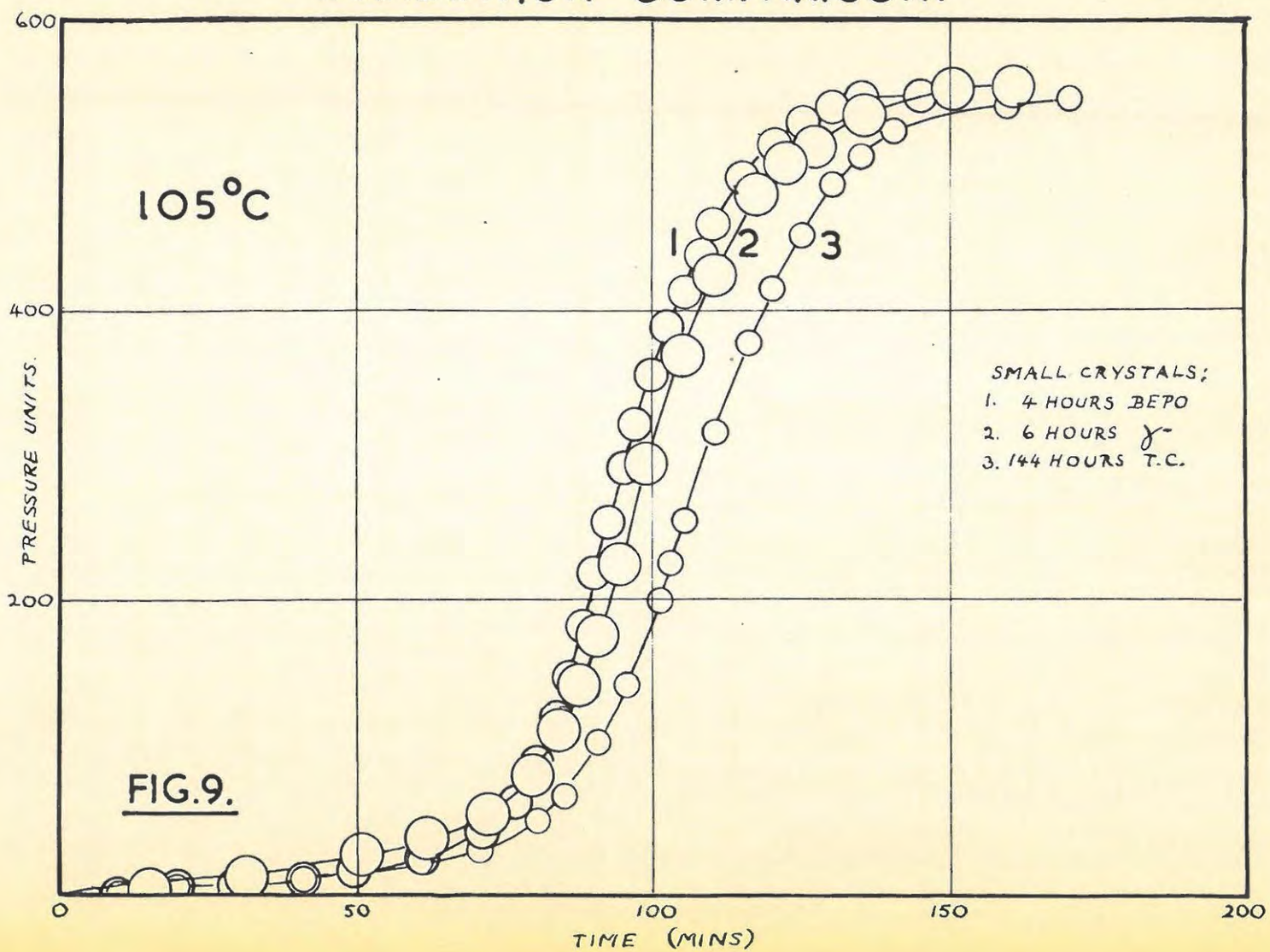
IRRADIATION COMPARISON.
105°C
1
2
3
SMALL CRYSTALS;
1. 4 HOURS BEPO
2. 6 HOURS γ
3. 144 HOURS T.C.
600
400
200
0
50
100
150
200
PRESSURE UNITS.
TIME (MINS)

FIG.9.

of small, large and ground crystals, The crystals were irradiated in the normal way and then thermally decomposed. In the case of the large crystals the decompositions were carried out at 115°C and as final pressures varied somewhat, the curves were normalised. The other two batches were done at 105°C. The results are shown in figs. 10, 11 and 12. Readings are tabulated below.

TABLE 7.

(SMALL CRYSTALS)

64.8 hrs. ✓					
t	p	t	p	t	p
8.0	1.1	52.0	109.3	71.0	467.1
15.0	4.2	53.0	165.0	73.0	486.0
20.0	8.3	55.0	202.3	78.5	526.1
25.0	12.5	57.0	243.5	80.0	533.0
30.5	17.1	59.0	281.5	83.0	544.4
35.0	22.1	61.0	318.5	85.0	546.4
40.0	27.9	63.0	353.0	90.0	552.0
45.5	40.1	65.0	388.1	100.0	553.1
47.5	51.3	67.0	417.0		
49.0	66.6	69.0	442.3		

16.3 hrs. ✓					
t	p	t	p	t	p
10.0	2.0	70.5	95.4	100.0	489.1
20.0	6.5	75.0	162.3	105.0	515.9
31.0	12.4	80.0	236.0	111.0	532.0
40.0	18.1	85.0	308.5	120.0	541.1
50.0	25.4	90.5	390.5	127.5	544.0
60.5	36.0	95.0	442.0	135.0	547.9

6 hrs. ✓					
t	p	t	p	t	p
10.0	2.2	77.0	68.1	110.0	418.5
20.0	7.3	80.0	84.2	116.5	473.0
25.0	10.7	84.0	112.0	121.0	499.0
30.0	13.6	87.0	143.7	127.0	526.3
42.5	21.7	90.0	174.0	136.5	538.5
51.0	27.8	94.0	222.5	142.0	540.0
57.0	33.6	99.0	290.0	150.0	548.0
65.0	42.0	105.0	363.5	160.0	548.0
74.0	56.9				

SMALL CRYSTALS: γ-IRRADIATED.

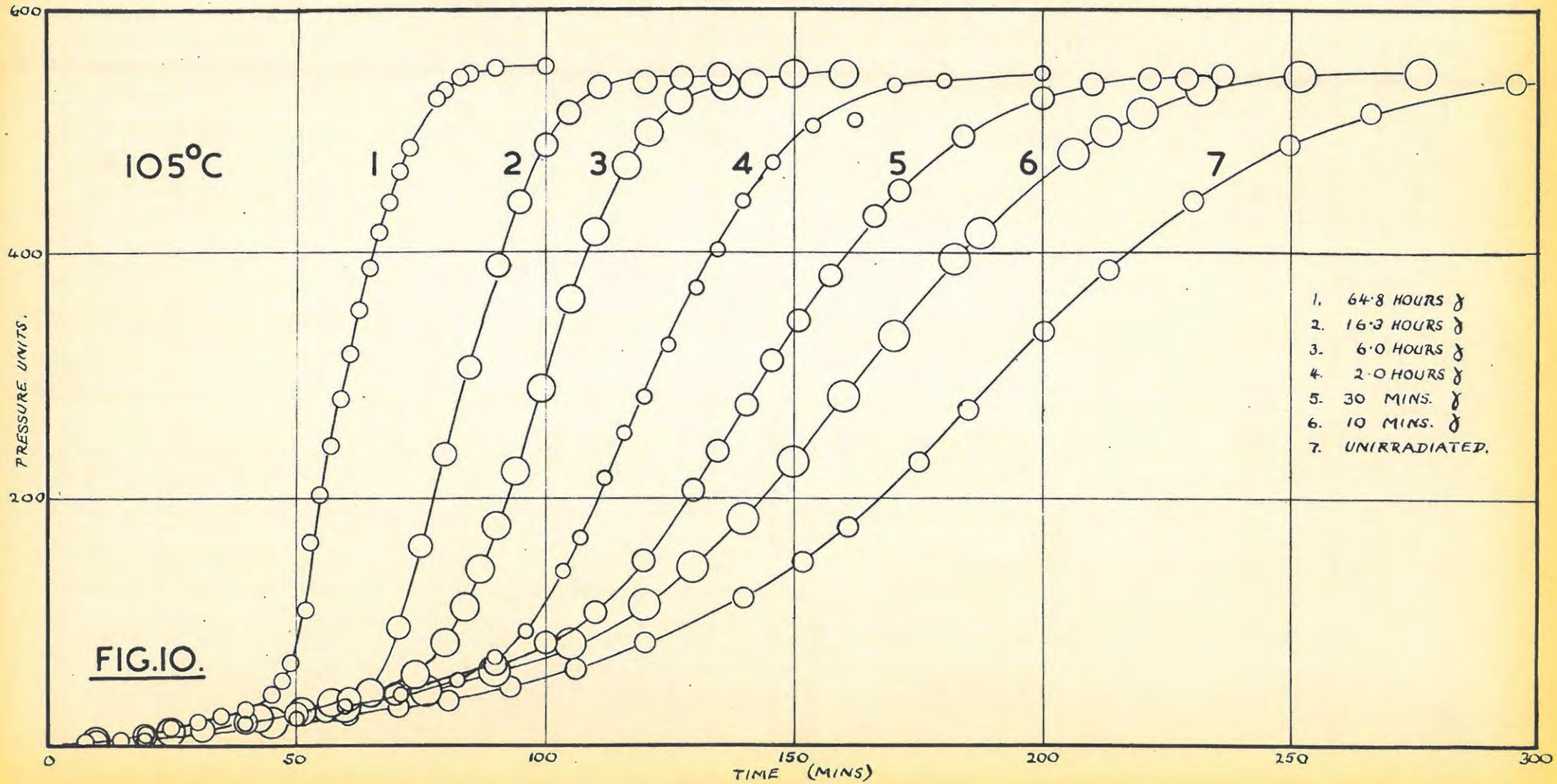

FIG.10.

2 hrs. γ					
t	p	t	p	t	p
11.0	1.7	96.0	92.1	135.0	404.1
20.0	5.2	103.5	141.0	140.0	445.0
32.0	10.6	107.0	168.5	146.0	475.2
40.0	16.4	112.0	217.0	154.0	506.0
50.0	21.6	116.0	253.5	162.0	509.0
60.0	30.8	120.0	284.0	170.0	539.1
71.0	40.3	125.0	326.5	180.0	542.0
82.5	53.1	130.5	372.0	200.0	549.0
90.0	71.2				

30 mins. γ					
t	p	t	p	t	p
25.0	6.9	120.0	150.0	171.0	452.9
35.0	12.2	130.0	207.1	184.0	497.0
56.0	26.2	135.0	240.0	200.0	528.1
70.0	41.0	141.0	277.3	210.0	539.0
80.0	52.8	146.0	313.0	221.0	543.0
90.0	65.4	151.0	346.0	329.0	544.0
100.0	83.1	157.5	383.3	336.0	547.4
110.0	108.5	166.0	433.0		

10 mins. γ					
t	p	t	p	t	p
15.5	2.0	130.0	144.6	206.0	483.3
30.0	7.9	140.0	185.0	212.5	501.0
45.0	17.5	150.0	230.5	220.0	515.1
60.0	28.3	160.0	284.0	232.0	534.0
76.0	44.3	170.0	334.4	251.5	546.4
90.0	60.8	182.0	396.0	276.0	549.0
105.0	83.2	187.5	418.1	300.0	553.2
120.0	114.0				

TABLE 8.

(LARGE CRYSTALS).

220 hrs. γ					
t	p(norm)	t	p(norm)	t	p(norm)
5.0	5.5	17.5	223.5	24.0	528.0
7.0	12.8	18.0	295.8	26.0	553.5
14.0	18.4	19.0	341.0	30.0	581.6
15.5	85.2	20.0	392.1	37.0	590.0
16.5	137.2	22.0	473.4	43.0	591.0 (pf = 467.1)

TABLE 8. CONTINUED: LARGE CRYSTALS.

63 hrs. γ					
t	p(norm)	t	p(norm)	t	p(norm)
5.0	2.4	21.0	295.0	27.0	485.2
14.0	12.3	22.0	331.5	30.0	541.1
18.0	14.6	23.0	362.5	35.0	585.9
19.0	42.1	24.0	393.0	39.0	589.0
20.0	101.2	25.0	421.0	44.0	591.0 (p_f=542.3)

21 hrs. γ					
t	p(norm)	t	p(norm)	t	p(norm)
11.0	2.3	25.0	179.8	38.5	568.1
18.0	7.1	26.0	211.3	44.0	589.0
22.0	10.1	28.0	283.0	49.0	591.0
23.0	24.4	31.0	397.1	56.0	591.0
24.0	74.1	34.0	492.0		(p_f=554.1)

6.3 hrs. γ					
t	p(norm)	t	p(norm)	t	p(norm)
16.0	11.9	37.0	152.5	50.0	553.4
21.0	14.3	40.0	367.3	60.0	584.0
27.0	17.1	43.5	404.0	70.0	589.0
33.0	54.4	46.0	486.1	80.0	591.0
35.0	85.3				(p_f=513.8)

2.1 hrs. γ					
t	p(norm)	t	p(norm)	t	p(norm)
19.0	7.5	41.0	129.8	50.0	520.3
31.0	16.7	42.0	166.5	52.0	571.1
36.0	33.9	43.0	203.5	56.0	589.0
38.0	53.6	44.0	245.0	62.0	591.0
39.0	72.3	45.0	285.0	68.0	(p_f=564.0)
40.0	96.4	47.0	373.2		

TABLE 8. CONTINUED Overleaf/.....

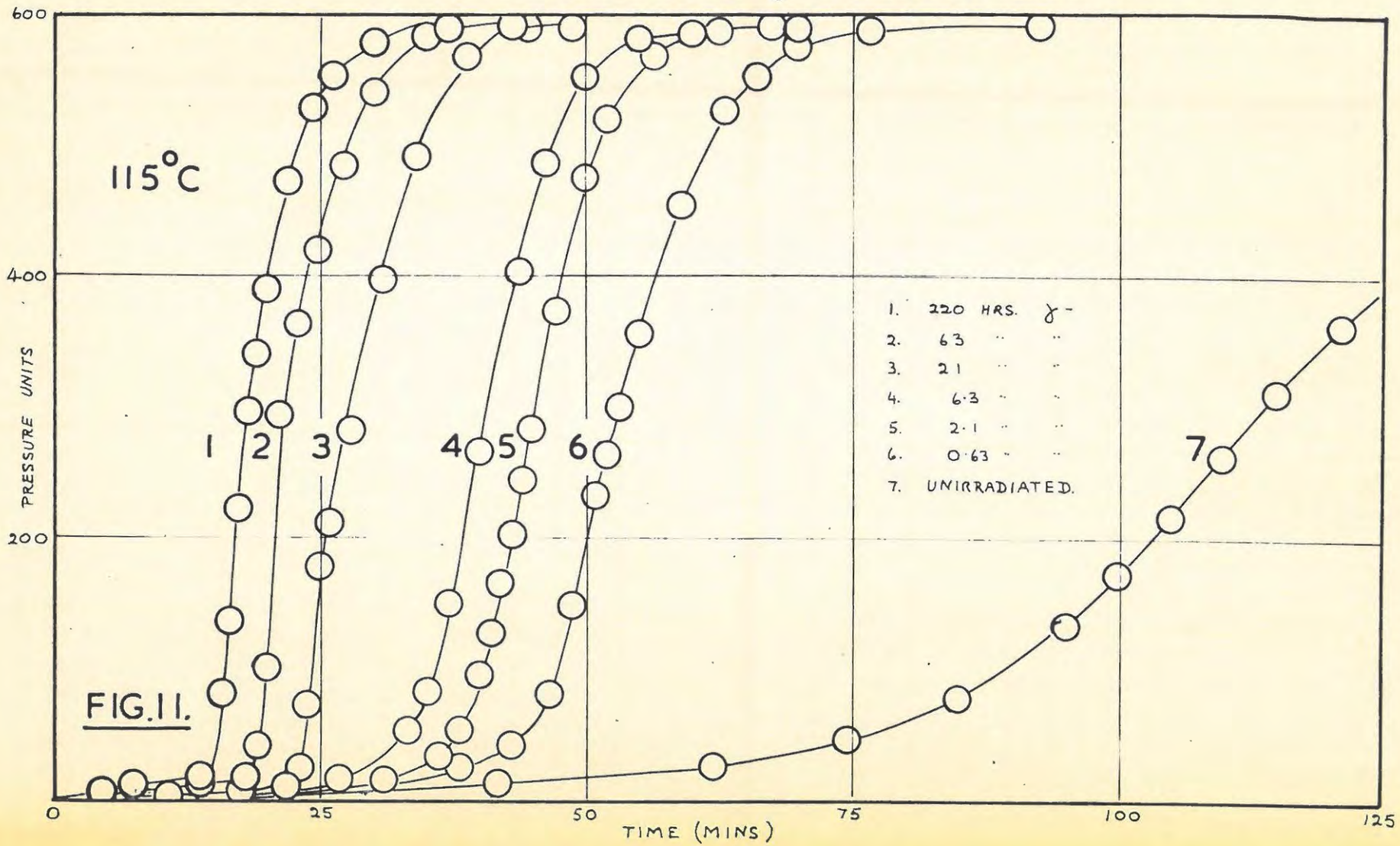
LARGE CRYSTALS: γ-IRRADIATED.
115°C
600
400
200
PRESSURE UNITS
0
25
50
75
100
125
TIME (MINS)
1
2
3
4
5
6
7
1. 220 HRS. γ-
2. 63 " "
3. 21 " "
4. 6·3 " "
5. 2·1 " "
6. 0·63 " "
7. UNIRRADIATED.

FIG.11.

0.63 hrs.					
t	p(norm)	t	p(norm)	t	p(norm)
15.0	5.2	48.5	151.1	63.0	524.9
21.0	7.1	51.0	233.0	66.0	553.0
29.0	14.2	52.0	264.3	70.0	578.1
38.0	26.2	53.0	300.5	77.0	588.4
43.0	43.4	55.0	357.0	93.0	591.0
46.5	81.0	59.0	456.1		(p_f=563.2)

UNIRRADIATED.					
t	p	t	p	t	p
27.0	7.6	100.0	173.1	136.0	466.0
42.0	14.6	105.0	214.9	147.5	515.0
62.0	28.5	110.0	263.8	161.0	552.4
75.0	48.2	115.0	312.0	180.0	575.0
85.0	79.4	121.0	363.2	200.0	588.0
95.0	135.0	127.0	407.1	220.0	591.0

TABLE 9.

(GROUND CRYSTALS)

64.8 hrs.					
t	p	t	p	t	p
11.0	0.5	33.0	130.5	60.0	408.5
20.0	4.2	35.0	157.0	65.5	452.1
23.0	12.0	37.0	175.7	72.5	495.0
25.0	20.0	40.0	208.0	83.5	529.3
27.0	34.2	45.5	267.5	91.5	536.0
29.0	54.1	50.0	313.0	96.0	534.1
31.0	94.7	55.0	362.4	106.0	536.0

16.3 hrs.					
t	p	t	p	t	p
10.0	0.2	40.0	158.0	87.5	482.0
20.0	1.7	43.0	183.5	92.0	496.1
25.0	10.7	46.0	203.5	98.0	515.0
28.0	26.2	50.0	238.0	103.0	522.1
30.0	48.1	55.0	275.5	112.0	534.0
32.5	98.9	60.5	314.8	121.0	537.1
35.0	120.3	68.0	365.1	134.0	539.0
37.5	138.0	75.0	412.7		

TABLE 9 CONTINUED. Overleaf/...

GROUND CRYSTALS: γ-IRRADIATED.

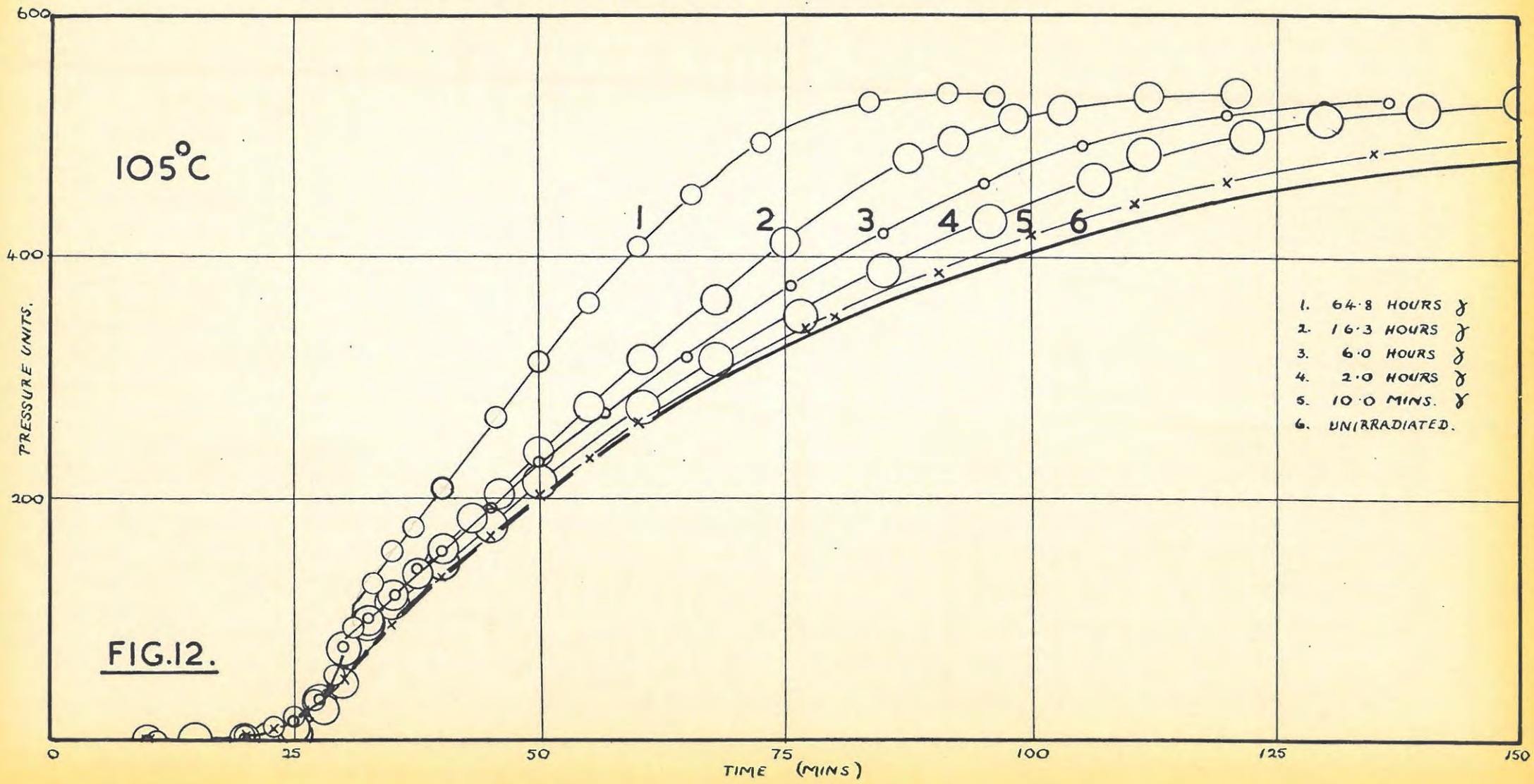

FIG.12.

6 hrs. γ					
t	p	t	p	t	p
10.0	0.2	35.0	121.0	75.5	377.5
20.0	3.0	37.5	142.4	85.0	421.1
22.5	7.5	40.0	156.5	95.0	462.0
25.0	16.1	43.0	193.5	105.0	491.8
27.5	34.0	50.0	230.0	120.0	519.2
30.0	77.6	56.5	271.5	130.0	526.5
32.5	101.6	65.0	318.0	157.0	536.0

2 hrs. γ					
t	p	t	p	t	p
15.0	0.9	40.0	146.8	106.5	465.0
20.0	2.6	45.0	182.5	116.5	501.1
22.5	4.1	50.0	214.5	130.0	515.2
25.0	6.4	60.5	276.5	140.0	523.3
27.5	32.5	68.0	316.0	150.0	530.1
30.0	76.0	76.5	352.2	160.0	532.0
32.5	97.0	85.0	390.0	172.0	535.0
35.0	114.1	95.0	431.0		

10 mins. γ					
t	p	t	p	t	p
10.0	0.5	50.0	204.0	110.5	446.1
20.5	4.6	55.0	234.4	120.0	461.9
23.0	10.9	60.0	263.2	135.0	488.2
26.0	23.9	77.0	342.0	150.0	503.2
30.0	51.8	80.0	353.5	167.0	522.1
35.0	97.3	90.5	390.0	181.0	526.1
40.0	136.7	100.0	420.2	200.0	530.0
45.0	170.7				

UNIRRADIATED.					
t	p	t	p	t	p
5.0	0.2	38.0	122.5	105.0	416.0
10.0	1.3	40.0	137.0	130.0	463.0
15.0	4.7	45.0	172.0	150.0	485.0
20.5	12.5	51.0	208.0	170.0	503.0
25.0	29.0	57.0	247.5	190.0	509.0
27.5	42.1	65.0	283.0	205.0	514.0
31.0	67.7	75.0	330.1	220.0	520.0
35.0	103.0	85.0	362.0		

-60-/.....

6.6 EFFECTS OF INTERRUPTING THERMAL DECOMPOSITIONS FOR γ-IRRADIATION.

Prout and Tompkins (32) had shown that when the thermal decomposition of unirradiated $AgMnO_4$ crystals was interrupted and then continued, the decomposition curve remained unchanged. It was therefore of interest to investigate the effects of interrupting thermal decompositions at various times, irradiating at room temperature, and then continuing the decomposition.

Decompositions of large crystals were carried out at 115°C. Pyrex buckets were used. After decomposing the crystals in the normal way for various times, the buckets were removed from the reaction chamber and sealed off. The samples were then irradiated with γ-rays for 21 hours. After irradiation the decompositions were continued at the same temperature.

The results are shown graphically in fig.13 and are tabulated below. The curves were normalised to the same final pressure.

TABLE 10.

UNINTERRUPTED.					
t	p(norm)	t	p(norm)	t	p(norm)
11.0	2.3	25.0	179.8	38.5	568.3
18.0	7.1	26.0	211.3	44.0	589.0
22.0	10.1	28.0	283.0	49.0	591.0
23.0	24.4	31.0	397.2	56.0	591.0
24.0	74.1	34.0	492.2		

INTERRUPTED AFTER 25 MINS.					
t	p(norm)	t	p(norm)	t	p(norm)
25.0	7.0	44.0	22.4	52.0	330.5
30.0	7.6	46.0	26.7	55.0	459.0
33.0	9.5	47.0	50.3	61.0	569.2
35.0	10.4	48.0	131.3	69.0	589.0
39.0	16.3	49.0	171.0	81.0	591.0
42.0	18.4	50.0	217.1		

TABLE 10 CONTINUED. Overleaf/.....

γ - INTERRUPTED RUNS ON LARGE CRYSTALS.

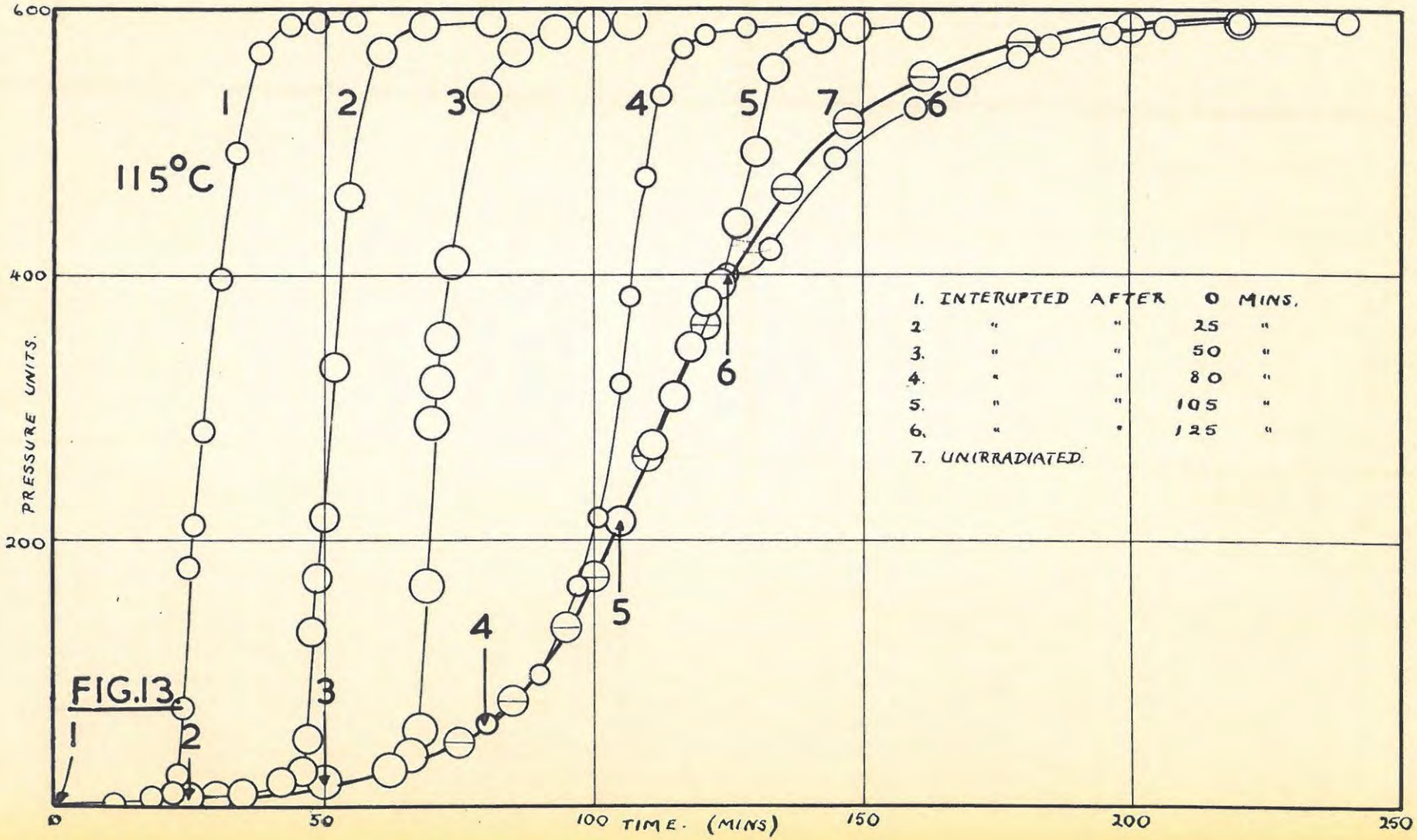

FIG.13.

TABLE 10 CONTINUED.

INTERRUPTED AFTER 50 MINS.					
t	p(norm)	t	p(norm)	t	p(norm)
50.0	18.0	69.0	166.0	80.0	536.9
53.0	18.4	70.0	289.1	85.5	570.2
55.0	20.1	71.0	320.0	93.0	584.1
62.0	27.1	72.0	351.1	100.0	588.2
66.0	38.2	74.0	409.4	107.0	591.0
68.0	56.6				

INTERRUPTED AFTER 80 MINS.					
t	p(norm)	t	p(norm)	t	p(norm)
80.0	64.0	101.0	217.0	117.0	572.0
86.0	73.1	105.0	319.1	121.0	581,0
90.0	99.7	107.0	383.2	129.0	587.0
94.0	132.4	110.0	473.8	140.0	591.0
97.0	166.3	113.0	536.3		

INTERRUPTED AFTER 105 MINS.					
t	p(norm)	t	p(norm)	t	p(norm)
105.0	116.0	121.0	380.0	142.5	579.0
111.0	272.5	124.0	394.3	149.0	581.0
115.0	309.0	130.5	494.4	160.0	590.0
118.0	345.6				

INTERRUPTED AFTER 125 MINS.					
t	p(norm)	t	p(norm)	t	p(norm)
125.0	400.0	168.0	545.5	205.0	588.1
133.0	416.1	179.0	565.5	220.0	591.0
145.0	488.5	185.0	573.1	240.0	592.0
160.0	527.6	196.0	584.0		

6.7 EFFECTS OF INCREASED GRINDING FOLLOWED BY FIXED γ-RAY DOSAGE.

Small crystals of $AgMnO_4$ were ground in an agate mortar for increasing times. Three samples, one ground lightly for~5 minutes, another ground more heavily for ~10 minutes, and a third ground very heavily for ~15 minutes were all irradiated for 63 hours and then thermally decomposed at 105°C. Curves were normalised to the same

-62-/.....

INCREASED GRINDING: γ-IRRADIATION

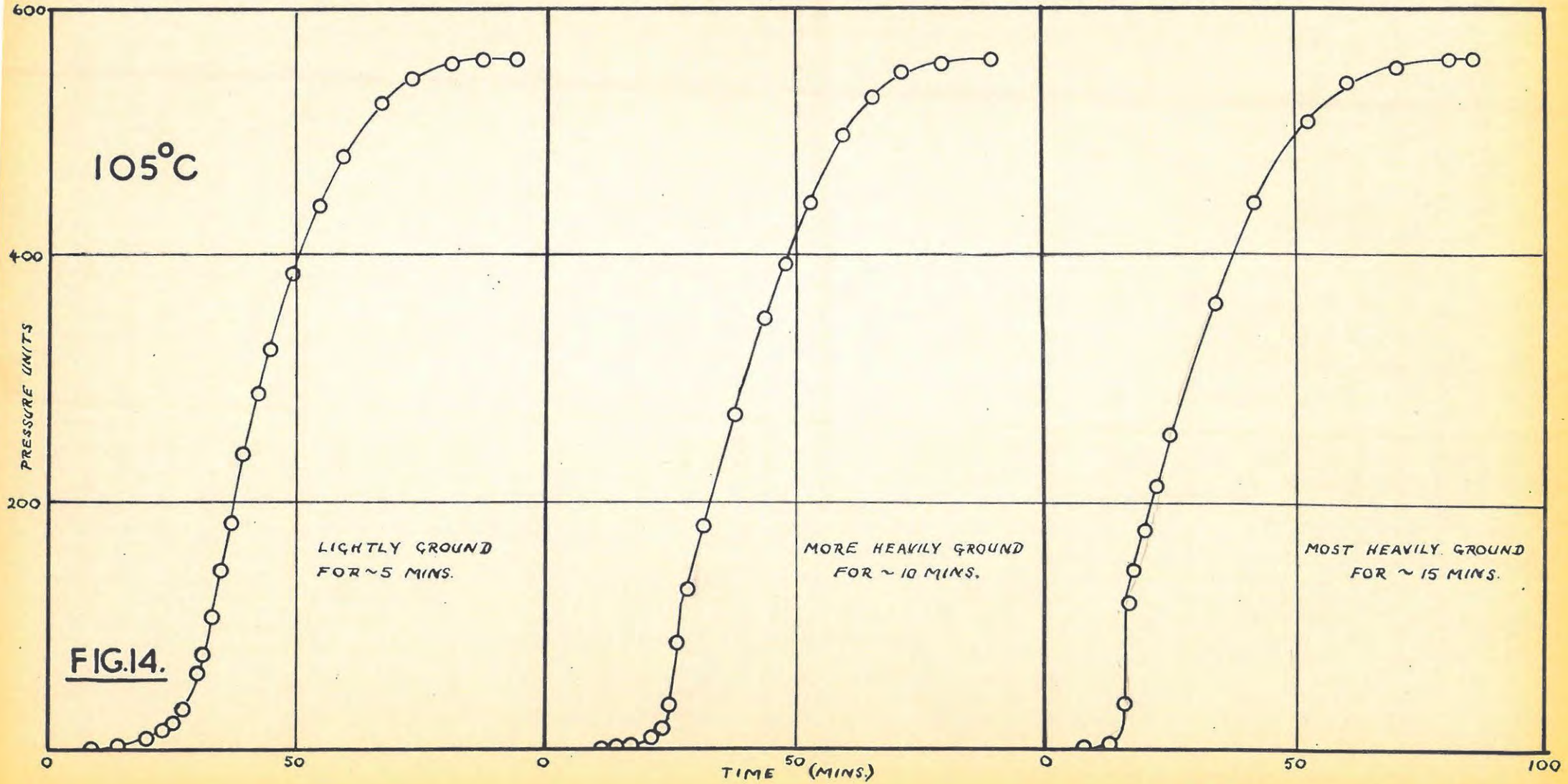

FIG.14.

final pressure.

The results tabulated below and shown graphically in fig.14 indicate that increased grinding shortens the induction period and increases the maximum rate of decomposition. The decay period remains unaffected.

TABLE 11.

GROUND 5 MINS.					
t	p(norm)	t	p(norm)	t	p(norm)
9.0	1.7	33.0	107.8	55.0	440.0
14.0	4.5	35.0	146.2	60.0	480.3
20.0	9.6	37.0	183.9	68.0	524.4
23.0	15.0	40.0	239.0	73.5	543.8
25.0	22.5	42.5	287.2	81.0	553.1
27.0	32.0	45.0	322.5	87.0	560.0
30.0	62.3	50.0	385.0	94.0	560.0
31.0	77.7				(p_f=550.5)

GROUND 10 MINS.					
t	p(norm)	t	p(norm)	t	p(norm)
11.0	2.7	29.0	130.7	60.0	499.0
14.0	4.0	32.0	182.0	65.0	526.5
17.0	5.4	38.0	274.0	71.0	549.0
21.0	12.0	44.0	351.5	80.0	556.1
23.0	19.8	48.0	392.9	90.0	560.0
25.0	38.4	53.0	442.1	100.0	560.0
27.0	88.7				(p_f=550.3)

GROUND 15 MINS.					
t	p(norm)	t	p(norm)	t	p(norm)
8.0	1.7	23.0	213.5	60.0	542.0
13.0	4.3	26.0	258.0	70.0	553.0
16.0	37.9	34.0	360.4	77.0	553.1
17.0	119.0	42.0	443.1	81.0	560.0
18.0	145.7	53.0	507.8	85.0	560.0
20.0	177.5				(p_f=501.0)

6.8 VISUAL OBSERVATIONS.

Visual observations were made of the behaviour of crystals during thermal decomposition. In the case of small, large and ground unirradiated crystals there was no sign of movement or splintering at

-63-/.....

any time during decomposition. After decomposition microscopic examination revealed that there was no apparent change in the external morphology of the crystals except that they were somewhat darker in colour.

However, specimens pre-irradiated in the pile or "hotspot" showed a different behaviour altogether. During the induction period they showed no signs of movement but began to disintegrate at the commencement of the acceleratory period and the disintegration continued until the commencement of the decay period. The pattern of the disintegration varied somewhat but in the case of small and large γ-irradiated crystals two features were marked. Firstly, at the end of induction period the crystals began to jump about violently before splintering into fragments. These fragments then disintegrated to a fairly fine powder. In the case of heavily dosed samples the process could be regarded as an explosion, the material often flying right out of the reaction bucket. As the amount of pre-irradiation was decreased the extent of fracture and disintegration became less.

Further, it was found for both pile- and γ-irradiated specimens, that the time at which physical fracture began coincided with the intercept on the time axis made by the tangent at the point of maximum velocity. The lengths of induction periods were therefore defined in this manner.

Typical behaviour patterns are tabulated below. The corresponding graphs are shown in fig.15.

TABLE 12.

CURVE 1: LARGE CRYSTALS, 63 hrs. γ-, DECOMPOSED AT 115°C.	
t	Behaviour of crystals.
0 - 21 mins.	Crystals remained motionless.
21 - 22 mins.	Crystals started jumping about violently.
22 - 24 mins.	Crystals fractured and disintegrated to a powder.
24 - 50 mins.	No further change.

-64-/.....

VISUAL OBSERVATIONS.

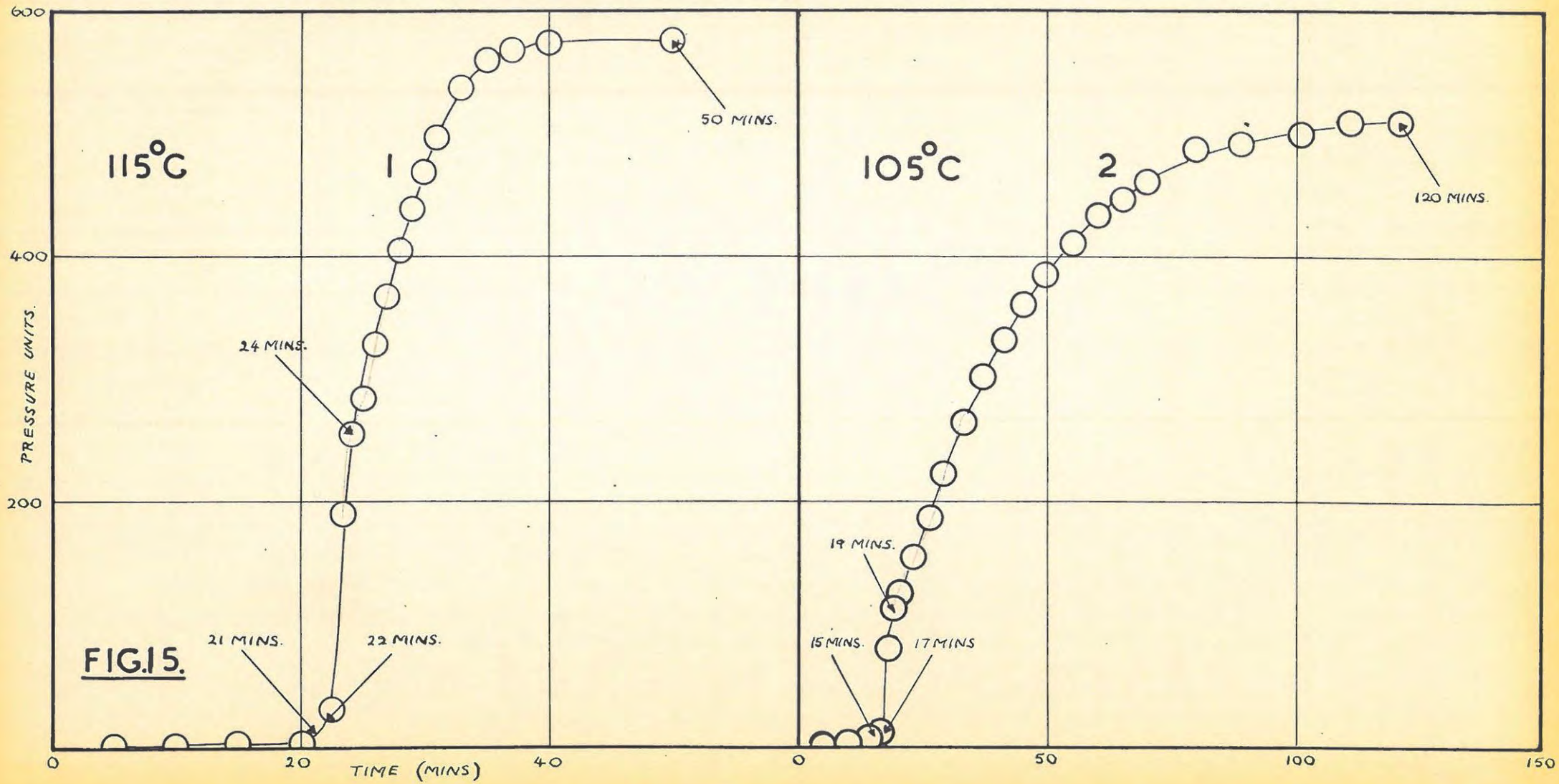

FIG.15.

CURVE 2: GROUND CRYSTALS, 21 hrs. γ-, DECOMPOSED AT 105°C.	
t	Behaviour of particles.
0 - 15 mins.	Particles remained motionless.
15 - 17 mins.	Movement of particles observed.
17 - 19 mins.	Virtual explosion, powder being expelled from reaction bucket.
20 - 120 mins.	No further change.

6.9 ANALYSIS OF PERCENTAGE DECOMPOSITIONS.

Assuming the equation for the decomposition suggested by Prout and Tompkins (32)

$$4AgMnO_4 \longrightarrow 2Ag_2O + 4MnO_2 + O_2$$

percentage decompositions were calculated and are analysed below.

(i) EFFECTS OF AGEING AND GRINDING.

The percentage decomposition was found to decrease slowly with time. This has been attributed to a slow decomposition occurring at room temperature (72). The results are shown in table 13. From this table it is apparent that grinding too decreases the percentage decomposition, a result which was also obtained by Prout and Tompkins (32).

TABLE 13.

SAMPLE.	DECOMPN. TEMP.	AGE.	% DECOMPN.
Small crystals, unirradiated.	105°C	freshly prepared	92.8
Small crystals, unirradiated.	105°C	~2 years.	86.1
Ground crystals, unirradiated.	105°C	freshly prepared	87.4
Ground crystals, unirradiated.	105°C	~ 2 years.	78.6

(ii) EFFECTS OF VARIOUS RADIATIONS.

The percentage decompositions obtained for various irradiated samples are compared in table 14.

TABLE 14 Overleaf. -65-/.....

TABLE 14.

SMALL CRYSTALS.		GROUND CRYSTALS.	
SAMPLE.	% DECOMPOSITION	SAMPLE.	% DECOMPOSITION.
Unirradiated	86.1	Unirradiated	78.6
6 hrs. γ-rays.	86.1	6 hrs. γ-rays.	84.4
4 hrs. BEPO.	86.9	4 hrs. BEPO.	84.3
144 hrs. T.C.	86.0	144 hrs. T.C.	73.7

All the samples in table 14 were aged about 2 years and were decomposed at 105°C.

(iii) EFFECTS OF INCREASING γ-RAY DOSAGE.

A comparison of the effects of increasing γ-ray dosage on various types of crystals is given in table 15.

TABLE 15.

SMALL CRYSTALS.		GROUND CRYSTALS.		LARGE CRYSTALS.	
SAMPLE.	% DECOMPN.	SAMPLE.	% DECOMPN.	SAMPLE.	% DECOMPN.
Unirrad.	86.1	Unirrad.	78.6	Unirrad.	93.3
10 mins	87.1	10 mins	84.4	0.63 hrs	88.8
30 mins	85.6	30 mins	82.3	2.1 hrs	88.9
2 hrs	86.3	2 hrs	84.1	6.3 hrs.	81.1
6 hrs	86.1	6 hrs	84.4	21 hrs	87.0
16.3 hrs	86.1	16.3 hrs	84.7	63 hrs	84.8
64.8 hrs	86.9	64.8 hrs	84.4	220 hrs	72.5

The small and ground crystals in table 15 were all decomposed at 105°C and were aged about 2 years. The large crystals were decomposed at 115°C and were all aged about 4 months except for the unirradiated sample which was freshly prepared.

(iv) REPRODUCIBILITY.

The data of table 16 gives an indication of the degree of reproducibility obtainable. The duplicates refer to decomposition

-66-/.....

carried out within a month of each other.

TABLE 16.

SAMPLE.	% DECOMPOSITION.
Large crystals, 6.3 hrs. γ-	84.1, 85.3, 83.0
Small crystals, 16.3 hrs. γ-	87.1, 86.1.
Ground crystals, 16.3 hrs. γ-	84.8, 80.8.

6.10 EFFECT OF TEMPERATURE.

Several samples were decomposed at varying temperatures to obtain the critical increment of the processes taking place.

(i) Small unirradiated crystals.

The results are tabulated below and shown graphically in fig.16. The graphs were all normalised to the same final pressure for comparison purposes.

TABLE 17.

131.5°C.					
t	p(norm)	t	p(norm)	t	p(norm)
4.0	1.4	21.0	239.9	30.0	491.0
10.0	16.0	22.0	288.5	32.0	507.8
14.0	35.8	23.0	334.1	35.0	513.2
18.0	86.7	24.0	371.2	40.0	520.0
19.0	117.0	25.0	411.0	45.0	520.0
20.0	178.0	27.0	460.0		

125°C.					
t	p(norm)	t	p(norm)	t	p(norm)
7.0	4.0	25.0	98.4	40.0	428.0
11.0	15.7	27.5	138.1	42.5	463.8
15.0	24.0	30.0	196.0	45.5	490.0
17.5	35.6	32.5	272.3	50.0	508.1
20.0	51.3	35.0	326.2	60.0	520.0
22.5	71.8	37.5	388.0	70.0	520.0

-67-/.....

UNIRRADIATED SMALL CRYSTALS: TEMPERATURE VARIATION.

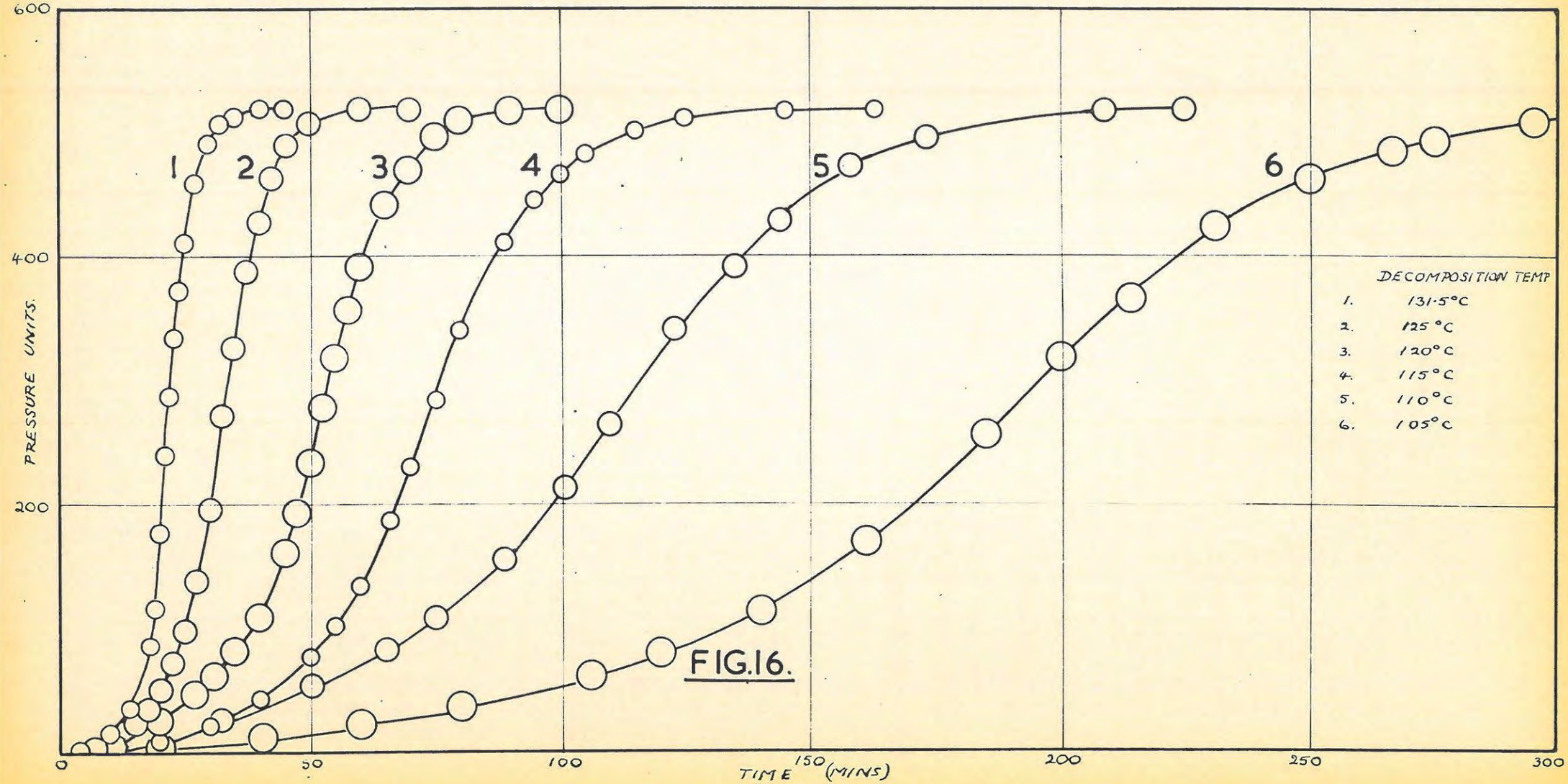

FIG.16.

TABLE 17. CONTINUED.

120°C					
t	p(norm)	t	p(norm)	t	p(norm)
10.0	4.5	47.5	193.5	65.0	442.0
20.0	28.0	50.0	233.3	70.0	471.0
27.0	47.5	52.5	278.0	75.0	499.3
31.0	61.8	55.0	319.0	80.0	510.0
35.0	81.9	57.5	356.8	90.0	520.0
40.0	110.5	60.0	392.1	100.0	520.0
45.0	161.5				

115°C					
t	p(norm)	t	p(norm)	t	p(norm)
10.0	3.6	66.0	187.0	100.0	468.3
20.0	9.3	70.0	230.5	105.0	485.9
30.0	22.1	75.0	285.0	115.0	503.0
40.0	44.6	80.0	341.1	125.0	513.2
50.0	76.3	89.0	412.2	145.0	520.0
55.0	102.0	95.0	446.0	163.0	520.0
60.0	134.4				

110°C					
t	p(norm)	t	p(norm)	t	p(norm)
10.0	3.2	89.0	156.5	158.5	472.3
20.0	16.1	101.0	214.5	173.5	498.0
32.0	27.2	110.0	265.5	187.0	511.2
43.0	43.1	124.0	343.0	209.0	520.0
50.0	54.1	135.0	394.1	225.0	520.0
65.0	83.0	144.0	431.1		
75.0	109.2				

105°C.					
t	p(norm)	t	p(norm)	t	p(norm)
20.0	5.1	140.0	114.0	250.0	463.2
40.5	12.0	161.0	170.6	266.5	486.0
60.0	23.0	185.0	257.0	274.0	494.4
80.0	37.7	200.0	319.4	295.0	511.2
106.0	61.6	214.0	367.1	318.0	520.0
120.0	80.7	231.0	425.0		

(ii) Large unirradiated crystals.

The results are tabulated below and shown graphically in fig. 17.

TABLE 18. Overleaf. -68-/.....

TABLE 18.

130°C.					
t	p(norm)	t	p(norm)	t	p(norm)
10.0	5.0	33.0	214.0	43.0	512.0
20.0	19.1	34.0	256.5	45.0	531.3
25.0	38.0	35.0	299.1	48.0	560.0
27.0	54.5	36.0	355.1	51.0	574.2
29.0	84.5	37.0	373.1	55.0	580.1
30.0	109.2	39.0	434.2	61.0	583.0
31.0	137.5	41.0	478.8	88.0	593.0
32.0	174.3				

125°C					
t	p(norm)	t	p(norm)	t	p(norm)
10.0	3.0	45.0	166.0	65.0	522.1
20.0	13.5	47.5	220.5	71.0	555.9
25.0	20.6	50.0	279.1	75.0	570.0
30.5	31.9	52.5	336.4	80.0	576.3
36.0	55.0	58.0	440.0	87.5	588.0
41.0	98.1	61.0	482.3	100.0	593.0

120°C.					
t	p(norm)	t	p(norm)	t	p(norm)
10.0	1.5	65.0	157.5	100.0	535.2
20.0	8.7	70.0	227.0	110.0	570.1
31.0	16.4	75.0	299.1	124.0	586.3
40.0	26.8	80.0	368.3	133.0	590.2
50.0	49.6	85.0	426.1	145.0	593.0
61.5	121.0	90.5	477.0		

115°C.					
t	p(norm)	t	p(norm)	t	p(norm)
10.0	1.0	100.0	173.4	136.0	466.2
27.0	7.6	105.0	215.2	147.5	515.0
42.0	14.6	110.0	263.1	161.0	551.8
62.0	28.5	115.0	311.9	180.0	575.1
75.0	48.2	121.0	363.0	200.0	588.1
85.0	79.4	127.0	407.0	230.0	593.0
95.0	135.0				

-69-/.....

UNIRRADIATED LARGE CRYSTALS: TEMPERATURE VARIATION.

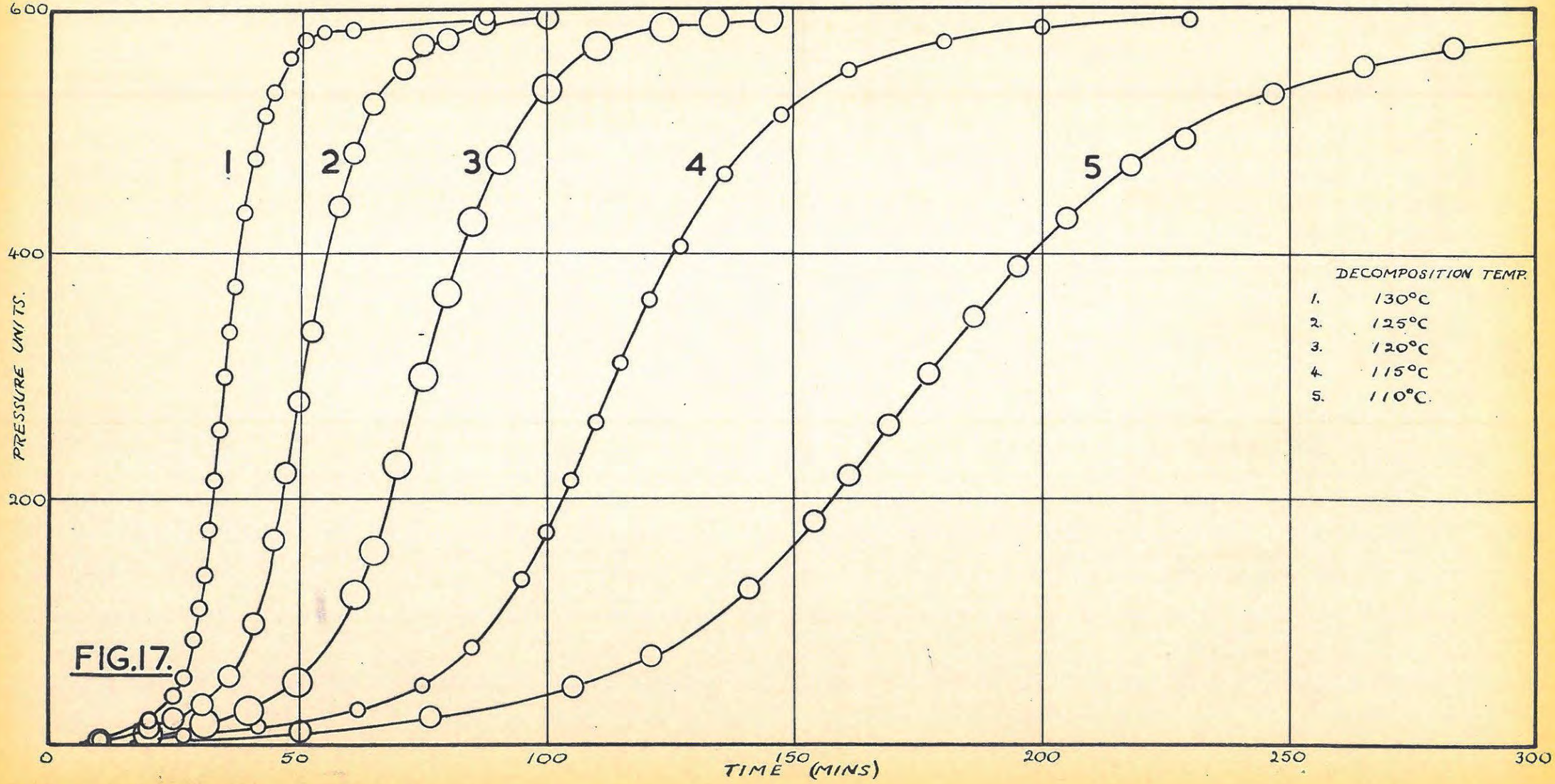

FIG.17.

TABLE 18. CONTINUED.

110°C.					
t	p(norm)	t	p(norm)	t	p(norm)
20.0	3.0	161.0	219.0	218.0	472.5
50.0	11.5	169.0	260.0	229.0	495.1
76.5	22.9	177.0	301.8	247.0	532.4
105.0	47.5	186.0	349.0	265.0	553.2
121.0	72.0	195.0	390.2	283.0	569.0
141.0	126.5	205.0	430.0	340.0	593.0
154.0	181.5				

(iii) Small crystals, 15 hrs. BEPO.

The results are tabulated below and shown graphically in fig.18.

TABLE 19.

124°C.					
t	p(norm)	t	p(norm)	t	p(norm)
9.0	4.9	19.0	144.1	24.0	481.2
11.0	9.6	20.0	266.3	25.0	495.0
13 0	13.2	21.0	350.0	26.5	517.4
15.0	19.0	22.0	412.1	30.0	515.2
17.0	29.0	23.0	452 9	35.0	520.0
18.0	45.5				

120°C.					
t	p(norm)	t	p(norm)	t	p(norm)
10.0	5.8	22.0	154.3	28.0	477.0
15.0	14.1	23.0	244.4	29.0	492.3
17.0	19.1	24.0	315.5	30.0	506.1
19.0	27.4	25.0	374.2	32.0	515.3
20.0	33.8	26.0	418.8	34.0	520.0
21.0	66.0	27.0	452.0	41.0	520.0

115°C.					
t	p(norm)	t	p(norm)	t	p(norm)
5.0	1.0	27.0	134.3	35.0	412.8
10.0	6.5	28.0	176.0	37.0	449.9
15.0	13.3	29.0	220.1	39.0	482.0
20.0	24.2	30.0	256.5	41.0	498.0
22.0	30.3	31.0	391.0	43.0	503.2
24.0	39.9	32.0	328.0	45.0	514.2
25.0	47.5	33.0	356.4	54.0	519.6
26.0	87.8	34.0	390.0	60.0	520.0

-70-/.....

SMALL, 15 HRS. BEPO: TEMPERATURE VARIATION.

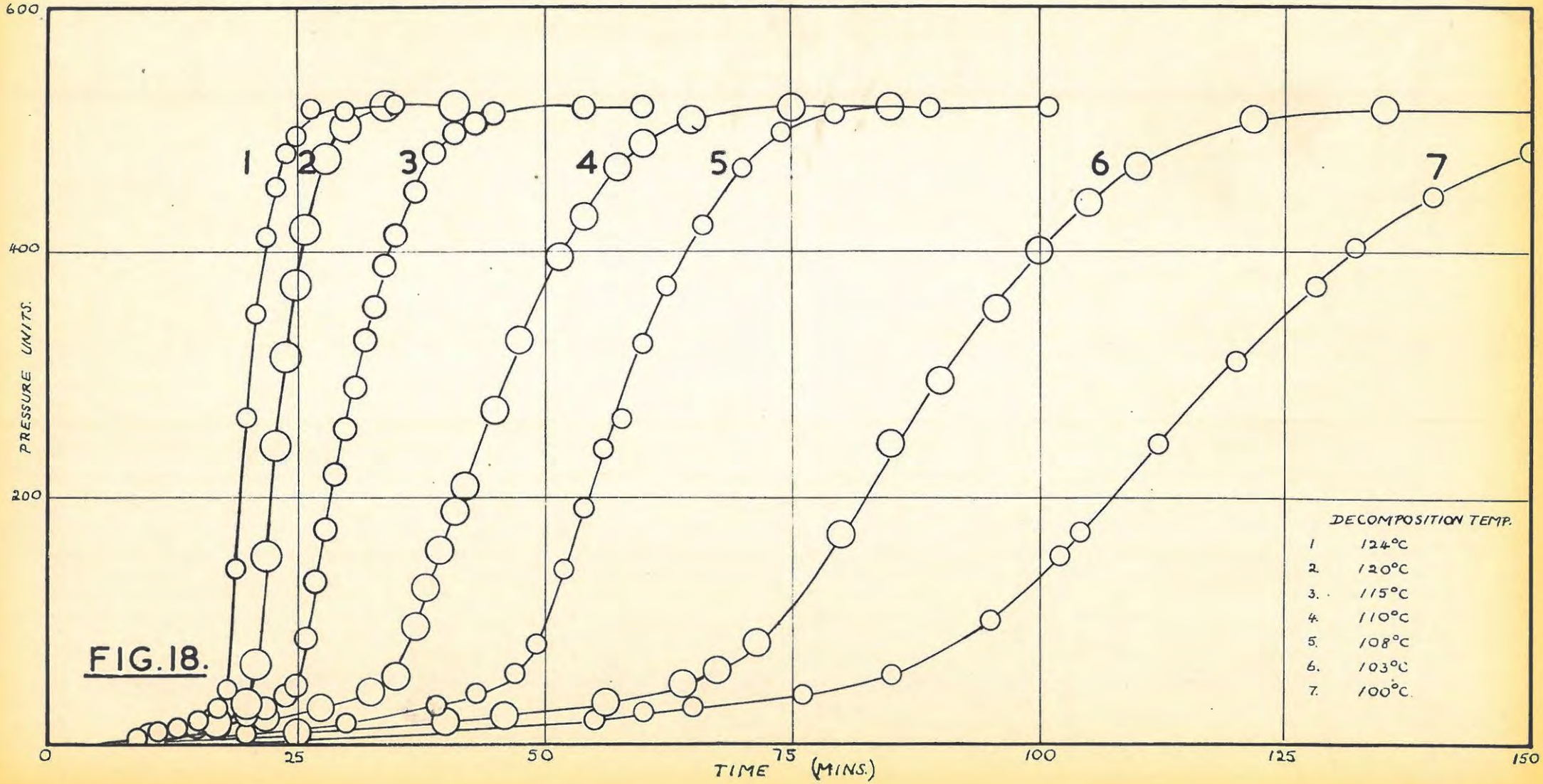

FIG. 18.

110°C.					
t	p(norm)	t	p(norm)	t	p(norm)
10.0	6.4	38.0	128.0	54.0	430.0
17.0	15.8	39.5	159.4	57.5	471.1
22.0	21.0	41.0	190.2	60.0	490.0
27.5	30.1	42.0	211.5	65.0	510.0
32.5	42.8	45.0	273.0	75.0	519.6
35.0	55.0	47.5	328.9	85.0	520.0
37.0	97.3	51.5	398.0		

108°C.					
t	p(norm)	t	p(norm)	t	p(norm)
10.0	1.4	52.0	144.0	66.0	425.0
20.0	9.5	54.0	193.5	70.0	471.1
30.0	17.1	56.0	241.4	74.0	500.3
39.0	32.1	58.0	266.3	79.0	516.2
43.0	42.3	60.0	328.1	89.0	520.0
47.0	59.6	62.5	374.1	101.0	520.0
49.0	83.4				

103°C.					
t	p(norm)	t	p(norm)	t	p(norm)
11.0	1.8	67.5	60.4	95.5	356.2
25.0	10.9	71.5	83.3	100.0	403.9
40.0	19.0	75.0	104.0	105.0	442.8
46.0	24.5	80.0	172.5	110.0	472.0
56.0	35.5	85.0	246.3	122.0	510.3
64.0	50.6	90.0	296.5	135.0	520.0

100°C.					
t	p(norm)	t	p(norm)	t	p(norm)
20.0	6.7	102.0	155.3	150.0	483.4
55.0	21.6	104.0	174.0	161.0	502.1
60.0	26.6	112.0	245.0	180.5	511.8
65.0	30.1	120.0	311.9	196.0	516.3
76.0	41.3	128.0	374.2	215.0	520.0
85.0	58.2	132.0	405.5	230.0	520.0
95.0	102.1	140.0	448.4		

(iv) Small crystals, 6 hrs.

The results are tabulated below and shown graphically in fig.19.

TABLE 20. Overleaf.

-71-/.....

TABLE 20.

120°C.					
t	p(norm)	t	p(norm)	t	p(norm)
5.0	1.9	25.0	107.3	32.0	437.5
10.0	11.0	26.0	198.0	34.5	488.9
15.0	20.7	27.0	253.2	36.0	502.2
17.0	25.2	28.0	293.1	38.0	513.1
20.0	35.2	29.0	332.2	40.0	519.2
22.0	42.3	30.0	372.4	50.0	520.0
23.0	47.6	31.0	406.4	60.0	520.0
24.0	58.5				

115°C.					
t	p(norm)	t	p(norm)	t	p(norm)
15.0	13.0	40.0	68.5	54.0	439.2
20.0	17.7	42.0	95.2	58.0	488.0
26.5	28.5	44.0	149.1	60.0	501.8
29.0	32.6	46.0	221.1	62.0	512.3
32.0	40.7	48.0	286.5	64.0	516.4
34.0	45.1	50.0	344.2	70.0	520.0
36.0	51.0	52.0	394.1	79.0	520.0
38.0	57.0				

113°C.					
t	p(norm)	t	p(norm)	t	p(norm)
13.0	5.2	50.0	142.0	65.5	469.0
20.0	12.0	52.0	197.6	70.0	500.1
30.0	26.3	54.0	250.9	78.0	518.3
40.0	47.3	56.0	320.0	85.0	520.0
44.0	60.1	60.0	392.1	90.0	520.0
48.0	97.7	62.0	424.8		

110°C.					
t	p(norm)	t	p(norm)	t	p(norm)
12.0	2.0	63.0	117.5	85.0	437.7
20.0	11.0	64.0	131.0	89.0	469.1
26.0	16.5	66.0	160.2	94.0	491.3
35.0	25.6	70.0	225.9	99.0	507.8
41.0	34.4	72.0	264.1	105.0	508.4
47.0	43.7	74.0	293.1	113.5	513.6
54.0	55.2	78.0	354.0	138.0	520.0
62.0	104.3	82.0	406.0		

-72-/.....

SMALL, 6 HRS. γ: TEMPERATURE VARIATION.

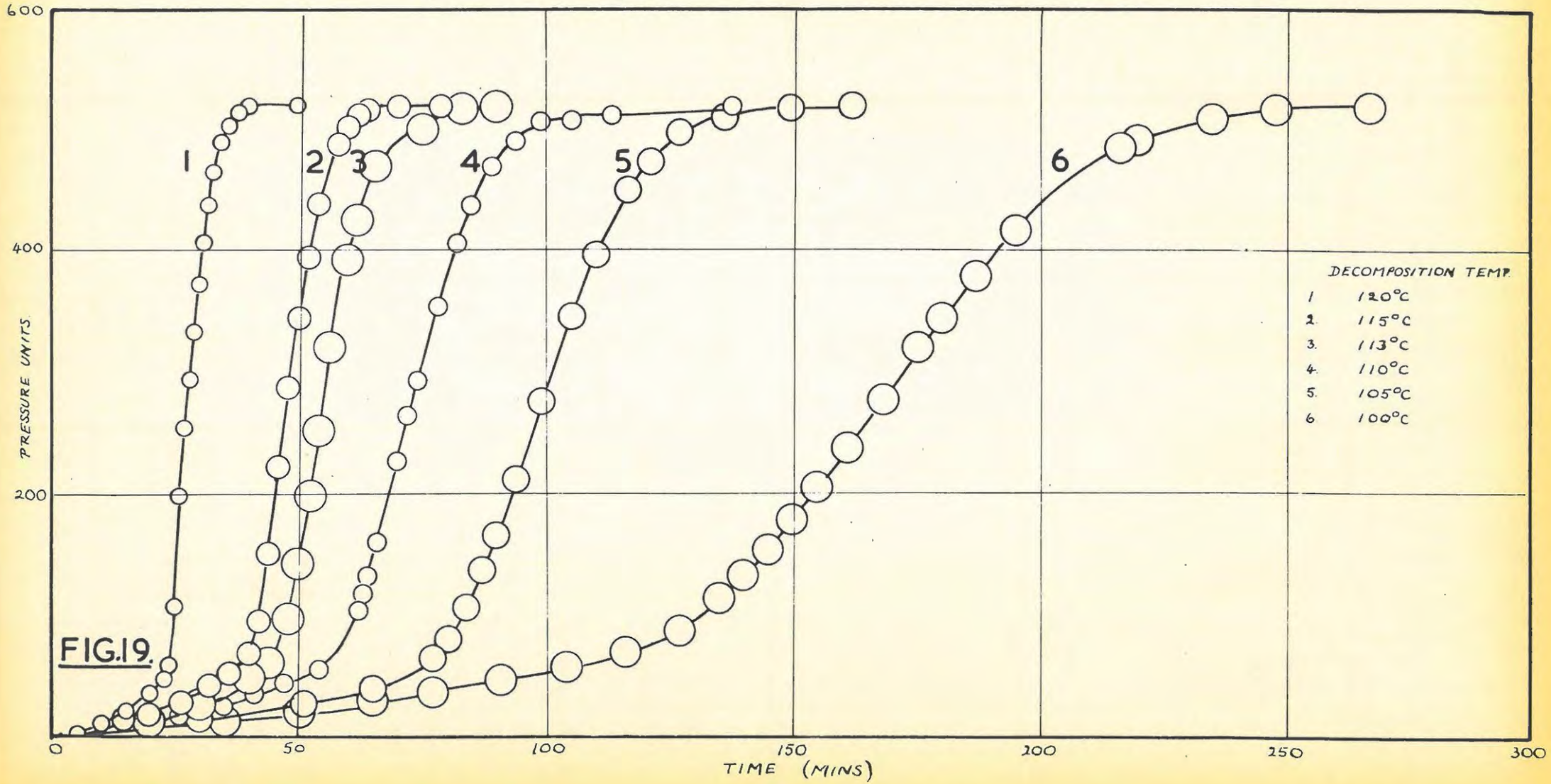

FIG.19.

TABLE 20. CONTINUED.

105°C.					
t	p(norm)	t	p(norm)	t	p(norm)
10.0	2.9	84.0	106.3	116.5	450.0
20.0	6.9	87.0	136.5	121.0	474.3
30.0	12.9	90.0	165.0	127.0	499.0
51.0	26.4	94.0	211.5	136.5	511.0
65.0	39.9	99.0	276.0	150.0	520.0
77.0	64.6	105.0	346.5	162.0	520.0
80.0	79.8	110.0	396.9		

100°C.					
t	p(norm)	t	p(norm)	t	p(norm)
35.0	12.6	135.0	113.0	180.0	345.3
50.0	19.6	140.0	132.5	187.0	380.0
65.0	29.2	145.0	153.0	195.0	418.3
77.0	36.3	150.0	178.9	216.5	485.7
91.0	47.3	155.0	205.0	220.0	492.2
104.0	58.0	161.0	238.0	235.0	510.4
116.0	70.5	168.0	277.8	248.0	517.1
127.0	88.7	175.0	321.1	267.0	520.0

6.11 APPLICABILITY OF MATHEMATICAL EQUATIONS.

Prout and Tompkins showed that the p-t plots for the decomposition of small crystals of $AgMnO_4$ were well fitted by the equation

$$\log \frac{p}{p_f - p} = k \log t + c \qquad \text{(6.1)}$$

In their determinations of the activation energies of the acceleratory and decay periods they employed the relationships

$$\log \frac{p}{p_f - p} = kt + c \qquad \text{(6.2)}$$

and $\log (p_f - p) = kt + c.$ (6.3)

respectively. These two equations were used both for small and ground crystals.

The above equations and others which have previously been used were tested for applicability. A summary of the results obtained is given in fig.20.

It is evident that a given section of any curve is fitted by more than one equation. This fact emphasises again that, as such, these equations provide little knowledge about processes occurring during

-73-/.....

APPLICABILITY OF EQUATIONS.

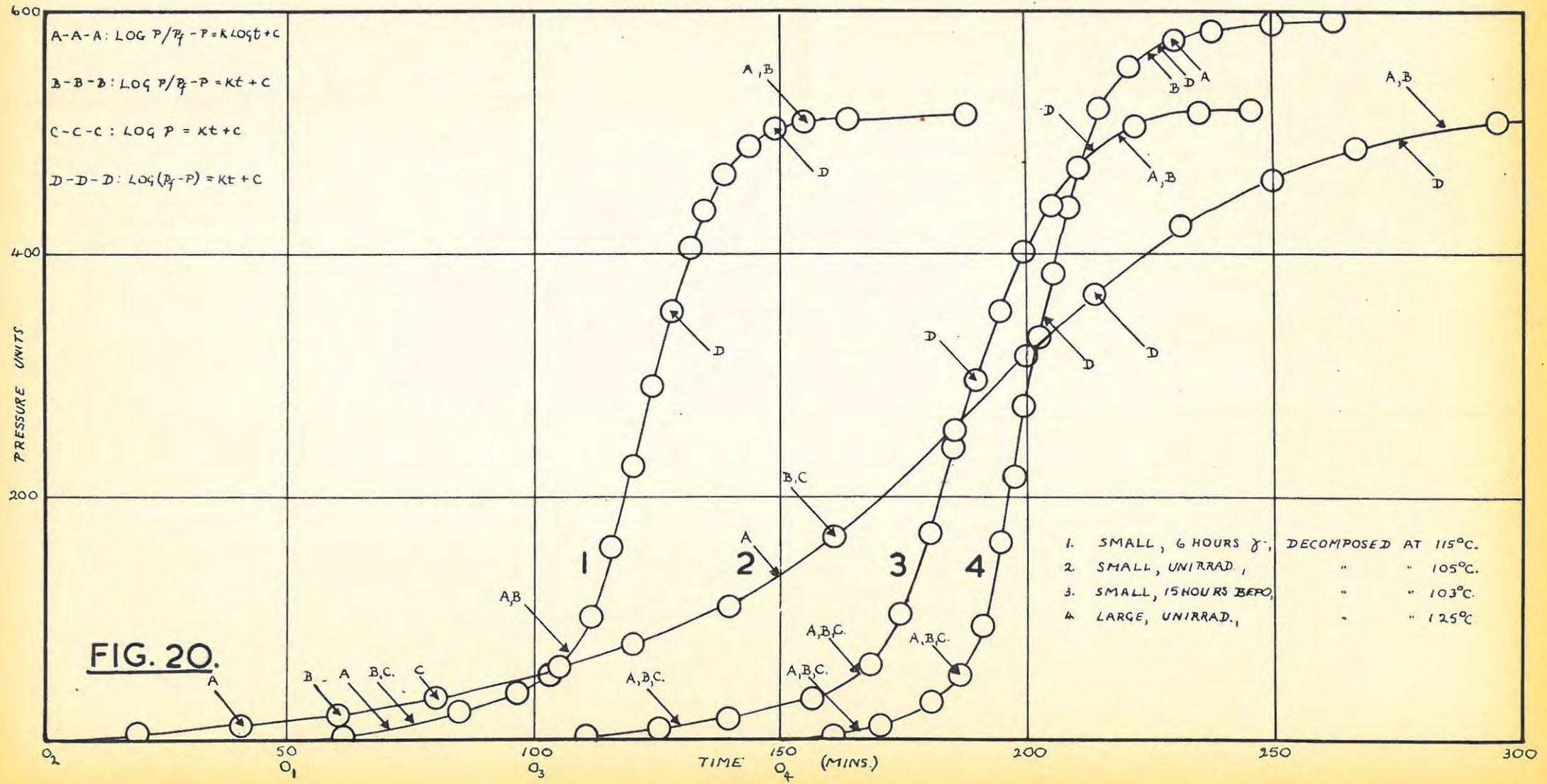

FIG. 20.

DEGREE OF FIT.

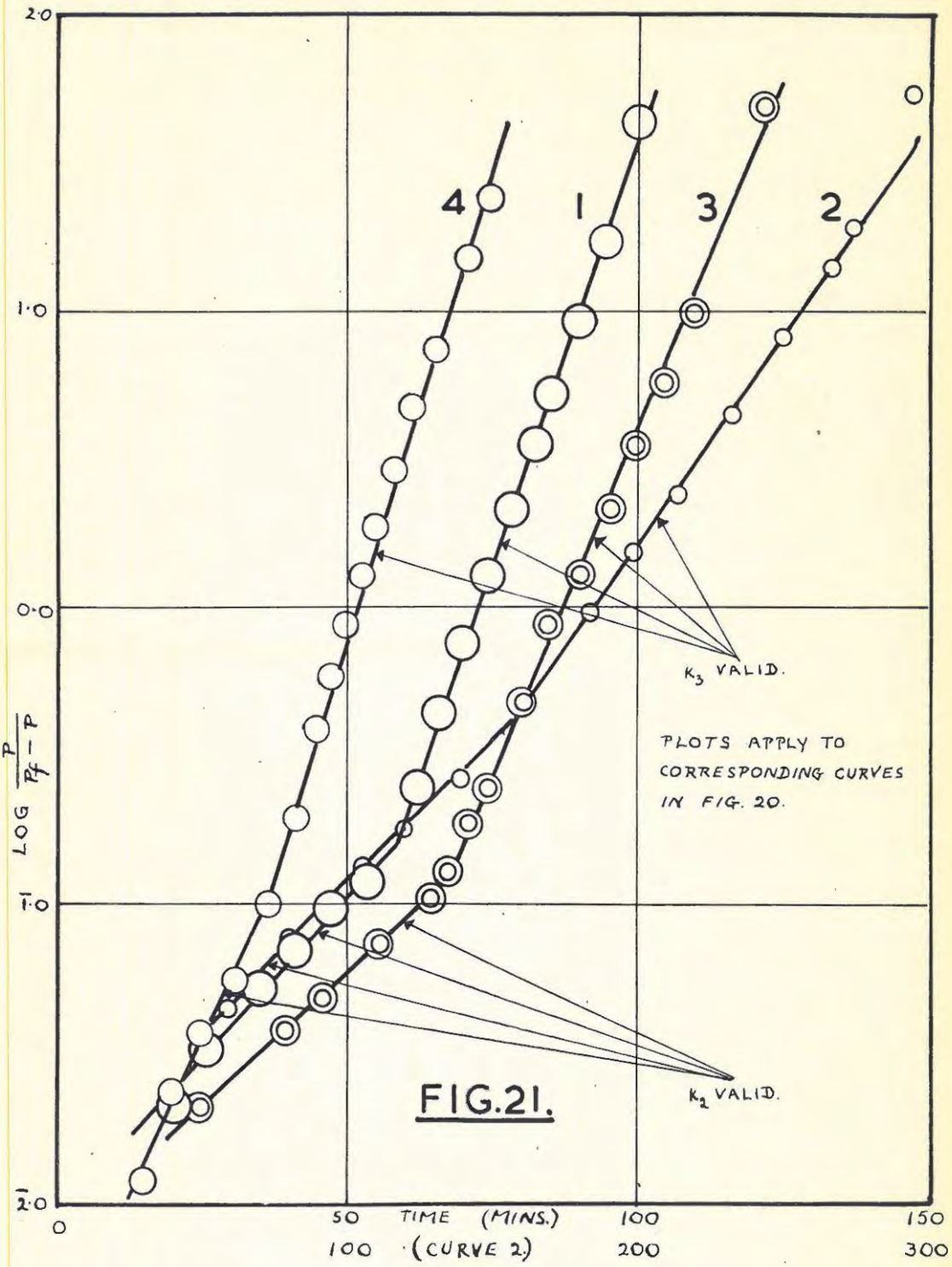

FIG.21.

decomposition.

In the subsequent determination of activation energies it was found convenient to use equation (6.2). Fig.2.1 shows the degree of fit obtainable when it is used. K_2 and K_3 represent the values of k in (6.2) which hold over the acceleratory and decay periods respectively.

7. ANALYSIS OF RESULTS.

7.1 INDUCTION PERIODS (I.P.)

Silver permanganate does not have a true induction period as is the case with potassium permanganate. Thus for unirradiated crystals there is no sharp distinction between the end of the induction period and the commencement of the acceleratory period.

In the case of irradiated crystals, however, it has already been shown that the end of the induction period may be more sharply defined. Using the criterion stated in section 6.8 activation energies (E_1) were calculated from the plot of log $\frac{1}{\text{I.P.}} / \frac{1}{T^{\circ}A}$ for various irradiated specimens. The results are shown in Tables 21 and 22 and in Fig.22.

TABLE 21.

SMALL CRYSTALS, 6 HRS. γ -		SMALL CRYSTALS, 15 HRS. BEPO.	
Decompn. Temp.	I.P. (mins)	Decompn. Temp.	I.P. (mins)
100°C	116.0	100°C	86.5
105°C	77.0	103°C	68.0
110°C	56.0	108°C	46.5
113°C	46.0	110°C	32.5
115°C	39.5	115°C	24.5
120°C	24.5	120°C	20.2
LARGE CRYSTALS, 38 MINS. γ -		LARGE CRYSTALS, 220 HRS. γ -	
Decompn. Temp.	I.P. (mins)	Decompn. Temp.	I.P. (mins)
110°C	67.0	105°C	51.0
115°C	43.0	110°C	35.0
120°C	30.6	117.5°C	20.0
125°C	21.0	120°C	16.0
		125°C	9.7

TABLE 22.

SPECIMEN	E_1 (eV)
Small crystals, 6 hrs. γ -	1.03
Small crystals, 15 hrs. BEPO	1.02
Large crystals, 38 mins. γ -	1.02
Large crystals, 220 hrs. γ -	1.06

-75-/.....

INDUCTION PERIOD: ACTIVATION ENERGIES.

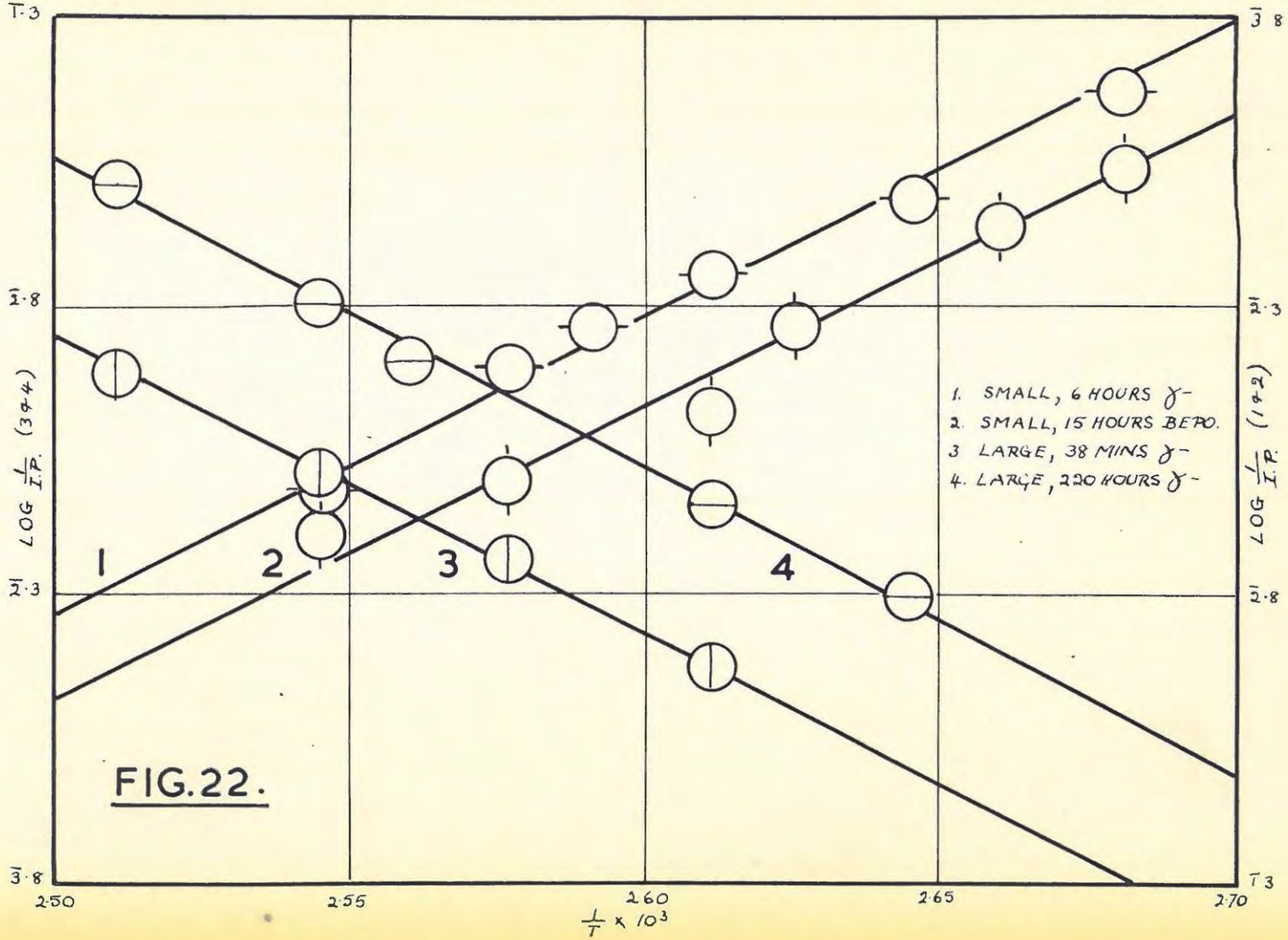

FIG.22.

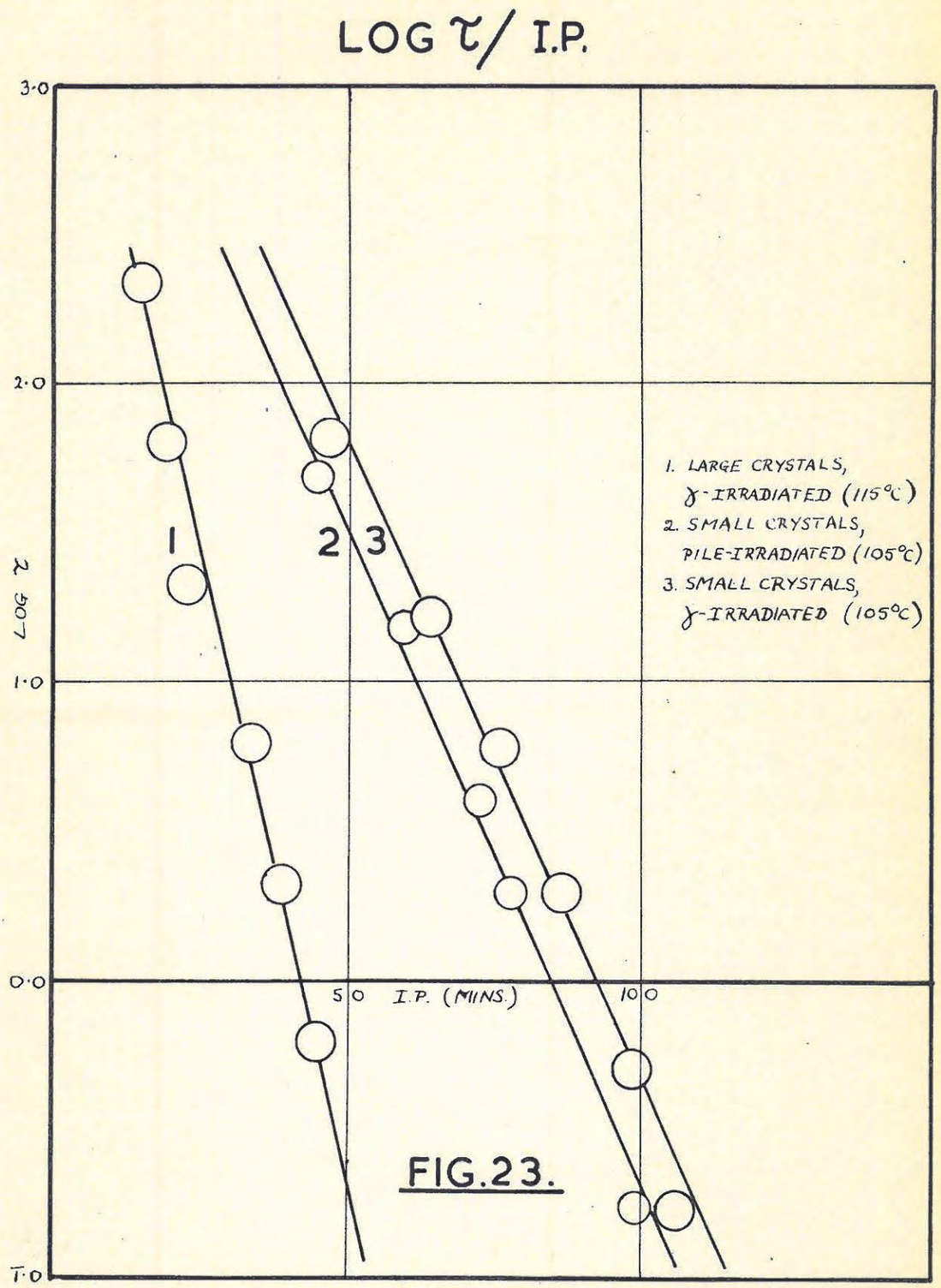
LOG τ/ I.P.
3·0
2·0
1·0
0·0
1·0
LOG τ
1
2
3
50
I.P. (MINS.)
100
1. LARGE CRYSTALS, γ-IRRADIATED (115°C)
2. SMALL CRYSTALS, PILE-IRRADIATED (105°C)
3. SMALL CRYSTALS, γ-IRRADIATED (105°C)

FIG.23.

The variation of the lengths of induction period with increasing dose (at fixed decomposition temperature) was found to obey the equation.

$$\log \tau = k_I(I.P.) + c \qquad (7.1)$$

where τ = time of irradiation,

k_I and c are constants.

The results are shown in Table 23 and Fig.23.

TABLE 23.

Large, γ-irradiated, decomposed at 115°C.		Small, γ-irradiated, decomposed at 105°C.		Small, BEPO-irradiated, decomposed at 105°C.	
I.P.(mins)	τ (hrs)	I.P.(mins)	τ(hrs)	I.P.(mins)	τ (hrs.)
15.2	220.0	47	64.8	45.0	48.0
19.7	63.0	64	16.3	60.0	15.0
22.8	21.0	76	6.0	73.0	4.0
34.0	6.3	87	2.0	78.0	2.0
38.3	2.1	98.5	0.5	99.0	0.17
44.5	0.63	106	0.17		
k_I =	0.0834	k_I =	0.0435	k_I =	0.0431

7.2 ACCELERATORY PERIODS.

The decomposition curves for small and large unirradiated crystals have been shown to fit the equation.

$$\log p/p_f - p = k_2 t + c \qquad (7.2)$$

over the acceleratory region.

(i) Unirradiated small crystals.

Using the above equation and the data of Table 17, values of k_2 were obtained for various temperatures. These are summarised in Table 24.

TABLE 24.

Decompn. Temp.	k_2 mins^{-1}
105°C	.00929
110°C	.01466
115°C	.03020
120°C	.04325
125°C	.06653
131.5°C	.10470

-76-/.....

ACCELERATORY PERIOD: ACTIVATION ENERGIES.

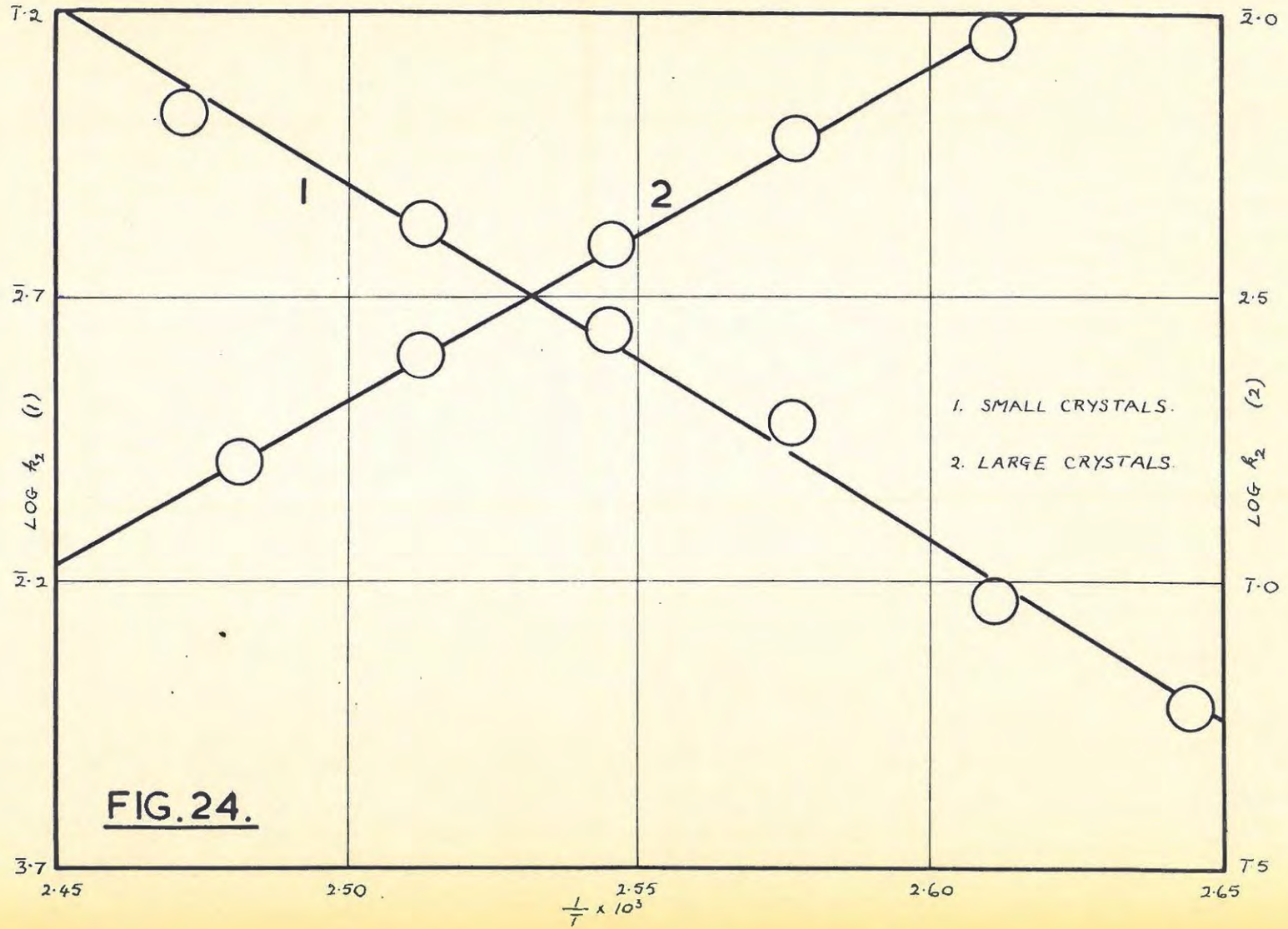

FIG. 24.

The activation energy (E_2) was calculated from the log $k_2 / \frac{1}{T^oA}$ plot (Fig.24) and found to be 29.0 Kcals mole^{-1}. This is in good agreement with the value of 29.4 Kcals mole^{-1} obtained by Prout and Tompkins.

(ii) Unirradiated large crystals.

The values of k_2 obtained from the data of Table 18 are summarised in Table 25.

TABLE 25.

Decompn. Temp.	k_2 mins^{-1}
110°C	.01104
115°C	.01660
120°C	.02582
125°C	.03999
130°C	.06166

The activation energy in this case was found to be 27.3 Kcals mole^{-1}.

(iii) Irradiated crystals.

In some cases the Prout-Tompkins equation fitted the acceleratory periods for irradiated crystals but for heavily dosed specimens an 'explosion' often occurred over this region. Thus activation energies for this period are of little value and were not calculated. A fuller discussion of this is presented later.

7.3 Decay Periods.

The Prout-Tompkins equation was found to fit the decay periods for unirradiated, γ-, and pile-irradiated crystals. As the decay processes are probably similar irrespective of treatment, activation energies (E_3) were determined for various specimens.

(i) Small unirradiated crystals.

The rate constants k_3 were determined from the data of Table 17 and are summarised below.

TABLE 26 Overleaf. -77-/.....

DECAY PERIOD: ACTIVATION ENERGIES.

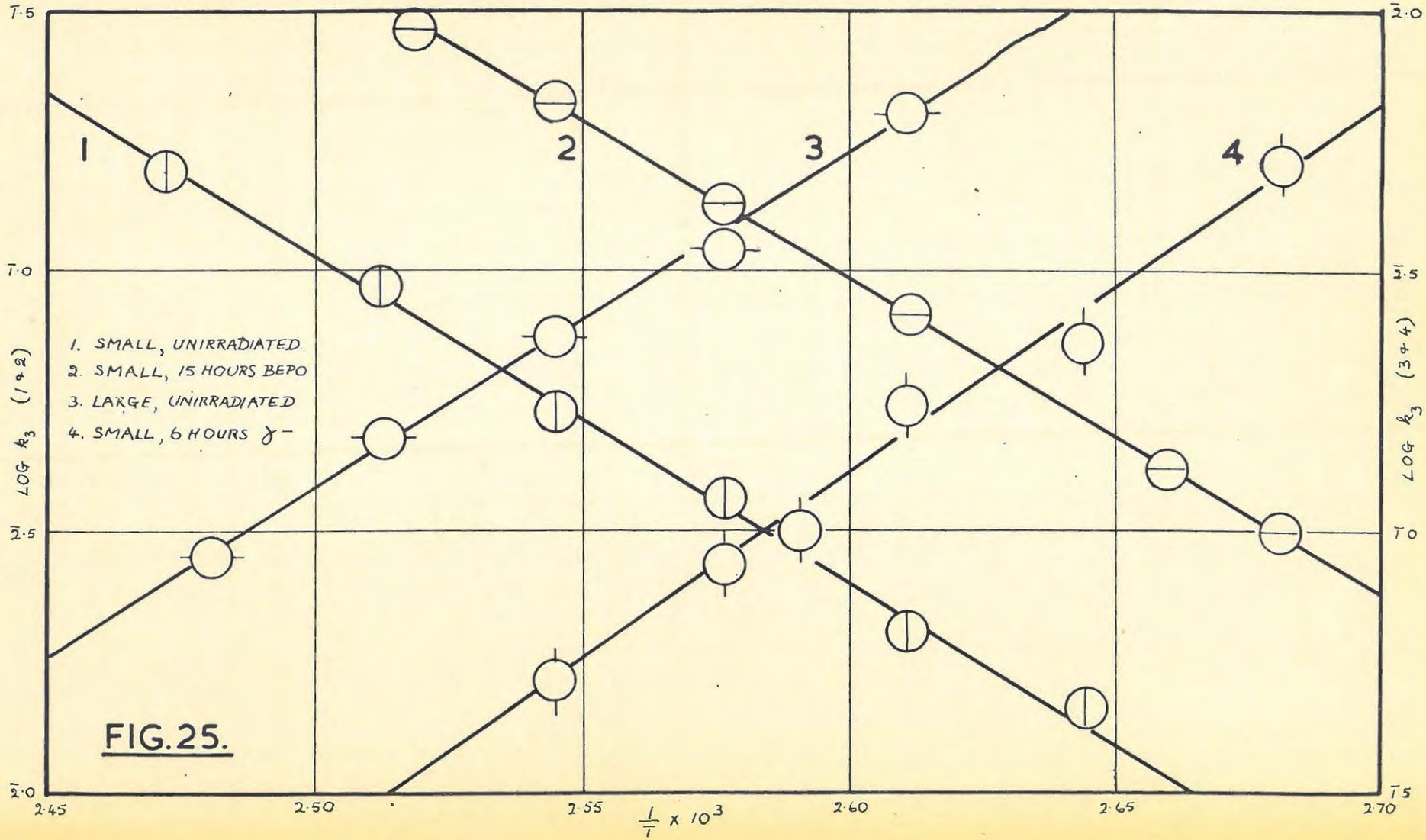

FIG.25.

TABLE 26.

Decompn. Temp.	k_3 $mins^{-1}$
105°C	0.01459
110°C	0.02000
115°C	0.03681
120°C	0.05333
125°C	0.09290
131.5°C	0.15490

The activation energy of decay was found to be 28.8 Kcals $mole^{-1}$, again in good agreement with the value of 29.4 Kcals $mole^{-1}$ obtained by Prout and Tompkins.

(ii) Large unirradiated crystals.

The rate constants k_3 tabulated below were obtained from the data of Table 18.

TABLE 27.

Decompn. Temp.	k_3 $mins^{-1}$
110°C	0.01563
115°C	0.02858
120°C	0.04207
125°C	0.06561
130°C	0.1127

The activation energy of decay was found to be 29.5 Kcals $mole^{-1}$.

(iii) Small crystals, 15 hours BEPO.

The rate constants k_3, tabulated below, were obtained from the data of Table 19.

TABLE 28.

Decompn. Temp.	k_3 $mins^{-1}$
100°C	0.03162
103°C	0.04169
108°C	0.09506
110°C	0.08318
115°C	0.1334
120°C	0.2109
124°C	0.2858

The activation energy of decay was found to be 28.0 Kcals $mole^{-1}$.

(iv) Small crystals, 6 hours γ - .

The rate constants k_3 tabulated below were obtained from the

-78-/.....

data of Table 20.

TABLE 29.

Decompn. Temp.	k_3 $mins^{-1}$
100°C	0.01972
105°C	0.04365
110°C	0.05754
113°C	0.1000
115°C	0.1148
120°C	0.1928

The activation energy of decay was found to be 32.3 Kcals $mole^{-1}$.

8. X-RAY INVESTIGATION.

A complementary study of the thermal decomposition of silver permanganate and the effects produced by pre-irradiation was undertaken during a seven week period at the National Physical Research Laboratory, Pretoria. This work can only be regarded as a preliminary to further study.

8.1 EFFECTS OF GRINDING CRYSTALS.

Since grinding has a marked effect on the rate of thermal decomposition, diffractometer traces were made for three samples in order to determine the effects of grinding on the quality of the crystals.

The samples investigated were:

1. Small crystals (0.3 x 0.03 mm)
2. Small crystals lightly ground for two minutes.
3. Small crystals heavily ground in a mechanical mortar for one hour.

Sample 1. showed a high degree of preferred orientation, and when this was reduced by using sample 2. there were marked changes in intensity, some peaks appearing and some disappearing. However, no peak broadening was noticeable. Sample 3. showed further slight intensity changes as well as a very slight amount of peak broadening. There was no suggestion that even heavy grinding for one hour can destroy the crystallinity of the crystal.

8.2 STUDY OF THE PROGRESS OF THE THERMAL DECOMPOSITION.

Laue photographs taken using unfiltered Mo radiation (exposure 1 hour at 45 kV and 20 mA) proved to be the most sensitive way of detecting changes produced on heating. Photographs of single unirradiated large crystals mounted about the [100] axis were taken after varying times of decomposition at 115°C in vacuo. (Fig.11 Curve 7; Plates B,C,D & E) The results are summarised below:

(a) Undecomposed crystal: The spots were sharp both in the high and low angle regions. There was also some thermal scattering.

-80-/.....

(b) After 25 minutes: Slightly more general diffuse scattering was evident but the spots were still well defined.

(c) After 50 minutes: Thermal scattering appeared to be more pronounced and there was more general diffuse scattering, but the spots were still well defined though slightly more diffuse in the high angle region.

(d) After 68 minutes: The thermal spots were more prominent and the crystalline spots showed signs of crystal break-up. Symmetrical diffuse scattering in the form of a circular ring in the region $\frac{\sin\theta}{\lambda} \approx 0.18A^{-1}$ was evident for the first time.

(e) After 78 minutes: The intensity of the diffuse ring had increased and the number of crystalline spots in the high angle region had diminished.

(f) After 105 minutes: The ring was more intense and a second outer ring in the region $\sin\frac{\theta}{\lambda} \approx 0.33A^{-1}$ was now visible. There were no high angle spots and thermal scattering was less.

(g) After 120 minutes: The two rings were now very distinct but the crystalline spots were still present.

(h) After 135 minutes: The crystalline spots were noticeably reduced in number but were still definitely present, as were the two diffuse rings.

(i) After 145 minutes: The crystalline spots had disappeared entirely leaving only the rings remaining.

(j) Completely decomposed: The position was unchanged from (i).

Thus the Laue photographs show that the diffuse rings increase in intensity approximately proportional to the amount of decomposition. The appearance of the crystalline spots is considerably more variable possibly because the effect of heating upon them depends very much on the initial state of the crystal. Consequently it would be rewarding to repeat these experiments by heating a single crystal in in situ in a camera and taking photographs at various stages of decomposition.

Oscillation and Weisenberg photographs were also taken using Cu radiation but were too underexposed to show amorphous scattering.

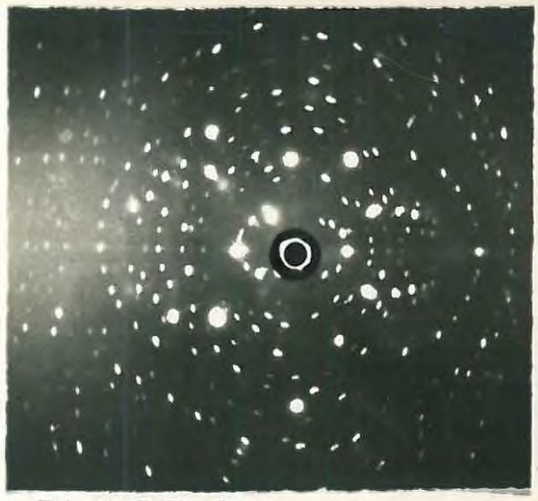

PLATE B.
UNIRRADIATED,
UNDECOMPOSED.

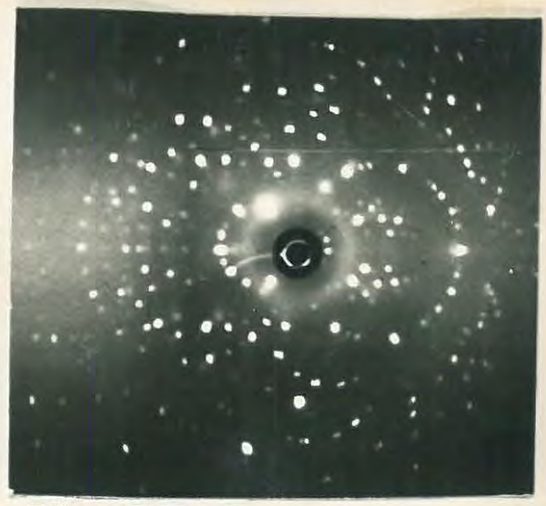

PLATE C.
UNIRRAD., DECOMP.
FOR 78 MINS. AT 115°C.

PLATE D.
UNIRRAD., DECOMP.
FOR 135 MINS. AT 115°C.

PLATE E.
UNIRRAD., DECOMP.
FOR 145 MINS. AT 115°C.

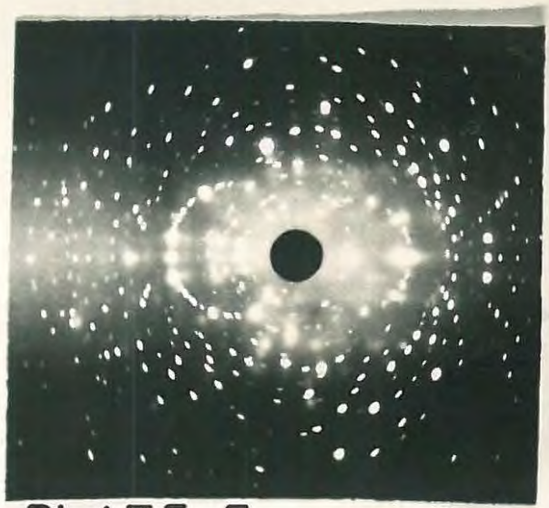

PLATE F.
220 HRS. γ- IRRAD.,
UNDECOMPOSED.

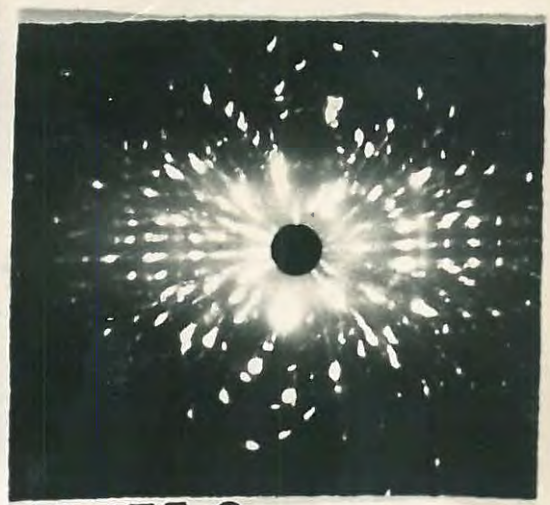

PLATE G.
220 HRS. γ-, DECOMP.
FOR 14 MINS. AT 115°C.

The behaviour of the crystalline spots was in general agreement with the results from the Laue photographs. Briefly, the Weisenberg and oscillation photographs showed a general weakening of the crystalline pattern with increased decomposition. There was some small broadening of the high angle spots but even after 78 minutes the Cu $K_{\alpha 1 \alpha 2}$ doublet remained fairly well resolved in the high angle region. There was no resolution on the 105 minute oscillation photograph. In addition there was no weakening of the high angle reflections relative to the low angle reflections.

8.3 SURFACE AND VOLUME DECOMPOSITION.

Surface and volume decomposition of large unirradiated crystals were also examined. Crystals decomposed for only 5 minutes at 115°C were immersed in water for 1 hour without the appearance of the characteristic permanganate colour. Undecomposed crystals from the same preparation coloured the water within 10 seconds. The partially decomposed crystals when broken under water rapidly coloured the water from the newly exposed surfaces. Similar results were obtained for crystals decomposed for 13 minutes and 78 minutes, indicating in all cases a sheath of product round the crystal. Using Cu radiation, oscillation spots were visible on the X-ray photograph of material decomposed for 78 minutes, indicating that the product sheath must be less than ~ 0.01 mm. thick.

Laue photographs were then taken of two different interior fragments of crystals decomposed for 78 minutes at 115°C. These photographs showed two differences from the analogous photograph of the unbroken crystal:-

(i) There was general unsymmetrical scattering in the low angle region for the photograph taken with white radiation, but when the photograph was repeated using filtered Mo K_α radiation a diffuse ring of the usual kind was obtained. The reason for the difference is not understood at present, but the diffuse ring does show that amorphous material has been produced in the interior of the crystal as well as on the surface.

-82-/.....

(ii) There appeared to be extra reflections on the Laue photographs of the fragments. These spots were quite different in appearance from the normal Laue spots and were very similar both in shape and position to first layer line spots found in oscillation photographs. The explanation for these is not certain.

8.4 IRRADIATION EFFECTS.

Laue and Weisenberg photographs were taken of an undecomposed crystal which had been irradiated for 220 hours with γ-rays. The Weisenberg photograph was identical with that of the unirradiated undecomposed crystal. The Laue photograph (Plate F) is similar to Plate B except that there is more thermal and diffuse scattering in the former.

A Laue photograph of a crystal from the same batch but decomposed for 6 minutes at 115°C (Fig.11., Curve 1) was also taken. If anything this was a better photograph than Plate F. Possibly it was just a better crystal.

Another Laue photograph of the same irradiated crystals decomposed for 14 minutes at 115°C (Fig.11., Curve 1; Plate G) showed broken up spots, considerable asterism, and faint extra spots due to fragmentation of the crystal. On the other hand a Weisenberg photograph of the same crystal was only generally weaker showing no drastic changes in the quality of the reflections. This is a striking example of how much more sensitive the Laue method is for showing crystal fragmentation and distortion.

Laue photographs of γ-irradiated fully decomposed crystals were identical with Plate E.

9. DISCUSSION.

The results obtained with irradiated whole and ground crystals of silver permanganate are similar to those found for irradiated potassium permanganate (12). The p-t curves of whole crystals, irradiated for increasing times, are characterised by:

(a) A progressive shortening of the induction period,

(b) An increase in the maximum velocity until a 'saturation velocity' is reached, and

(c) A lowering of the point of inflexion after this point.

A saturation effect was observed in the case of irradiated ground crystals.

These effects have been interpreted for irradiated $KMnO_4$ in terms of the production and annealing of cation vacancy-interstitial (V-I) pairs. Prout (12) irradiated $KMnO_4$ crystals with 145 Mev protons, thermal neutrons and γ-rays from ^{60}Co. The effective changes produced by the latter two radiations were considered to arise from the displacement of K^+ ions into interstitial positions as a result of collisions with Compton electrons generated by γ-rays. These γ-rays are those of capture, γ-rays in the pile or those from the ^{60}Co 'hot-spot'. Since collisions are heavily biased towards small energy transfer, the knocked-on atoms seldom have energies to produce secondaries and so the damage will consist of isolated V-I pairs randomly distributed in the crystal, the separation of vacancies from interstitials being about four or five interatomic distances.

At the temperature of decomposition there is annealing or recombination of vacancies and interstitials with the release of the associated Wigner energy. This energy may be quite considerable. As the crystal is already at its decomposition temperature, and since the material in the region of recombination is temperature sensitive, a centre of decomposed material will result. The presence of decomposition product will cause deformation of the $KMnO_4$ lattice and will result in a lowering of the activation energy for vacancy jump. There is thus preferential annealing around this region, which will increase

-84-/.....

in size to form a 'decomposition spike'.

During the induction period annealing takes plane and results in an increase in the number of these decomposition centres. A steady accumulation of strain in the crystal will result and this is sufficient to produce physical fracture at the end of the induction period. With moderate radiation doses the strain at various points within the crystal will not reach the critical disruptive calue at exactly the same time so that an extension of the fracturing process into the acceleratory period is probable. With heavy doses, and consequent increase in density of defects, the times between the attainment of critical strain will have decreased and the fracturing process should consist of the instantaneous break-up of the crystal. This would account for the lowering of the inflexion point with increased dosage. The shorting of the induction period with increased dosage is attributed to the increased number of defects produced, so that the time for critical strain to be produced is lessened.

Grinding is considered to be similar to 'cold-working' in metals which results in an increased number of vacancies (73). Consequently, since the rate of recombination depends on these, the induction periods of ground crystals, irradiated for the same time and decomposed at the same temperature, will be shorter than those for whole crystals. Saturation effects are easily accounted for since with high dosages a point will be reached during irradiation where there will be almost instantaneous recovery of the displaced atoms owing to the presence of excess vacancies produced by grinding.

The activation energies for the decay periods of both irradiated and unirradiated were similar, and as the Prout-Tompkins equation was applicable to both, the processes occurring in the decay of irradiated crystals were considered to be the same as those previously suggested for unirradiated $KMnO_4$ (1).

The mechanisms outlined above are based upon the annealing of point defects. As this standpoint will be adopted in applying these ideas to irradiated $AgMnO_4$, it is appropriate at this juncture to review various annealing processes which have been suggested.

In most cases irradiation of materials produces changes in certain physical properties (optical, electrical etc.) (57). These properties usually revert to normal when the materials are warmed. In general this has been attributed to a recombination of vacancies and interstitials.

Fletcher and Brown (74) have studied the annealing of electron irradiated germanium using resistance measurements. Annealing is considered to be a three stage process. Firstly those vacancy-interstitial pairs having small initial separation will recombine under the influence of short range forces. In the region of the interstitial the lattice will be deformed and this lowers the potential barrier between an atom adjacent to a vacancy and between it and the interstitial. The nett result is that the atom tends to jump into the vacancy or, alternatively, the vacancy jumps towards the interstitial. The rate of recombination is then given by

$$\frac{dN}{dt} = - N \nu \qquad \text{(9.1)}$$

where N = number of close pairs / cm^3.

ν = frequency of movement.

The second and third stages involve the movement of vacancies outside the deformed regions of their respective interstitials. These vacancies are considered to move according to a random walk process. Some will return to the distorted regions of their own interstitials and recombine in a bimolecular process whose rate of recombination is

$$\frac{dN}{dt} \propto N_v^2 \qquad \text{(9.2)}$$

where N_v = density of vacancies after stage 1. is completed. The remaining vacancies will wander away and become annihilated at defects other than the ones of origin or become trapped at the surface or at dislocations. This comprises stage 3. of the mechanism and the process is intermediate between a uni- and bimolecular reaction.

Waite (75) has extended the work of Fletcher and Brown to embrace the aspect of diffusion. Vacancies and interstitials are considered to diffuse with a combined activation energy of $\sim$ 1.35 ev.

-86-/.....

The individual contributions to this process are not assessed but vacancy diffusion is considered to predominate. A capture radius r_o is defined and the average separation of a vacancy-interstitial pair is found to be $\sim 1.5r_o$. The first 65% of the annealing is due to the recombination of each interstitial with the vacancy from which it was produced.

Overhauser (76) suggests that at low temperatures, annealing is due to recombination of vacancy-interstitial pairs, but at higher temperatures is due to volume diffusion of vacancies and their annihilation with interstitials. Lomer and Cottrell (77) consider the annealing of damage in metals to be a two-stage process. During the first stage, defects become trapped (e.g. on impurity atoms). The unexpectedly large number of jumps in this stage is accounted for by postulating an interstitial mechanism which provides a random walk in only one dimension. During the second stage the defects evaporate from their traps and then recombine.

In the annealing processes discussed above, a point of significance is that both interstitials and vacancies can migrate but that their respective activation energies are different. Thus the migration of one species often predominates over the migration of the other. It is therefore of interest to mention some theoretical and experimental values of the activation energies of migration of interstitials and vacancies in various materials. These will provide a guide in assessing which occurs in the case of $AgMnO_4$. Huntington (78) has calculated the activation energies of interstitials and vacancies in copper to be $\sim$ 0.2 ev and $\sim$ 0.9 ev respectively. The latter value is in good agreement with the value of 1.0 ev obtained by Granato et al (79) using ultrasonic methods. Brinkman et al (80) suggest that the movement of interstitials in Cu_3Au occurs with an activation energy of 0.7 ev while the activation energy of vacancy migration is 1.2 ev. The migration of vacancies in cold-worked molybdenum (63) has been associated with an activation energy of $\sim$ 1.25 ev and the migration of interstitial Ag^+ ions in AgBr with an activation energy of 0.11 ev (81).

-87-/.....

At this stage it is of interest to consider the nature and magnitude of the Wigner energy release when vacancies and interstitials are mutually annihilated. The energy of formation of the vacancy in copper has been calculated by Huntington (78) to be 1.5 - 1.8 ev and that of an interstitial to be 5.1 - 6.1 ev. It has generally been accepted that the energy stored in a vacancy-interstitial pair is $\sim$ 5 ev (56). This energy will be released in the form of lattice phonons and be degraded into heat on the annihilation of the pair (82). Kinchin (83) has measured calorimetrically the energy release when graphite, after a dose of 3×10^{20} slow neutron/cm^2, was annealed to 400°C. This was equivalent to a rise of temperature of the material of about 200°C! Similar results were obtained by Austermann (84).

Before attempting to apply the ideas discussed above to irradiated $AgMnO_4$, it is necessary to consider whether the damage produced is similar. Reference to fig.9 indicates that, as with $KMnO_4$, the effective damage is due to γ-rays. Comparison with $KMnO_4$ suggests that the damage is caused by displacement of Ag^+ ions into interstitial positions. That this is possible will now be shown.

Following the method of Seitz (59) and assuming that E_d for a silver ion in $AgMnO_4$ is 25 ev, the threshold energy for displacement of silver ions by electrons is 0.72 Mev. The maximum energy of a Compton electron produced by a photon of energy $h\nu$ is given by (85)

$$E_c\ (max) = h\nu \frac{2\alpha}{1 + 2\alpha} \qquad \text{(9.3)}$$

where $\alpha = \frac{h}{m_o c^2}$

$m_o c^2$ = rest energy of the electron.

For incident γ-rays of mean energy 1.25 Mev, $E_c(max)$ is 1.04 Mev. Thus Compton electrons scattered through small angles will have energies in excess of threshold and can produce displacement.

Kinchin and Pease (57) state that the most likely process for atoms of high atomic number is displacement by photoelectric recoil. This is expected to predominate here as the probability of absorption depends on Z_2^5 in this case (86) while that for Compton scat-

-88-/...

tering is only proportional to Z_2. The photoelectrons themselves can produce further displacements since the energy of a photoelectron (E_p) is given by

$$E_p = h\nu - w \qquad \text{(9.4)}$$

where w = the binding energy of the electron. For an electron in the K shell, w is given by (87)

$$w \approx R_H (Z_2 - 1)^2 \qquad \text{(9.5)}$$

$$\approx 0.16 \text{ Mev for silver.}$$

where R_H = Rydberg constant ($\sim$ 13.5 ev)

The energy of photoelectrons produced by γ-rays of energy 1.25 Mev is therefore 1.09 Mev, again in excess of the threshold for displacement. The number of secondary displacements will not be greatly in excess of the number of photoelectrons as the knock-on atoms will seldom have sufficient energy to produce secondaries.

The analysis of the results for irradiated $AgMnO_4$ may be divided into three sections which relate to the induction period, the accelleratory period, and the decay respectively.

During the induction period it is assumed, as before, that close V-I pairs anneal according to stage 1. of Fletcher and Brown's theory. The energy released on recombination causes the formation of a centre of decomposed material, and this grows, due to the lowered energy for vacancy jump around it, to produce a 'decomposition spike'. It should again be stressed that the undecomposed material is already at decomposition temperature when the Wigner energy is released. The 'decomposition spikes' will be formed preferentially along dislocation lines since their initial formation is favoured in regions of deformation. Strain will thus be produced along dislocations and, it is important to note, this will thus be interior strain as distinct from surface strain for which there is some evidence in the unirradiated crystals (see later). Fracture will probably originate in these regions. This view is supported by the X-ray results (Plate G) which indicate distortion and fragmentation of the lattice at the end of the induction period. The strain produced in the irradiated crystal must therefore be due to solid product. It should be pointed out that

-89-/.....

though the product has been shown to the amorphous it will still have a "lattice" with short range order and this lattice will be different from that of the $AgMnO_4$. Moreover the density of the product has been found to be less than that of the undecomposed crystal (88).

The progressive shortening of the induction period with increasing dosage is due to an increase in the density of point defects with a consequent decrease in the time required for the strain to attain a critical value. The degree of disintegration at the end of the induction period should increase with dosage since with the greater numbers of defects present a larger number of dislocation will contribute to the fracturing.

The activation energies (E_1) obtained from the plot of $\log \frac{I}{I.P}$ against absolute temperature for fixed irradiation time may be given physical significance as follows. Fletcher and Brown consider that by comparing the times at which the same degree of annealing occurs for different temperatures, the barrier energy, E, for vacancy jump, can be determined. The variation with temperature of the length of the induction period can therefore be assumed to reflect the average jump time of the moving defect. The average value of E_1 (1.03 ev) is in general agreement with the value obtained for $KMnO_4$. Reference to the activation energies of migration of vacancies given previously would suggest that the above value is to be associated with the movement of vacancies.

The saturation effects observed for irradiated ground material are in agreement with those obtained for $KMnO_4$. They may again be explained in terms of the production of vacancies during grinding resulting in almost instantaneous recovery of some of the displaced atoms during irradiation. The shortening of the induction period with increased grinding and fixed radiation dose may be explained in terms of the increased number of vacancies. The increase in the maximum rate of reaction and in the degree of splintering is explained by there being increased numbers of dislocations, produced as a result of grinding.

The nature of the processes occurring during the acceleratory

period is complex. Because of fracture (which does not occur in the unirradiated case) two distinct processes are considered to operate. The production of fragments will result in the rapid spread of the reaction over the new surfaces which are formed. This is followed by the inward progression of the reactant-product interface. In addition it is expected that reaction occurring by the previously suggested mechanism for the unirradiated decomposition will also be occurring. In lightly dosed crystals the latter will predominate and the Prout-Tompkins equation is still expected to apply, as was found to be the case (cf. Fig.20, curve 1.) As with $KMnO_4$, for lightly dosed samples, the strain developed in various parts of the crystal will not reach a critical value simultaneously and the fracturing process and hence the acceleration will be time extended. With increased dosages the times for the attainment of critical strain will be less so that almost instantaneous break up of the crystal will occur. As is to be expected therefore, the Prout-Tompkins equation fails in these cases. In view of the complicated nature of the processes occurring, the determination of an activation energy for the acceleratory period is not possible.

As has been mentioned previously, the acceleratory period is characterised with increasing dosage by an increasing velocity which reaches a maximum. This can be attributed to the increased surface area of the solid as a result of increased disintegration. However, the latter will reach a maximum which is dependent on the density of crystal dislocations.

The lowering of the point of inflexion with increased dose may be explained as follows. Reaction during the period of fracture will involve in addition to the acceleratory surface reaction, the decay reaction of particles produced in the early stages. Irradiation times greater than that first giving rise to the limiting velocity will cause a shortening of the period of fracture since with heavy doses and a consequent increase in the density of defects, the times between the attainment of the critical strain at various dislocations will have decreased. This will lower the pressure at the

-91-/.....

end of the fracture period since there will be a decrease in the extent of the decay reaction of the fragments formed during fracture.

The decay period, as has been suggested above, is to be associated with the inward progression of the product-reactant interface. The activation energies (E_3) for this process are similar to the unirradiated case. As the Prout-Tompkins equation again applies and the end product is the same, the mechanism for this progression is assumed to be the same as previously postulated for $KMnO_4$ where equation (6.2) was valid.

The interrupted runs (Fig.13) suggest that two different types of nuclei operate, in the case of the irradiated and unirradiated material. The onset of fracturing with irradiated crystals always occurs at a pressure above that given by unirradiated crystals at the same time, indicating the formation of product molecules additional to those produced by the "normal decomposition". If the former are, as suggested, favourably placed for crystal fracture whereas the latter are not, it is likely that the initiation of fracturing is up to a point independent of the unirradiated decomposition. Reference to fig.13 shows that this is the case. If curve 1. diverges after 23 minutes, it is to be expected that curve 2. (which was interrupted after 25 minutes and then given the same dose) will diverge at t = 48 minutes. In fact it diverges at t = 46 minutes. Then again, curve 3., interrupted after 50 minutes decomposition, should diverge at t = 73 minutes. Actually it diverges at t = 68 minutes. Likewise, curves 4 and 5 diverge at t = 97 minutes and t = 125 minutes respectively, instead of at t = 103 minutes and at 128 minutes. Interrupting the decomposition once the decay has begun, and then irradiating, has no real effect. This is reasonable since the accelerator mechanism suggested above would not apply, due to the decomposition of a large percentage of the reactant, with consequent destruction of dislocation lines.

The preceding research has also provided a clearer picture of the unirradiated decomposition. Solubility studies have shown that initial reaction consists of the rapid spread of product over the sur-

-92-/.....

face. This occurs in five minutes at 115°C. Over the induction period, before the Prout-Tompkins equation becomes applicable, the p-t plot is almost linear. This may be explained as follows. Once the layer of product has been formed reaction will proceed at the product-reactant interface. In the initial stages of decomposition, the area of the interface will be approximately constant, so that a linear rate of decomposition will occur. (89). This slow decomposition will result in a thickening of the product sheath over the induction period. The resultant surface strain will produce cracks along which reaction may proceed inwards in a manner analogous to that for unirradiated $KMnO_4$ (1). This will be marked by the commencement of the acceleration.

Now, if a surface reaction is occurring over the induction period, it would seem that the Prout-Tompkins equation might be modified to take account of this. If p_I is the pressure developed at time t_I, (the time at the end of the induction period) then the Prout-Tompkins equation may be rewritten in the form

$$\log \frac{p - p_I}{p_f - p} = k.t + c \qquad \text{(9.6)}$$

Taking t_I as 60 minutes, (the time when the Prout-Tompkins equation becomes inapplicable), equation (9.4) was plotted for small unirradiated crystals decomposed at 105°C. Reference to fig.26 shows that the fit equation (9.4) is good, and that moreover, only one value of the constant k is necessary.

That reaction is proceeding in the interior of the crystal during the acceleratory period has been definitely established. Laue photographs of interior fragments of crystals decomposed for 78 minutes show the presence of amorphous product as evidenced by the usual diffuse ring.

Three broad possibilities for the structural changes occurring in the crystals when they are decomposed may be envisaged from the appearance of the Laue photographs taken of crystals after various stages of decomposition. The increasing diffuseness of the crystalline spots suggest that there is distortion and break-up of the

-93-/.....

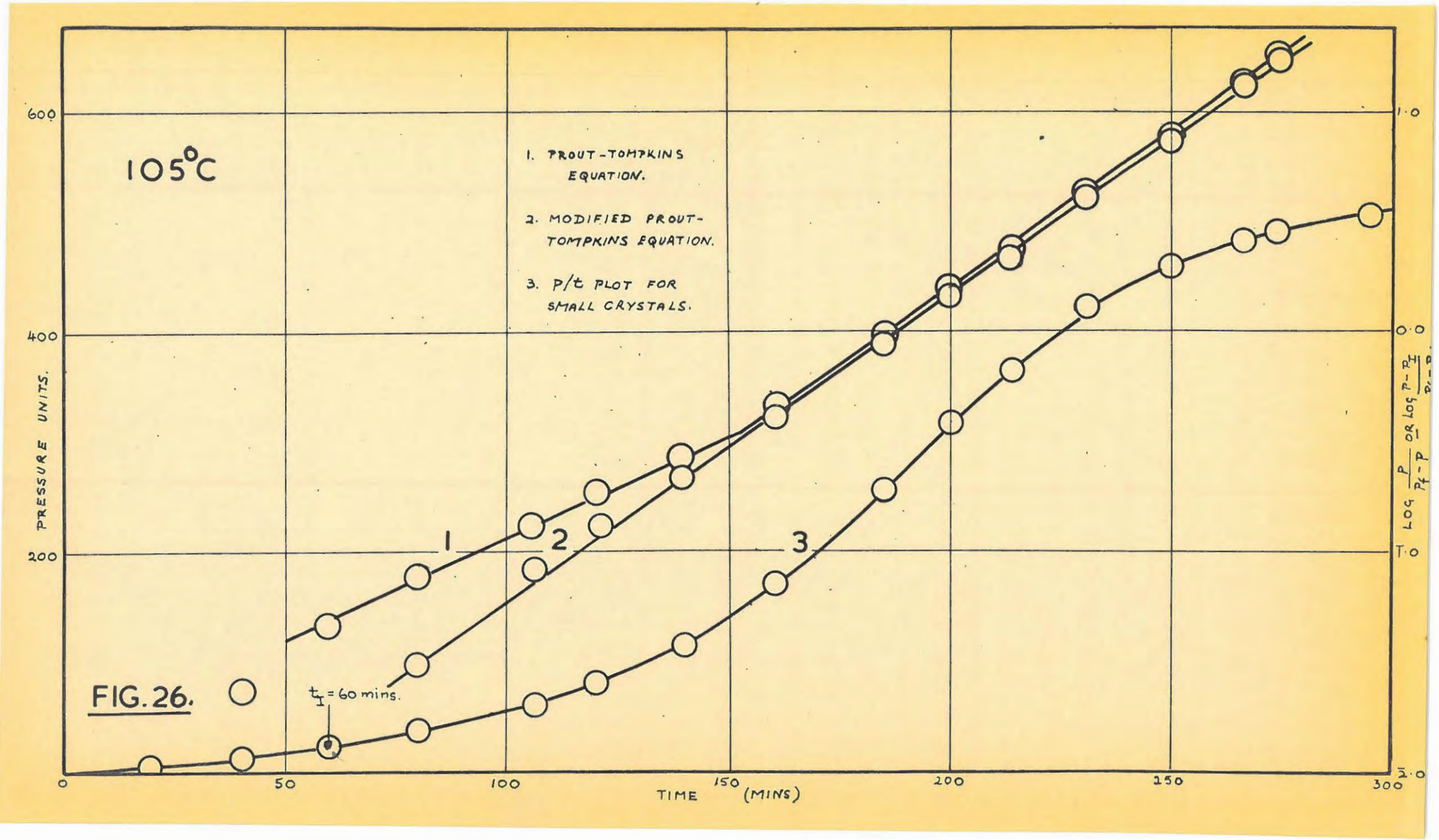
105°C
1. PROUT-TOMPKINS EQUATION.
2. MODIFIED PROUT-TOMPKINS EQUATION.
3. P/t PLOT FOR SMALL CRYSTALS.
1
2
3
t_I = 60 mins.
PRESSURE UNITS.
600
400
200
0
50
100
150
200
250
300
TIME (MINS)
1·0
0·0
1·0
2·0
LOG $\frac{P}{P_f - P}$ OR LOG $\frac{P - P_I}{P_f - P}$

FIG. 26.

crystal. However, the fact that physical fracture is not observed and that the $Cu_K \alpha_1 \alpha_2$ doublet remains fairly well resolved in the high angle region for a crystal decomposed for 78 minutes at 115°C, would seem to indicate that the distortion is not great. What distortion there is, is probably associated with the formation of cracks caused by the product, in the reactant surface adjacent to the product. There is also evidence for increased thermal vibrations as shown by the increasing numbers of 'thermal spots' with increased decomposition. However, the predominant process must be the conversion of crystalline into amorphous material without marked reduction of the crystallinity of the unreacted material. This is emphasised by the striking fact that even when crystals are 78% decomposed (Plate D) the crystalline spots still remain.

The exact nature of the product of decomposition and its relation to the reactant are still not clear. However, it has been established that, while retaining the external morphology of the undecomposed crystals, the product is amorphous and is probably in the form of a glass. This confirms the work of Hein (90) and of Grant and Katz (91) who also reported an amorphous product. In this respect $AgMnO_4$ differs from $KMnO_4$ where the products have been shown to be K_2MnO_4 and γ-MnO_2. (88)

The foregoing account may be briefly summarised. The unirradiated decomposition proceeds along the surface and along self-created planes of reaction. X-rays show that this gives rise to only slight distortion. The irradiated decomposition occurs with the formation of additional reaction centres near dislocations. These result in faster reaction and strain which causes fragmentation at the end of the induction period. The decay mechanisms for both irradiated and unirradiated are essentially the same and involve the interference of planes of product resulting in a series of contracting interfaces.

10. SUMMARY.

The thermal decomposition of silver permanganate, pre-irradiated in BEPO and in a ^{60}Co γ 'hot spot' has been investigated in the temperature range 100 - 125°C. The results are similar to those for irradiated $KMnO_4$ and the mechanism proposed for the latter is again suggested. The activation energy for the migration of point defects over the induction period is 1.03 ev. The decompositions of unirradiated and irradiated crystals differ in that the latter undergo physical disintegration over the acceleratory period. X-ray studies immediately prior to disintegration show strain and fragmentation in the irradiated crystal. An explanation involving the annealing of point defects at dislocations is advanced to explain the changes produced in the p/t plots with increased dosage, and fixed decomposition temperature.

BIBLIOGRAPHY.

1. Prout and Tompkins, Trans. Faraday Soc., 40, 488, (1944)
2. Hailes, ibid, 29, 544, (1933).
3. Prout and Tompkins, ibid, 43, 148, (1947).
4. Garner and Gomm, J. Chem. Soc., 2123, (1931).
5. Garner and Marke, ibid, 657, (1936).
6. Garner and Haycock, Proc. Roy. Soc., A211, 335 (1952).
7. Garner and Tanner, J. Chem. Soc., 47, (1930).
8. Thomas and Tompkins, Proc. Roy. Soc., A210, 111, (1951).
9. Garner and Maggs, ibid, A172, 299, (1939).
10. Groocock and Tompkins, ibid, A223, 267, (1954).
11. Bowden and Singh, Nature, 172, 378, (1953).
12. Prout, in the press.
13. Gray and Waddington, Proc. Roy. Soc., A241, 110, (1951).
14. Wischin, ibid A172, 314, (1939).
15. Hume and Colvin, ibid, A125, 635, (1929).
16. Garner and Southon, J. Chem. Soc., 1705, (1935).
17. Garner and Pike, ibid, 1565, (1937).
18. Sawkill, Proc. Roy. Soc., A229, 135, (1953).
19. Finch, Jacob and Tompkins, J. Chem. Soc., 2053, (1954).
20. Mott and Gurney, Proc. Roy. Soc., A164, 151, (1938).
21. Bright and Garner, J. Chem. Soc., 1872, (1934).
22. Cooper and Garner, Trans. Faraday Soc., 32, 1739, (1936).
23. Benton and Cunningham, J. Amer. Chem. Soc., 57, 2227, (1935).
24. Garner, "The Chemistry of the Solid State", (Butterworth), 188, (1955).
25. Tompkins and Young, unpublished work.
26. Garner and Reeves, Trans Faraday Soc., 50, 254, (1954).
27. Bartlett and Tompkins, unpublished work.
28. Garner and Hailes, Proc. Roy. Soc., A139, 1393, (1933).
29. Bircumshaw and Edwards, J. Chem. Soc., 1800, (1950).
30. Dodé, Bull. Soc. Chim., 170, (1938).
31. Bircumshaw and Harris, J. Chem. Soc., 1637, (1939); 1898, (1948).
32. Prout and Tompkins, Trans. Faraday Soc., 42, 468, (1946).
33. Burgers, Proc. Phys. Soc., (London), 53, 23, (1940).

34. Frank, Advances in Physics, 1, 91, (1952).

35. Turnbull and Hoffmann, unpublished work.

36. Seitz, Rev. Mod. Phys. 23, 328, (1951).

37. Kittel, "Introduction to Solid State Physics", (Wiley), 478, (1956).

38. Shulman, Journ. Phys. Chem., 57, 749, (1953).

39. Pohl, Phys. Z., 39, 36, (1938).

40. Estermann, Leivo and Stern, Phys. Rev. 75, 627, (1949).

41. Haynes and Shockley, ibid 82, 935, (1951).

42. Mitchell, Phil. Mag., 40, 249, (1949).

43. Sheppard, Photo. J., 65, 380, (1925).

44. Sheppard and Hudson, J. Amer. Chem. Soc., 49, 1814, (1927).

45. Mott, Proc. Roy. Soc., A172, 325, (1939).

46. Thomas and Tompkins, J. Chem. Phys., 20, 662, (1952).

47. Bagdassarian, Acta Physicochim U.S.S.R., 20, 441, (1945).

48. Garner and Moon, J. Chem. Soc., 1398, (1933).

49. Maggs, Trans. Faraday Soc., 35, 433, (1939).

50. Prout and Tompkins, ibid 43, 148, (1947).

51. Seitz and Koehler, "Theory of Lattice Displacements Produced During Irradiation," Proc. Intern. Conf. Peaceful Uses of Atomic Energy, 7, 615, (United Nations, 1956).

52. Klontz and Lark-Horowitz, Phys. Rev., 86, 643, (1952).

53. Loferski and Rappaport, ibid, 98, 1861, (1955).

54. Eggen and Laubenstein, ibid, 91, 328, (1953).

55. Denney, ibid, 92, 531, (1953).

56. Cottrell, Jour. Brit. Nucl. Energy Conf., 3, 50, (1958).

57. Kinchin and Pease, Rep. Progr. Phys., 18, 1, (1955).

58. Snyder and Neufeld, Phys. Rev., 97, 1636, (1955).

59. Seitz, "Solid State Physics" (Academic Press Inc.) 2, 305, (1955).

60. Brooks, U.S. Atomic Energy Commission Document KAPL (declassified report 360, (1950).

61. Brinkman, Amer. J. Phys., 24, 246, (1956).

62. Brooks, Annual Rev. Nucl. Science, 6, 215, (1956).

63. Dugdale, "Defects in Crystalline Solids", 246, (Proc. Bristol Conf. Phys. Soc. London, 1955).

64. Cleland, Crawford and Holmes, Phys. Rev., 102, 722, (1956).

65. Seitz, ibid, 89, 1299, (1953).

66. Dexter, ibid, 93, 985, (1954).

67. Varley, J. Nuclear Energy, 1, 130, (1954).

68. Moles and Crespi, Anales de la Sociedad Espanola de Fisic. y Quimica, 198, (1925).

69. Roginsky, Trans, Faraday Soc., 34, 959, (1938).

70. Handbook of Chemistry and Physics (Chemical Rubber Publishing Co), 289, (1952-1953).

71. Eastwood, Nucleonics, 13, 52, (1955).

72. Mellor, "Inorganic and Theoretical Chemistry", 12, 332.

73. Dugdale and Green, Phil. Mag., 45, 163, (1954).

74. Fletcher and Brown, Phys. Rev. 92, 585, (1953).

75. Waite, ibid, 107, 471, (1957).

76. Overhauser, ibid, 90, 393, (1953).

77. Lomer and Cottrell, Phil. Mag., 46, 711, (1955).

78. Huntington, Phys. Rev., 61, 325, (1942).
ibid, 91, 1092, (1953).

79. Granato, Hikata, and Lucke, ibid, 108, 1344, (1957).

80. Brinkman, Dixon and Meechan, Acta Met., 2, 38, (1954).

81. Kittel, "Introduction to Solid State Physics", (Wiley), 487, (1956).

82. Seitz, "Imperfections in Nearly Perfect Crystals", (Wiley), 35, (1952).

83. Kinchin, Proc. Int. Conf. Peaceful Uses of Atomic Energy, (Geneva, 1955), 7, 472, (1956).

84. Austermann, "Solid State Physics Quarterly Progress Report, April-June 1955". U.S.A.E.C. Rep., 1955, No. NAA-SR-1942.

85. Semat, "Intro. Atomic and Nuclear Physics", (Rinehart), p.157.

86. Friedlander and Kennedy, "Introduction to Radiochemistry", (Wiley), p.166, (1949).

87. Fermi, Orear, Rosenfeld and Schluter, "Nuclear Physics", (Chicago Press), p.38, (1950).

88. Herbstein, private communication.

89. Garner, "Chemistry of the Solid State", (Butterworth), p.198, (1955).

90. Hein, Z. anorg. allgem. Chemie, 235, 25, (1937).

91. Grant and Katz, Can. J. Chem. 32, 1068, (1954).